STUDY ON THE CHAOTIC SYSTEMS CONTROL AND SYNCHRONIZATION

Thesis submitted to

Mahatma Gandhi University

in partial fulfillment of the requirements

for the award of the Degree of

DOCTOR OF PHILOSOPHY

in

PHYSICS

under the

Faculty of Science

Submitted by

SUNSU KURIAN THOTTIL

Under the guidance of

Dr. Rose P. Ignatius

DEPARTMENT OF PHYSICS

ST.TERESA'S COLLEGE, ERNAKULAM

Mahatma Gandhi University Kottayam-686 560

Kerala, India

December 2019

MAHATMA GANDHI UNIVERSITY

CERTIFICATE ON PLAGIARISM CHECK

1.	Name of the Research Scholar	**SUNSU KURIAN THOTTIL**
2.	Title of the Thesis/Dissertation	Study on the Chaotic Systems Control and Synchronization
3.	Name of the Supervisor	Dr. Rose P. Ignatius
4.	Department/Institution/ Research Centre	Department of Physics St.Teresa's College, Ernakulam
5.	Similar Content (%) identified	**1% (One)**
6.	Acceptable Maximum Limit	25%
7.	Software Used	Urkund
8.	Date of Verification	19-12-2019

**Report on plagiarism check, items with % of similarity is attached*

Checked by (with Name, Designation & Signature) :

Annu George
19.12.2019
ANNU GEORGE
Deputy Librarian in-charge
University Library
Mahatma Gandhi University
Kottayam - 686 560

Name & Signature of the Researcher : Sunsu Kurian Thottil

Name & Signature of the Supervisors : Dr. Rose P. Ignatius

Dr. ROSE P. IGNATIUS
Assoc. Professor
Physics Department
St. Teresa's College
Ernakulam-682 035

Name & Signature of the HoD/HoI(Chairperson of the Doctoral Committee) :

ST. TERESA'S COLLEGE AUTONOMOUS
ERNAKULAM-682 011

Dr SAJIMOL AUGUSTINE M
PRINCIPAL
ST TERESA'S COLLEGE
Autonomous
Ernakulam

URKUND

Urkund Analysis Result

Analysed Document:	Sunsu Kurian Thottil - Study on the chaotic systems control and synchronization.pdf (D61426104)
Submitted:	12/19/2019 11:16:00 AM
Submitted By:	library@mgu.ac.in
Significance:	1 %

Sources included in the report:

https://www.researchgate.net/publication/231149423_Coherence_resonance_and_synchronization_of_Hindmarsh-Rose_neurons_with_noise
http://web.tuat.ac.jp/~gvlab/ronbun/ReadingGroupControl/mls-lyap.pdf
https://www.researchgate.net/publication/257448485_Simulated_test_of_electric_activity_of_neurons_by_using_Josephson_junction_based_on_synchronization_scheme

Instances where selected sources appear:

8

19/12/19

Annu George
19.12.2019

ANNU GEORGE
Deputy Librarian in-charge
University Library
Mahatma Gandhi University
Kottayam - 686 560

DECLARATION

I hereby declare that the matter embodied in this thesis entitled "STUDY ON THE CHAOTIC SYSTEMS, CONTROL AND SYNCHRONIZATION" is the result of original research work done by me under the supervision of Dr. Rose P. Ignatius, Research Guide, Department of Physics, St. Teresa's College, Ernakulam and it has not been submitted elsewhere for award of any other degree or diploma.

Kottayam **Sunsu Kurian Thottil**

27-12-2019

St. Teresa's College (Autonomous)
Department of Physics
Ernakulam-682011, Kerala,
India
Telephone: +91-9446490056 (Mobile)
E-mail: rosgeo@yahoo.com

Dr. Rose P. Ignatius
Research Guide

23.12-2019

Certificate

This is certify that the thesis entitled **"STUDY ON THE CHAOTIC SYSTEMS CONTROL AND SYNCHRONIZATION"** is an authentic record of the research work carried out by Smt. Sunsu Kurian Thottil, under my supervision, in partial fulfillment of the requirements for the award of the degree of Doctor of Philosophy in Physics under the Faculty of Science of Mahatma Gandhi University, Kottayam. This work presented in this thesis has not been submitted for any degree or diploma earlier. It is also certified that Smt. Sunsu Kurian Thottil has fulfilled the course requirements for Ph.D. degree of the University.

Rose P. Ignatius

Dr. Rose P. Ignatius
(Supervising Teacher)

Dr. ROSE P. IGNATIUS
Assoc. Professor
Physics Department
St. Teresa's College
Ernakulam-682 035

Acknowledgement

I thank Almighty God, beholder of ultimate and ever ending knowledge for giving blessings upon me all the time. I could never have completed this thesis without your devine help.

I would like to express my sincere gratitude to my Research supervisor Dr. Rose P. Ignatius who provided incredible support and advice in completing this thesis. Her kind and helpful nature had been a steady influence throughout my Ph.D career. I express my whole hearted indebtedness for her guidance, encouragement, insightful discussions and advices during the research work. I must thank her for encouraging me and for helping me to do research with freedom.

I express my profound sense of thankfulness to all my teachers, mentors, fellow research scholars and friends for their encouragement and motivation. I also express my sincere thanks to all faculties and staff members of physics department.

I greatly acknowledge Mahatma Gandhi University and Directorate of Collegiate Education for granting the fellowship during my research period.

I am thankful to my parents for their unconditional love and support. I must say that my partner in life, Savichen, has played a pivotal role by standing by me and constantly motivating me to accomplish this task. Our six year old son Jothem, kept me enthused with his antics, engulfed me with love and gave me a sense of purpose to complete my thesis.

Sunsu Kurian Thottil

PREFACE

The thesis entitled **'Study on the chaotic systems control and synchronization**' comprises the study of nonlinear dynamics of neurons. The nonlinear dynamics of a neuron can generate deterministic chaos under some conditions. The theoretical and experimental studies on chaotic neural dynamics shall help to understand functions of brain such as adaptation, perception, episodic memory, learning, awareness, intentionality and thought. Also studies on the effect of electromagnetism in brain gives a pathway to the quantum mind theories of brain dynamics. The work addresses how chaos in neural systems accomplishes synchronization, anti-synchronization, oscillation death, amplitude death and near death rare spikes which may eventually lead to different biologically important goals.

The thesis is divided into 7 chapters. Though each chapter may stand on its own, each contributes to the broader scope of the thesis which is the study of chaotic or nonlinear dynamics of selected systems.

Chapter 1

This chapter deals with introductory ideas of nonlinear dynamics and chaotic systems. Chaotic systems manifest itself in a number of phenomena in both laboratory and in day to day dealings. The dynamical characterization tools of chaotic systems such as phase portraits, attractors, time series analysis, Lyapunov Exponent, stability of dynamical systems, bifurcations and routes to chaos are described. Some ideas related to control and synchronization in chaotic systems are also addressed.

Chapter 2

Chapter 2 deals with basic principles of Neuronal Dynamics. Theoretical and computational neuroscience focuses on models of single neuron. Dynamical and structural basis of brain activities, various biological neural models and its importance are discussed. Brief ideas of neural excitability and different modes of spiking are also addressed in this section.

Chapter 3

Chapter 3 of the thesis presents the investigation on the possibilities of couplings like linear indirect synaptic, nonlinear cubic feedback and memristor based couplings in the H-R neuron model. The nano-scale two-terminal device, memristor acts like a resistor with memory and is therefore of great interest to be used as a synapse in hardware of artificial neural networks. It is relevant to study the possibilities of different memristor couplings in neuromorphic systems. The influence of different memristor couplings such as cubic, quadratic and exponential flux controlled memristor on the neurons is investigated. The linear stability analysis for the dynamics of H–R neurons for nonlinear feedback and for various types of flux-controlled memristor couling is done. The complex behaviour of neural systems are predicted with respect to Lyapunov Exponents. The simulation results of these coupling schemes show the presence of synchronization, amplitude death, oscillation death and behavior like near death rare spikes for the neuronal systems. In most of the schemes the coupling strength summarizes information distribution between neurons. The bifurcation diagrams show the qualitative change of dynamical behaviour of neurons and maximum Lyapunov Exponent plots show the range over which neuronal behaviour is chaotic.

Chapter 4

This chapter focuses on the effect of electromagnetic radiation in nonlinear response of biological neuron systems. The nonlinear response of four variable (improved) Hindmarsh-Rose neuron model is selected and memristor is incorporated to understand the fundamental mechanisms of the network of neurons on cellular level. Memristor acts as the bridge between magnetic flux and membrane potential of the neuron. Induction of multiple modes via electrical activities of neurons is analysed with single and coupled neurons with quadratic flux controlled memristor.

H-R model is also examined under the influence of Gaussian noise. When Gaussian noise is added to the system, the oscillation death is achieved for relatively smaller magnitude of external current and it also leads to the inhibition of quiescent activity under periodic current. Hamilton energy is calculated to understand the response of action potential of the neuron to the external forcing current. It would be helpful to study the energy consumption and supply in neurons. The changes of action potential and mode of transition in electrical activities among neurons are related to Hamilton energy estimated by Helmholtz theorem. Bifurcation of Inter Spike Interval (ISI) versus current is also plotted and it exhibits denser pattern as compared with that of cubic flux based electromagnetic induction. Stability analysis of the system and electrical activities of neuron with exponential flux controlled memristor is also studied. Hence the work gives a pathway to understand influence of electromagnetic flux on the overall activity of neurons and it is established that it introduces high nonlinearity to the neuron model.

Chapter 5

Effect of field coupling and memristor on electromagnetic induction of neurons are analysed in this chapter. It is possible to analyse the synchronization and pattern selection in neuronal network under chemical or electric synapse coupling. Field coupling is regarded as a form of communication within the nervous system caused by exchange of ions between cells or as a result of local electric fields. For isolated and coupled neurons multiple modes in electrical activities are analysed for increase in the intensity of field coupling. As the external forcing current increases the system shows various dynamics such as oscillation death, tonic spiking, desynchronization and synchronization. Further it is observed that under the high coupling strength the oscillation suppression of coupled systems is achieved by high value of external current.

It is observed that for network of 300 H-R neurons, the neuron oscillators show incoherent as well as synchronization behaviour. Control inputs for the system is analysed and stability of system is confirmed by the negative value of Transverse Lyapunov Exponent plot. It is observed that under field coupling excitability of neurons can be changed and hence this coupling can produce signal exchange between neurons even if synapse is absent.

Chapter 6

The superconducting circuit, like the Josephson Junctions can also model neurons. In Josephson Junctions it is possible to sustain action potentials upto picosecond range. Based on the law of electromagnetic induction, the Josephson Junction circuit model can be improved to consider effect of electromagnetic induction by introducing the magnetic flux variable in to the model. In this chapter, the influence of memristor on the dynamic behaviour of

Josephson Junctions is examined. This adds more nonlinearity to the selected systems. It is found that dynamical behaviours and electrical modes are much dependent on magnetic flux. Here cubic flux controlled and logarithmic flux controlled memristors are selected to introduce the flux to the model. Different dynamics such as fast periodic spiking, double periodic spiking and suppression of oscillations are resulted in. Modulation of chaotic oscillation in the model can be controlled by memristor.

Further, electric activity of H-R neuron is studied on coupling with the Josephson Junction chaotic circuit based on the Lyapunov stability theory. The possibility of synchronization of the Josephson Junction neurons with that of H-R neuron model is investigated. Depending on gain coefficients different chaotic phenomena such as spiking, bursting, tonic spiking and breaking of complete synchronization are observed between the Josephson Junction and the H-R neuron. Neuromorphic computing with in the frame work of ultra fast and low energy superconducting digital circuit can be achieved using this technology.

Chapter 7

Concluding remarks and discussions are included in chapter 7.

PUBLISHED WORKS

- *"Nonlinear Feedback coupling in Hindmarsh-Rose Neurons"*, Sunsu Kurian Thottil, Rose P. Ignatius**, Nonlinear Dynamics,** Vol.87, p.1879-1899(2017). ISSN 0924-090x.
- *"Influence of Memristor and noise on H-R neurons"*, Sunsu Kurian Thottil, Rose P. Ignatius, **Nonlinear Dynamics**, Vol.95, p.239(2019). ISSN 0924-091x.
- *"Study on Electromagnetic induction on neurons through field coupling and Memristor"*, Sunsu Kurian Thottil, Rose P. Ignatius (Communicated).
- *"Study on dynamics of Josephson Junction model with Memristor and H-R neuron"*, Sunsu Kurian Thottil, Rose P. Ignatius (Communicated).
- "*Neurons under noise and Memristor based Electromagnetic induction"*, Sunsu Kurian Thottil, Rose P. Ignatius, **International conference proceedings,** IISF, WSE10604, Chennai, October 2017.
- "*Electrical modes of neurons in the presence of noise and Memristor*", Sunsu Kurian Thottil, Rose P. Ignatius, **National conference proceedings**, APS(Annual physics symposium), St. Teresa's college, Ernakulam, 5, CP18, 28-29, 2017-18. ISBN:978-93-5291-017.
- "Dynamics of Hindmarsh –Rose Neurons with Memristor coupling", Sunsu Kurian Thottil, Rose P. Ignatius, **National conference proceedings**, APS (Annual Physics Symposium), St. Teresa's college, Ernakulam, CP7, 26, 2016-17. ISBN:978-93-5291-787-7.

Minor Projects

- *"Electrical activity of neuron under Josephson Junction model"*(**ASPIRE project, Directorate of Collegiate Education, Government of kerala, 2018-19)**.
- *"Study on Electromagnetic induction on neurons"* (**ASPIRE project, Directorate of Collegiate Education, Government of kerala, 2018).**
- Presented papers in **National conferences on 'Modern Trends in Research'** organised by Teresian Research and Consultancy Cell, St. Teresa's College (Autonomous), Ernakulam, sponsored by UGC(CPE) every year from 2015 to 2019
    - *"Dynamic behavior of H-R neuron model"*, **National conference on Modern Trends in Research,** Teresian Research and Consultancy Cell, 2015, St. Teresa's College (Autonomous), Ernakulam, UGC(CPE),14th October 2015
    - "*Nonlinear feedback coupling in Hindmarsh-Rose Neurons*", **National conferences on Modern Trends in Research,** Teresian Research and Consultancy Cell, 2016, St. Teresa's College (Autonomous), Ernakulam, UGC (CPE), 16th December 2016.
    - *"Electrical modes of neurons in the presence of Noise and Memristor"*, **National conferences on Modern Trends in Research**, Teresian Research and Consultancy Cell, 2017, St. Teresa's College (Autonomous), Ernakulam sponsored by UGC(CPE), 19th October 2017.
    - "*Study on the effect of electromagnetic induction in neurons through field coupling"*, **National conferences on Modern Trends in Research,** Teresian Research and Consultancy Cell, 2018, St. Teresa's College (Autonomous), Ernakulam sponsored by UGC(CPE), 23rd November 2018.

Contents

List of Tables

List of Figurers

Chapter 1
Introduction

Introduction

The ideas of dynamical chaos have altered the understanding of the origin of random behaviour in many fields. In this section some insights on introductory ideas of nonlinear dynamics and chaotic systems are given. Chaotic systems manifest itself in a number of phenomena in both laboratory and day to day dealings. The tools for characterization of chaotic systems such as phase portraits, attractors, time series analysis and Lyapunov Exponent are explored in this chapter. The stability of dynamical systems, bifurcations and routes to chaos are also described in the following sections. Some techniques related to control and synchronization in chaotic systems are also addressed.

1.1 Brief history of chaos

Since antiquity, historians and researchers have noted the idea that small causes can sometimes have larger effects. Chaos theory has claimed the attention of scientists from 19^{th} century onwards[1]. Many complex systems can be better understood through the lens of Chaos Theory. In 1890 Henri Poincarè [2]found sensitive dependence on initial conditions in a particular case of three –body problem and later proposed that such phenomena is common in the field of meteorology. He noted that very small fluctuations in initial conditions of the system could result in very diverse outcomes. The unpredictability of the problem is due to the extreme sensitiveness to initial conditions and it gives the notion of “chaos”. Also Jacques Hadamard pointed out the divergence of trajectories in spaces of negative curvature (1898) [2,3]. In the 1800s there had been work on nonlinear oscillators in connection with models of musical instruments. In 1927 Balthazar van der pol Balthazar [4] noted occasional "noisy" behaviour in a vacuum tube oscillator circuit which is governed by a simple nonlinear differential equation.

Other significant milestones in the theory of dynamical systems were initiated after discoveries of Henri Poincarè. In the 1950's, Kolmogorov, Arnold, and Moser focused their attention on the persistence of motion of quasi-periodic oscillators and proposed the fundamental KAM Theorem[5]. The discovery and subsequent work contributed to explain the inaccuracy of long-term weather forecasting and were summarized by E. Lorenz with famous statement: “Does the flap of a butterfly’s wings in Brazil set of a tornado in Texas?” [6]. That is how the sensitivity to initial conditions (‘SIC’ness) was also known as the ‘butterfly effect’. After this major turn, research on nonlinear dynamics stepped up. In 1971, David Ruelle and Floris Takens proposed an alternative mathematical explanation of the turbulence in fluid dynamics based on the existence of strange attractors [7]. A couple of years later, Tien-Yien Li and James A. Yorke used the term chaos to describe the erratic and unpredictable behaviours arising in deterministic nonlinear maps [8]. At the same period, Mitchell J. Feigenbaum unraveled universality of behaviour occurring in a particular class of systems as they make transition to chaos, and derived the Feigenbaum constant[9].

1.2 Fundamentals of chaotic systems

1.2.1 Sensitivity to initial conditions

Chaos is aperiodic long-term behaviour of deterministic systems. It exhibits sensitive dependence on initial conditions[10]. If the trajectories of the system do not settle down to fixed points, periodic orbits or quasiperiodic orbits as time progresses, then the system exhibits aperiodic long term behaviour [10]. ‘Deterministic’ means that the systems behaviour can be determined by analytical or numerical computations. The irregular behaviour arises from the system's inherent nonlinearity[11]. “Sensitive dependence on initial conditions” (‘SIC’ness) indicates that nearby trajectories separate exponentially fast. As a

result, any error in our knowledge of the initial conditions of the system will amplify rapidly, making its behaviour effectively unpredictable.

An example of 'SIC'ness can be demonstrated using the logistic map (Figure 1.1). Let us consider the logistic map. As we plot the orbits of the map for different initial conditions, it is observed that the two orbits are initially very close. However, they quickly lose correlation and eventually seem to be entirely different from each other after some time.

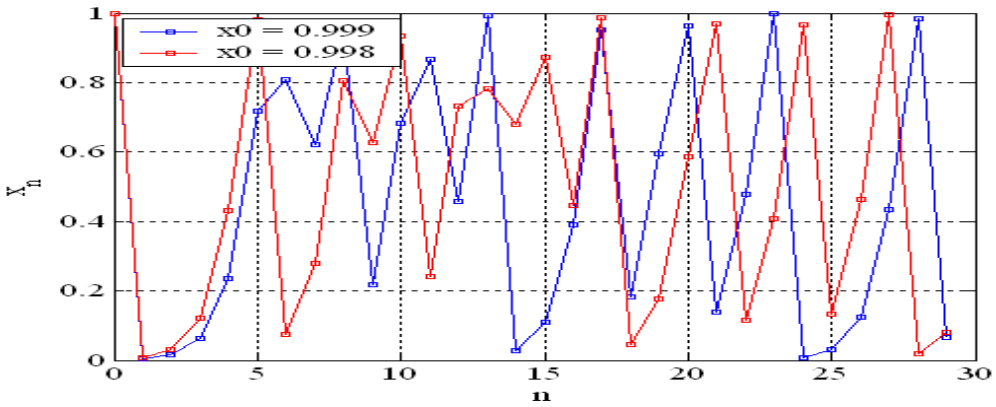

Figure 1.1: Logistic map: Sensitivity to initial conditions (adapted from [12])

1.2.2 Divergence in Phase Spae

The concept of the phase space was developed by Ludwig Boltzmann, Henri Poincaré and Willard Gibbs in the late 19th century [13]. A phase space is a space in which all possible states of the system are represented, with each possible state of the system corresponds to one unique point in the space. A plot of multiple phase curves corresponding to different initial conditions in the same phase plane is known as phase portrait. For mechanical systems, the phase space usually consists of all possible values of position and momentum variables (Figure 1.2 and Figure 1.3). Thus, for a single particle, there are three

degrees of freedom (x, y and z); and the state of the particle is defined by three position coordinates, and also by the three coordinates of the momenta.

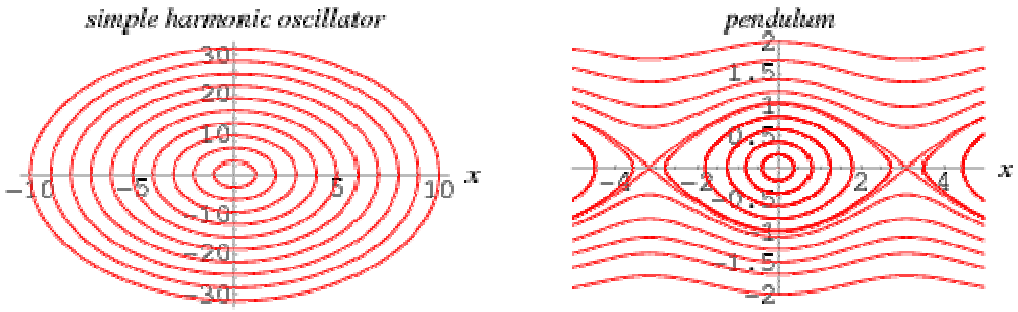

Figure 1.2: Phase portrait of SHM and for the pendulum rotations are resulted in as the energy is increased beyond a particular value (adapted from wolfram math world [14])

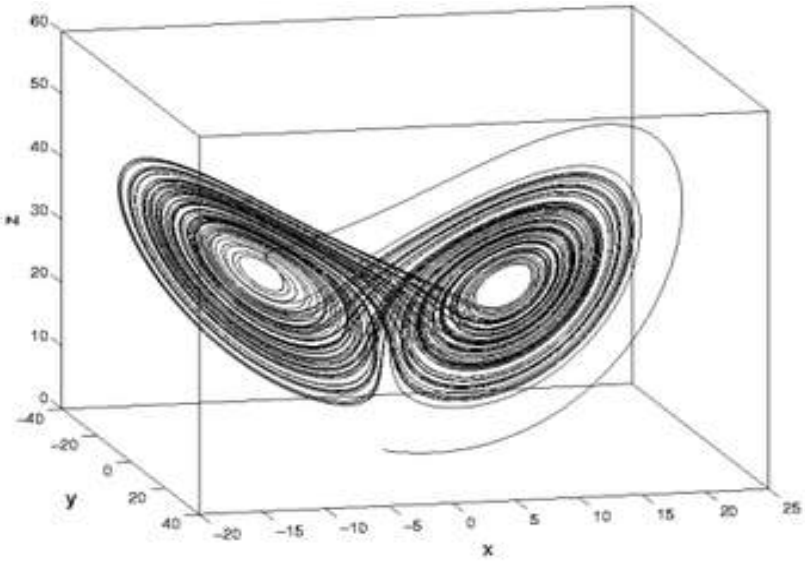

Figure 1.3: 3D phase plot of Lorenz attractor which exhibits the local and global divergence of the trajectory (adapted from[15,16])

1.2.3 Positive Lyapunov exponent

The Lyapunov Exponent (LE) or Lyapunov characteristic exponent of a dynamical system is a quantity that characterizes the rate of separation of infinitesimally close trajectories $x(t)$and $x_0(t)$ in phase space [17,18].

$$\delta x(t) = e^{\lambda t} x_0(t) \tag{1.1}$$

λ is the Lyapunov Exponent.

Lyapunov Exponent can be positive, negative or zero depending upon different orbits and this parameter decides whether the trajectory converges or diverges.

If a trajectory $x(t)$ given by the n dimensional linear ordinary differential equation, with constant coefficients

$$\dot{x} = Ax + f(t) \tag{1.2}$$

If the constant coefficient matrix A has n Eigenvalues $\lambda_1, \lambda_{2,\ldots\ldots\ldots}\lambda_n$ then the real part of n different eigenvalues are naturally Lyapunov Exponents.

The maximal Lyapunov Exponent can be written as

$$\lambda_{max} = \lim_{t\to\infty} \lim_{\delta x_0 \to 0} \frac{1}{t} ln \frac{\delta x(t)}{\delta x_0} \tag{1.3}$$

$\delta x_0 \to 0$, ensures the validity of the linear approximation at any time. It is required that the two limits cannot be exchanged, otherwise, in bounded attractors, the result would be trivially 0.

For a dynamical system with evolution equation f^t in an n–dimensional phase space, the spectrum of Lyapunov exponents $\{\lambda_1, \lambda_2, \ldots\ldots\ldots\ldots \lambda_n\}$generally depends on the starting point x_0

The Lyapunov Exponents describe the behaviour of vectors in the tangent space of the phase space and are defined from the Jacobian matrix

$$J^t(x_0) = \frac{df^t(x)}{dx}|_{x_0} \tag{1.4}$$

Where the Jacobian matrix J^t describes how a small change at point x_0 propagates to the final point $f^t(x_0)$. The limit

$$\lim_{t\to\infty}[J^t.(Transponse(J^t)]^{\frac{1}{2t}} \tag{1.5}$$

Defines a matrix $V(x_0)$. If $\Lambda_i(x_0)$ are the eigenvalues of $V(x_0)$

The Lyapunov Exponent λ_i are defined as

$$\lambda_i(x_0) = Ln\Lambda_i(x_0) \tag{1.6}$$

For a dissipative system, as criterions, it is proposed that, if the attractor reduces to

(a) Stable fixed point then all the exponents is negative;

(b) Limit cycle which indicates that an exponent is zero and the remaining ones are all negative;

(c) k-dimensional stable torus then the first k LEs vanishes and the remaining ones are negative;

(d) Strange attractor generated by a chaotic dynamics, then it implies that at least one exponent is positive.

1.2.4 Attractors

There are two types of attractors, namely, non-strange attractors and strange attractors. To which attractor does the trajectory ends up depends on the initial conditions. The closure of the set of initial conditions which approaches given attractor is called its basin of attraction. In many nonlinear systems, the boundary between basins is not smooth and has a fractal structure [19,20].

1.2.4a Non-Strange Attractors

Non-strange attractors are further classified into:-

- **Fixed point**: These are attractors whose orbits approach an equilibrium state. Here, the system converges to a single point known as the fixed point. It is stable if the particle displaced slightly away from it returns to the same point. Unstable fixed points are known as saddle points.

- **Limit cycle**: These are attractors whose orbits exhibit periodic motion. In the case of dynamical systems with two dimensional phase space, a limit cycle is a closed trajectory in the phase space having the property that at least one trajectory spirals into it as time approaches infinity or negative infinity[19]. Such behaviour is exhibited in some non linear systems. As time approaches infinity, if all the neighboring trajectories approach the limit cycle, then it is called an attractive or stable limit cycle. While on the other hand, if all the neighboring trajectories approach the limit cycle as time approach negative infinity, then it is called a non-attractive or unstable limit cycle.

- **Torus**: These are attractors whose orbits exhibit quasi-periodic motion which means it exhibits almost but not periodic motion. This means that they are the sum of periodic functions with incommensurate frequencies. It is a three dimensional doughnut shaped attractor.

1.2.4b Strange Attractor

Often, the term strange is used for attractors that show chaotic nature. But it is not necessary that an attractor should be chaotic in order to be called strange even though most of the strange attractors exhibit chaotic behaviour. An attractor is strange if it has a fractal structure [21]. In other words, if an attractor has a fractal attracting set, it is called a strange attractor. They are characterized with positive Lyapunov Exponent, which indicates exponential divergence of the trajectories. Another important feature is that they have three or more than three degrees of freedom. If a strange attractor is chaotic i.e., if it exhibits sensitivity to initial conditions, then any two arbitrarily close initial points on the attractor, after various number of iterations will be very far apart from each other. But after number of various iterations, it will lead to points that are arbitrarily close together. Thus a chaotic attractor associated with a dynamic system is said to be locally unstable but globally stable. The term strange attractor was put forward by David Ruelle and Floris Takens[21,22] to describe the attractors resulting from a series of bifurcation of a system that described fluid flow. Examples of strange attractors include the double scroll attractors, Hénon attractor, Rössler attractor, Tamari attractors and the Lorenz attractor (Figure 1.3)[15-24].

1.2.5 Bifurcation

The change in the qualitative character of a solution as a control parameter varied, is known as bifurcation[25]. This occurs where a linear stability analysis yields instability.

In the case of a dynamical system, its behaviour is influenced by the value of control parameters and this change in behaviour is studied by making use of the bifurcation plots of the system. The control parameters could be the amount of strength of an interaction, the amplitude and frequency of a periodic perturbation or some other quantity. The control parameters may suddenly change a stable equilibrium position into two such positions, or a system initially at rest may set into oscillations. This phenomenon of additionally arising solutions or solutions that all of a sudden changes its character is called bifurcation or branching. In brief, bifurcations are the most observed transitions in the dynamical system as the control parameter is varied.

There are local and global bifurcations. If the behaviour of a system in the neighborhood of an equilibrium solution is changed, it is called a local bifurcation. If the structure of the solutions is modified on a larger scale, it is called global bifurcation. Bifurcation from a steady solution with linear analysis predicts existence of two possible classes of behaviour as a single control parameter is changed. If complex conjugate pair of eigenvalues passes through the imaginary axis in the complex plane, then it is Hopf bifurcation. It is also possible to get bifurcation from periodic solution.

1.3 Routes to Chaos

Nonlinear systems can exhibit various dynamics apart from chaotic ones (If the dimension is large enough). This diversity and the transitions occurring

between each of them can be probed by varying one or several system's parameters is called bifurcation parameters. This makes it possible to observe a cascade of bifurcations to stable attractors until a strange attractor is reached. This is called a route to chaos. In the literature, the routes to chaos are graphically represented by a bifurcation diagram. Here the system's output is plotted as a function of the bifurcation parameter. The most commonly used scenarios are Intermittency route to chaos, Quasiperiodic route to chaos, and Period-doubling route to chaos.

Intermittency route to chaos

Here a single bifurcation is responsible for the alternation (or intermittence) of zones of chaotic motion with zones of smooth regular motion[26]. As the bifurcation parameter increases, the turbulent zones last longer and eventually, above a critical threshold, the system is always turbulent (or chaotic). Intermittency can be seen in Rayleigh-Bernad convention and in stirred chemical reactions.

Quasi-periodic route to chaos

It is also called the Ruelle-Takens-Newhouse route to chaos. It consists of the following succession of three bifurcations when the bifurcation parameter is steadily increased: First, a Hopf bifurcation that leads to a stable limit-cycle of period T, second a Torus bifurcation that leads to a quasi-periodic dynamics with two incommensurate frequencies associated with a torus attractor T2, and finally a last bifurcation turns the torus T2 into a new attractor T3 with three incommensurate frequencies, which rapidly destabilizes into a strange (chaotic) attractor. This type of transitions can be observed inconvection and solid state experiments.

Period-doubling route to chaos

It is also called Feigenbaum route to chaos. Here a steady state is first destabilized through a Hopf bifurcation resulting in a limit cycle of period T. Then, this limit cycle undergoes a cascade of period-doubling bifurcations until the n−th limit cycle of period 2nT destabilized and the strange attractor becomes stable. Period doubling cascades can be observed in fluid convention, in nonlinear circuits and in lasers.

1.4 Stability Analysis

The stability theory helps to draw conclusions about the behaviour of a system without actually computing its solution trajectories. The first person to study stability in the modern sense was Lagrange (1788)[26], who analyzed mechanical systems with Lagrangian mechanics. One of his conclusions was that, in the absence of external forces, an equilibrium of a conservative mechanical system is stable if it corresponds to a minimum of the potential energy. The Russian mathematician A. M. Lyapunov(1892), introduced the basic definitions of stability that are in use today which was helpful to prove many of the fundamental theorems.

Lyapunov stability[27] is concerned with the behaviour of the trajectories of a system when its initial state is near an equilibrium. From a practical viewpoint, this issue is very important because external disturbances such as noise, wind, and component errors are always present in a real system to knock it out of equilibrium. The Lyapunov theory is an indispensable tool in the analysis and synthesis of nonlinear systems. Lyapunov theory abounds in a variety of notions of stability namely: stability, asymptotic stability and exponential stability.

For a continuous system,

A vector $x_e = 0$ is an equilibrium point if

$$f(x_e)=0 \tag{1.7}$$

Several types of stabilities can be described as follows

- **Lyapunov stability**

An equilibrium point x_e is stable in the Lyapunov sense if for all $\varepsilon > 0$, there exist $\delta(t_0, \varepsilon)$ such that

$$\forall t > t_0 \,, \| \; x(t_0) - x_e \; \| < \delta(t_o, \varepsilon) \; \Rightarrow \| \; x(t) - x_e \; \| < \varepsilon \tag{1.8}$$

It guarantees that the trajectory of the system in phase space will remain in the vicinity of the equilibrium point if the initial state belongs to this vicinity. If δ does not depend on t_0, the stability is said to be uniform.

- **Asymptotic stability**

An equilibrium point is asymptotically stable if

$$\| \; x(t_0) - x_e \; \| < \delta(\varepsilon) \; \Rightarrow \| \; x(t) - x_e \; \| < \varepsilon \tag{1.9}$$

Asymptotic stability includes the Lyapunov stability, but it imposes for all trajectories initiated in the neighborhood of the equilibrium point to converge asymptotically to it.

A system is globally asymptotically stable if for all trajectories $x(t)$,

$$\lim_{t\to\infty} \| \; x(t) - x_e \; \| = 0 \tag{1.10}$$

here the system has a unique equilibrium point.

A major inconvenience with the definition of stability is that it requires to find the the system's trajectory.

- **The direct method of Lyapunov stability analysis**

It is also called the second method of Lyapunov stability analysis which allows to determine the stability of the system without explicitly integrating the differential equation

$\dot{x} = f(x,t)$ where $x(t_0) = x_0$ (1.11)

If there is some measure of energy in a system, it is possible to study the rate of change of energy of the system to ascertain stability.

- **The indirect method of Lyapunov stability analysis**

This method uses the linearization of a system to determine the local stability of the original system

Table 1.1 Summary of basic theorem of Lyapunov[27]

	Conditions on V(x,t)	Conditions on -$\dot{V}$(x,t)	Conclusion
1	Locally positive definite functions (lpdf)	≥ 0 locally	Stable
2	lpdf, decreasing	≥ 0 locally	Uniform stable
3	lpdf, decreasing	lpdf	Uniformly asymptotically stable
4	pdf, decreasing	pdf	Globally uniformly asymptotically stable

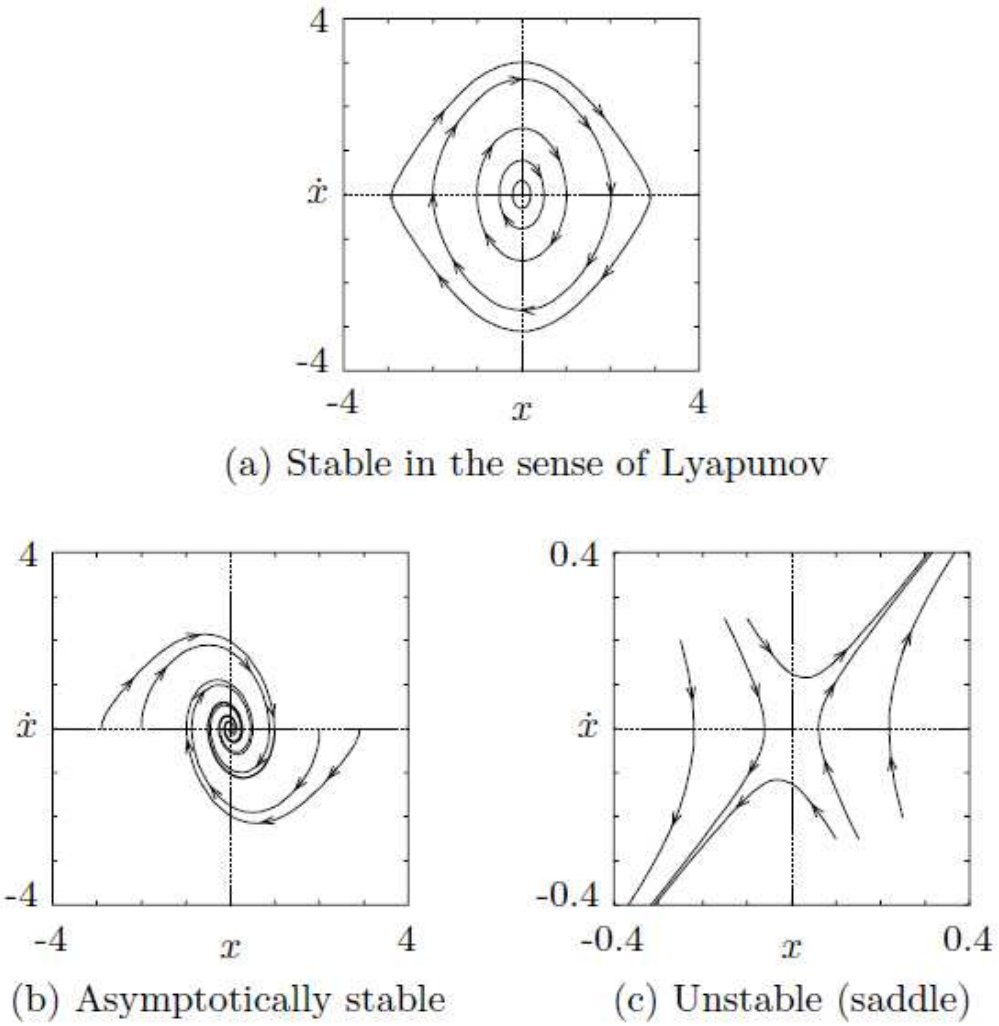

Figure 1.4: Phase portraits for stable and unstable equilibrium points (adapted from[27])

- **Transverse Lyapunov exponents**

When the chaotic systems are coupled they may exhibit identical oscillations with the onset of synchronization. There are several methods for investigating the synchronization problems. One of the method is based on conditional Lyapunov Exponents which are calculated along the typical

trajectory of the system[28]. This is also known as global Transversal Lyapunov Exponent. When all global Transversal Lyapunov Exponents of system driven by the signal are negative then the systems synchronize.

In the presence of noise, in the neighborhood of unstable periodic orbits there may exist regions where trajectories may be pushed away from synchronization subspace. Such situation occurs when one of the Lyapunov Exponents associated with the measure supported by the periodic orbit is positive. Small noise could force the trajectory to enter such a region.

Another method to check the possibility of the synchronization is based on Transversal Lyapunov Exponents which are computed along periodic orbits[29,30]. In order to ensure synchronization one should compute Transversal Lyapunov Exponents for all periodic orbits and check whether they are negative[29,30]. This is a difficult task. Even if a periodic orbit attracts the trajectory to the synchronization space it is possible that it repels trajectories locally. If all the eigen modes corresponding to the eigenvalues are in the range of negative Transverse Lyapunov Exponent, then the corresponding synchronous state is stable.

Lyapunov exponents $\lambda_i(x)$ of a trajectory based at x are the logarithms of the eigenvalues of the matrix[30]

$$\Lambda(x) = \lim_{L\to\infty}([T^L(x)]^T T^L(x))^{\frac{1}{2L}} \tag{1.12}$$

For discrete systems

$$T^L(x) = DF\left(F^{L-1}(x)\right) \dots\dots\dots DF\left(F(x)\right)DF(x) \tag{1.13}$$

It is the composition of L Jacobians. For continuous system $T^L(x)$ is the matrix of partial derivatives of the time –L map induced by the continuous time system.

Local Lyapunov Exponents $\lambda_i(x, L)$ are the logarithms of the eigen values of the matrix

$$\Lambda(x, L) = ([T^L(x)]^T T^L(x))^{\frac{1}{2L}} \tag{1.14}$$

Local Lyapunov Exponents shows how rapidly perturbations of the initial point x changes in L steps from the moment of perturbation[30].

Local Transversal Lyapunov Exponents are the local Lyapunov Exponents corresponding to eigenvectors transversal to the synchronization subspace[30]. It tells how trajectories of the coupled system are repelled or attracted to the synchronization subspace in time L.

Global Transversal Lyapunov Exponents, which are frequently used for the investigation of synchronization gives stability information which is averaged over the whole attractor.

1.5 Control of chaos

Control of chaos is a process where a very small perturbation is applied to a chaotic system. It helps to realize a desirable chaotic, periodic, or stationary behaviour[31]. Certain techniques employed for controlling chaos are feed-forward ('non-feedback'), control based on periodic excitation of the system, the 'Ott-Grebogi-Yorke method' (based on the linearization of the Poincaré map), the 'Pyragas method' (based on a time-delayed feedback) and the traditional control-engineering methods including linear, nonlinear and adaptive control[31].

1.5.1 Control goals: stabilization

A typical goal for control of chaotic systems is stabilization of an unstable periodic solution (orbit). Let x(t) be the T-periodic solution of the free system with initial condition $x(0) = x_0$ i.e, $x(t+T) = x_*(t)$ for all $t \geq 0$. If the solution $x_*(t)$ is unstable, then the stabilization solution will fulfill the condition

$$\lim_{t\to o}[x(t) - x_*(t)] = 0 \tag{1.15}$$

Let there is a driving output $y(t)$ to the desired output $y_*(t)$

$$\lim_{t\to o}[y(t) - y_*(t)] = 0 \tag{1.16}$$

For any solution x(t) there exist an initial solution $x(0) = x_0$ such that $x(0) = x_0 \in \varphi$. Where φ is the given set of initial conditions.

A control function can be foundin either open loop(feed forward) control

$$u(t) = U(t, x_o) \tag{1.17}$$

Or in the form of state feedback

$$u(t) = U\big(x(t)\big) \tag{1.18}$$

Or in output feedback

$$u(t) = U\big(y(t)\big) \tag{1.19}$$

inorder to ensure the equations (1.15) and (1.16).

This is the method of tracking problem for control theory. The key feature of the control of chaotic systems is to achieve goals by means of

sufficiently small control. A special case of above mentioned case is stabilization of unstable equilibrium of the state x_{*0} where stabilization should satisfy the equation $F(x_{*0}, 0) = 0$. Here additional restrictions such as small control solutions are used. This method even can be used for a simple pendulum, where nonlocal solutions of the stabilization problem with small control are nontrivial. The control laws also can be extended by introducing dynamic feedback described by differential or time-delayed models.

1.5.2 Methods of control of the chaotic processes

1.5.2a OGY Method

E. Ott, C. Grebogi and J. A. Yorke [33] were the first to make the key observation that the infinite number of unstable periodic orbits typically embedded in a chaotic attractor can be used for the purpose of achieving control by means of applying only very small perturbations. It is possible to get information about the chaotic system by analyzing a slice of the chaotic attractor. This slice is a Poincar*é* section. The information about the section has been gathered, then the system is allowed to run and wait until it comes near a desired periodic orbit. Later, the system is made to remain on that orbit by perturbing the appropriate parameter. When the control parameter is changed, the chaotic attractor is shifted and distorted. The new attractor helps the system to continue on the desired trajectory. This method does not require a detailed model of the chaotic system but only some information about the Poincaré section.

1.5.2b Pyragas method

In this method[33], an appropriate continuous controlling signal is injected into the system, for stabilizing a periodic orbit. Its intensity is

practically taken as zero when the system evolves close to the desired periodic orbit. But intensity increases when it drifts away from the desired orbit.

1.5.2c Adaptive Track control method

This method is a recursive design methodology for controller design[34]. It constructs associated Lyapunov functions and feedback control laws. The controller is selected such that it must adapt to a controlled system. The parameters may vary, or initially are uncertain. Its main purpose is to design the adaptive laws and virtual control functions to counteract the unknown nonlinearity of the system.

1.6 Synchronization

Synchronization of chaos may occur when two, or more, dissipative chaotic systems are coupled. Chaotic systems with positive Lyapunov Exponents resist synchronization phenomena. Synchronization occurs when the driving system loses its own dynamics and follows those of external force [4,35]. Quantitatively this can be measured by the largest Lyapunov Exponent: a negative exponent indicates synchronization. The stability of synchronization for coupled systems can be determined by master stability.

1.6.1 Synchronization by periodic forcing

In many systems chaos disappears if a periodic external force with sufficiently large amplitude is applied. Here synchronization means that periodic forced oscillations are observed instead of chaos. For very strong forces, dependence on the amplitude and frequency of the forcing does not follow any general rule. In the driven system the attractor is a limit cycle, so the

relation between driven and driving variables can be represented by a smooth function.

For example for periodically driven Lorentz system, periodic regimes are observed only if the amplitude of forcing is larger than critical value of parameter.

1.6.2 Synchronization by noisy forcing

Synchronization by external noise means that the system forgets its own dynamics and its own initial conditions and it follows the driving noise. For a particular system where the synchronization transition is not seen, it can be observed if a replica of system is considered. If the two identical systems which are having different initial conditions but are driven with the same noise, the synchronization is set in[4,35]. For the positive Lyapunov Exponents, the system trajectories will follow their initial conditions and will remain different. But for negative exponents they forget their initial conditions and approach each other, ie synchronization occurs.

Synchronization by common noise occurs without any direct interaction between the oscillators and is independent of number of oscillators. The same effect can be observed for any large ensemble of identical nonlinear systems driven by same noise. All systems will synchronize provided the Lyapunov Exponent is negative.

1.6.3 Synchronization by chaotic forcing

Complete synchronization, smooth and non- smooth Generalized synchronization, and Generalized synchronization by quasi periodic driving are examples of chaotic forcing. Complete synchronization via chaotic forcing is possible only when the system possesses a symmetry, so that a regime where all

variables of driven and driving systems are equal is possible. When the state of driven system is completely determined by the state of driving system, it is possible to use generalized synchronization[4]. If the driving force is described by a torus in phase space, then driving system can behave quasi periodically, then trajectories lies on a torus in enlarged phase space. This leads to strange nonchaotic attractor. It has negative largest Lyapunov Exponent but is fractal.

1.6.3.1 Different types of chaos synchronization

1.6. 3.1a Generalized Synchronization

This type of synchronization is observed when the coupled systems are completely different. The driven (slave) and the driving (master) systems can be represented by a one to one mapping given by,

$$y(t) = \varphi(x(t)) \tag{1.20}$$

Here, the trajectory of attracter in one system given by $x(t)$ transforms the trajectory of attracter in next system $y(t)$by the transformation φ[36]. Thus, $y(t)$can be determined if the evolution of the drive system is known. Once the two systems get synchronized, the difference in trajectories, with respect to time, reduces to zero. i.e.,

$$\lim_{t\to\infty}(x(t) - \varphi\big(x(t)\big) = 0 \tag{1.21}$$

1.6.3.1b Complete Synchronization

If the synchronization is displayed by coupled identical systems, then such synchronization is known as complete synchronization. Here, there is an equality of the state variables leading the synchronization. It is also known as identical or conventional synchronization[37]. Such systems show strong

coupling strength. This was the first recognized type and is the simplest one in chaotic synchronization provided with negative valued Lyapunov Exponents where the coupling is unidirectional. This is a special case of generalized synchronization where function φ becomes unity.

However, this is not the case with non-identical systems. Complete synchronization is not observed in such systems. Instead, phase synchronization and lag synchronization are observed in such systems.

1.6.2.1c Phase Synchronization

In phase synchronization, all the phases are locked while amplitudes are least affected and chaotic. This was first observed in the R$\ddot{o}s$sler system and can be simulated by a very weak external force. If m, n are integers and α, β represent the phases belonging to two different systems, then

$$m * \alpha - n * \beta = c \tag{1.22}$$

where c is a constant which represents phase synchronization relation between the two systems. This shows that, if either the phases change in the same way or if a constant ratio exists between the two, phase synchronization occurs. That means, perfect phase synchronization between two coupled oscillators will occur when the chaotic oscillators are phase coherent[4,36,37]. Phase synchronization finds application in neuroscience, laser technology etc.

1.6.3.1d Lag Synchronization

Phase synchronization is the weakest of all and it is achieved at very low coupling strengths. At larger values of coupling strengths, non identical systems may exhibit other types of synchronization also. An example for this is the lag synchronization. Lag synchronization lies intermediate to both phase

synchronization and complete synchronization. Here, both the phases and amplitudes are entrained but there is a time lag between the master and the slave. The two chaotic systems become indistinguishable in time, when shifted by a proper time lag. With a slight increase in the strength of coupling, complete synchronization can be achieved [4].

1.6.1.1.e Anti-Synchronization

Anti-synchronization occurs when the state variables of the both the driving and driven systems are the same in magnitude but opposite in sign. The synchronization which was first observed by Huygens in pendulums was of this kind [35]. They are characterized by the disappearance of certain relevant state variables that evolve in time. In this case, the relation between the slave, $y(t)$, and the master, $x(t)$, is given by,

$$y(t) = -x(t) \tag{1.23}$$

Under anti-synchronization,

$$\lim_{t\to\infty}(x(t) - \big(-x(t)\big) = 0 \tag{1.24}$$

1.6.3.1f Hybrid Synchronization

In hybrid synchronization of two chaotic oscillators, one part of the system is completely synchronized while the other part is anti- synchronized. Here, complete and anti-synchronization coexist in the process of synchronization [35].

1.7 Some Applications of Chaos

Chaos theory has successfully explained various phenomena in the natural sciences. There has been rapid and successful application of chaos

theory to mechanical systems, electrical circuits, lasers, chemical reactions due to the recent theoretical prediction that chaotic physical systems might be controllable with small perturbations[38]. The application of chaos theory to the physical and chemical sciences has resolved many problems, such as how to calculate a turbulent event in fluid dynamics or how to quantify the pathway of a molecule during Brownian motion.

Many unresolved problems are present in biology and medicine, such as how to predict the occurrence of lethal arrhythmias or epileptic seizures. In such cases, we can quantize the chaotic system, such as the nervous system, by calculating the correlation dimension of a sample of the data that the system generates. In chaos theory, the correlation dimension is a measure of the dimensionality of the space occupied by a set of random points, often referred to as a type of fractal dimension[38]. For biological systems, the point correlation dimension does not presume stationarity of the data. So it can track transient non-stationarities which occur when the system changes state. These types of non-stationarities arise during normal functioning (event related potential) or in pathology (epilepsy or cardiac arrhythmogenesis). The Point correlation dimension of a data can specify which patients will manifest sudden death [38].

Chaotic systems are deterministic. Hence there is greater sensitivity and specificity of the dimensional measures. It can be used for quantifying the time series. This accuracy in quantifying time series appears to be significant in detecting pathology in biological systems. Also the use of deterministic measures lead to breakthroughs in the diagnosis and treatment of some medical disorders. Chaos and its concepts are recently applied to psychology by researchers from the perspective of cognitive, developmental and clinical psychology[38].

Chapter 2
Neurons and Neuronal Dynamics

Chapter 2

Neurons and Neuronal Dynamics

Experimental and theoretical approaches of neuron dynamics for understanding the brain and its behaviour is an interesting research area. There are as many as 10^{11} neurons in the human brain, and each can have more than 10, 000 synaptic connections with other neurons. The applications of nonlinear dynamics to the study of brain activity began to flourish in the 1990s. Neuronal dynamics is fundamental for all aspects of mental activities such as perception, cognition and emotion since the main features of brain activity is always associated with the continuous change of the underlying brain states(even in a constant environment).

2.1 Elements of a Neuron

Neurons are the elementary processing units in the central nervous system, which are connected to each other in an intricate pattern. The ability to perceive surroundings – to see, hear, and smell what's around – depends on nervous system. The nervous system triggers involuntary responses. For example, increase in heart rate and blood flow to muscles, cope with danger etc. All of these processes depend on the interconnected cells.

The brain is made up of many types of cells, including neurons, neuroglia and Schwann cells[39]. The latter two types make up almost one half of brains volume, but neurons are key elements in signal processing. Neurons generate electrical signals called action potentials, which is quickly transmit information over long distances. Glia cells are also essential to nervous system functions, but they work mostly as supporting the neurons. They are required for energy supply and structural stabilization of brain tissue.

The ideal spiking neurons (Figure 2.1) have three distinct parts namely dendrites, soma, and axon. Dendrites play the role of input devices and collect signals from other neurons and transmit them to soma. The 'central processing unit' soma performs important non-linear processing step. If the total input to soma exceeds a threshold value, corresponding output signal is generated. The output signal is taken over by the axon which delivers the signal to other neurons.

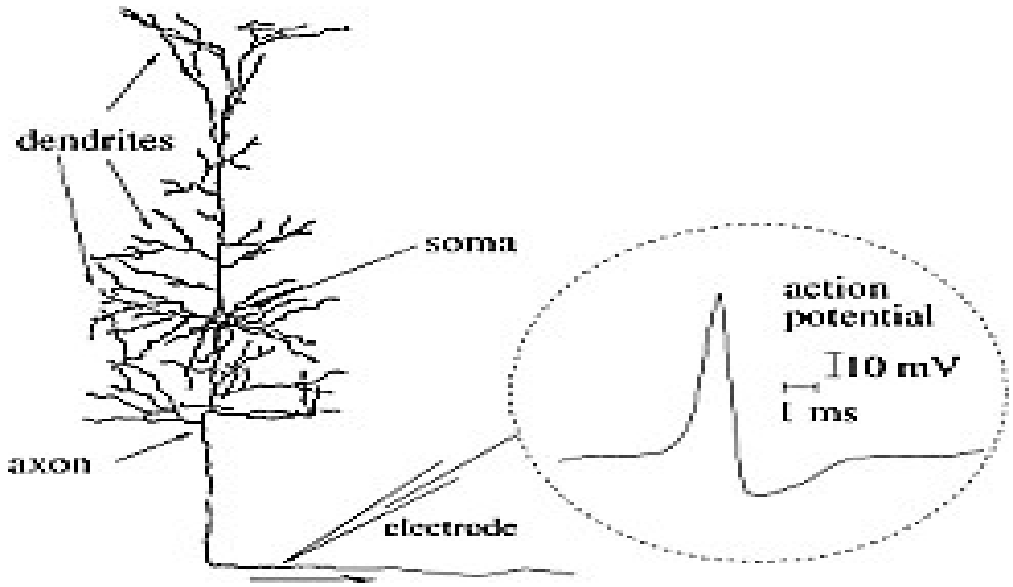

Figure 2.1: Ideal spiking neurons[adapted from elements of neuronal systems [39]]

A typical neuron receives inputs from other neurons and sends a signal (presynaptic cell) across a synapse which is received by another neuron (the postsynaptic cell). The electrical transmembrane currents produced by inputs change the membrane potential of the neuron. The change in synaptic currents produce postsynaptic potentials (PSPs)[40]. Small currents result in small PSP

s. The larger currents can produce postsynaptic potentials which can be amplified by voltage gated channels and cause the initiation of action potentials.

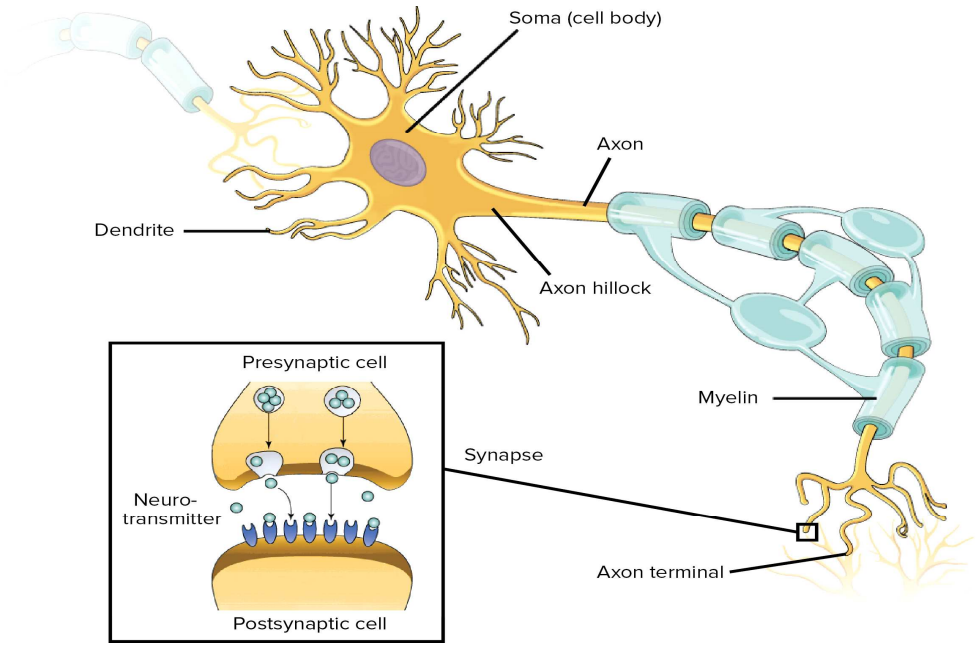

Figure 2.2: Basic structure of neuron (adapted from Neurons Boundless Psychology-Lumen Learning [courses lumenlearning.com])

A single neuron in vertebrate cortex often connects to more than 10^4 postsynaptic neurons. Many of its axonal branches end in the direct neighborhood of the neuron, here the axon can also stretch over several centimeters. So abrupt and transient changes of membrane voltage propagate to reach neurons in other areas of the brain.

2.2 Neuron as dynamical system

The coordination between brain and different organs is made possible with the help of neurons through electrical impulses. This means, every time an

input stimulus is given to a living body, brain initiates a propagating change in the membrane potential that essentially brings out the response to the stimuli.

2.2.1. Ionic mechanisms

Action potentials play an important role among the many mechanisms for communication between neurons. They are abrupt changes in the electrical potential across a cell's membrane and can propagate in essentially constant shape away from the cell body along axons.

Action potentials can be sustained by ionic currents through the cell membrane. The ions most involved are Sodium (Na+), Calcium (Ca++) and Potassium(K+). In the simplest case, an increase in the membrane potential activates (opens) Na+ and/or Ca++ channels, resulting in rapid inflow of the ions which further increases in the membrane potential[41,42]. Here positive feedback leads to sudden and abrupt growth of the potential. This triggers a relatively slower process of inactivation (closing) of the channels and/or activation of K+ channels. It leads to increased K+ current and it eventually reduces the membrane potential. These simplified positive and negative feedback mechanisms are responsible for the generation of action potentials[43]. There are more than a dozen of various ionic currents having diverse activation and inactivation dynamics and occurring on disparate time. Any combination of them would result in interesting nonlinear behaviour such as neural excitability.

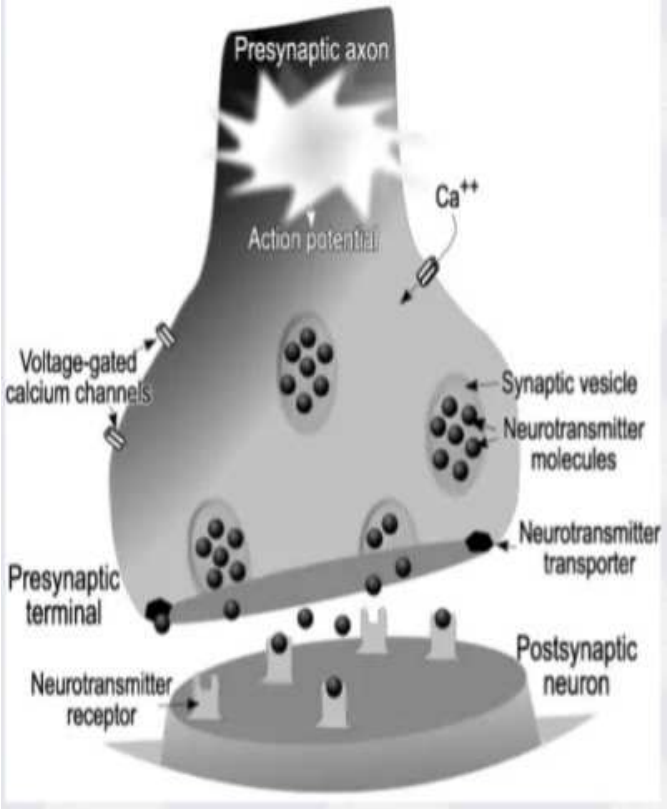

Figure 2.3: Impulse transmission among nervous system[adapted from[43]]

The inside of a neuron cell is approximately 70 millivolts more than that of outside(-70 mv). This can vary by neuron type and by species. The following Figure 2.4 shows the resting membrane potential, depolarization and hyperpolarization mechanisms in neurons.

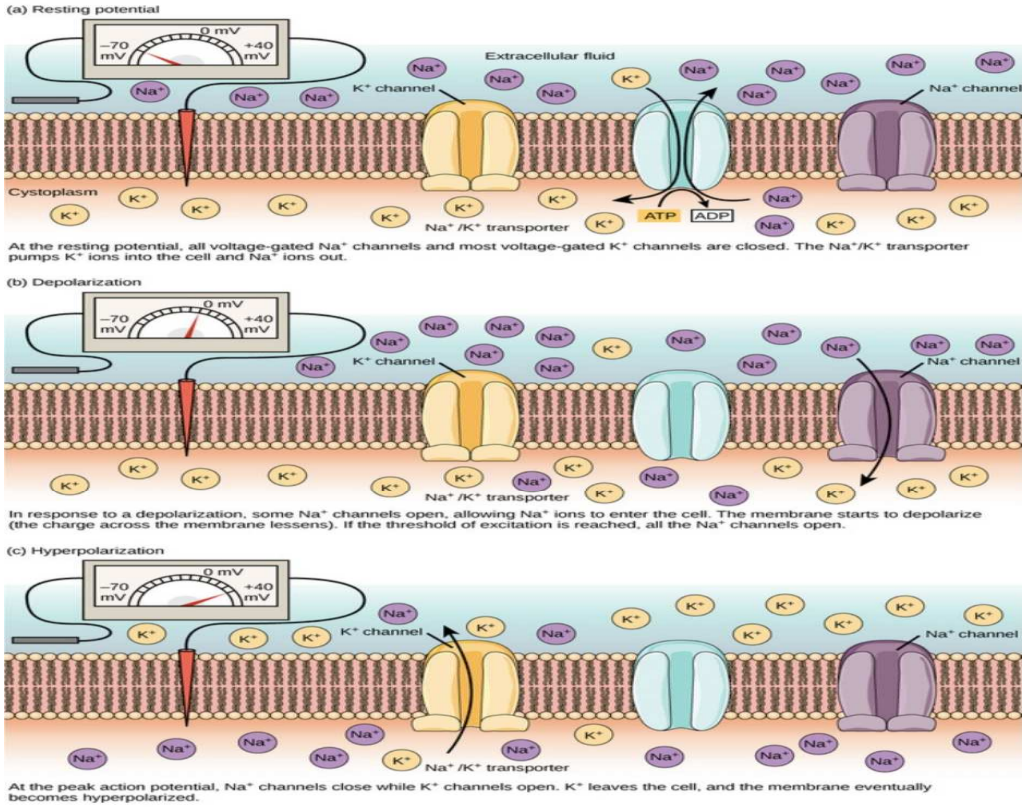

Membrane potential: The (a) resting membrane potential is a result of different concentrations of Na+ and K+ ions inside and outside the cell. A nerve impulse causes Na+ to enter the cell, resulting in (b) depolarization. At the peak action potential, K+ channels open and the cell becomes (c) hyperpolarized.

Figure 2.4: Mechanisms of Resting potential, depolarization and hyperpolarization among nervous system (Adapted from[43])

2.2.2 Dynamical mechanisms

A neuron is quiescent if its membrane potential is at rest or exhibits small amplitude(sub threshold) oscillations. In dynamical point of view this corresponds to the system residing at equilibrium or to a small amplitude limit cycle attractor. All the inward current causing depolarization will be balanced by the hyperpolarizing outward currents. If the neurons remain quiescent in spite of all the small perturbations, we can conclude that the equilibrium point is stable. A neuron is said to be excitable if a small perturbation away from a quiescent state can result in a large excursion of its potential before returning to quiescence. Here large excursions exist because the quiescent state is near a bifurcation.

2.2.2.1 Periodic spiking

Neurocomputational properties of cell depend on bifurcations of large amplitude limit cycles which corresponds to periodic spiking. This differs from bifurcations of quiescent states. When limit cycle is about to disappear or if it loses stability through subcritical flip bifurcations, there is a coexistence with stable quiescent state[44]. So weak perturbation having appropriate timing can shut down periodic spiking prematurely**.**

- **Tonic and phasic spiking**

Tonically spiking cells fire continuous trains of action potentials for the duration of the depolarizing pulse of injected current[Figure 2.5(A)]. While phasically spiking cells respond to a sustained depolarizing current pulse with a very brief train of action potentials followed by no further firing[Figure 2.5(B)].

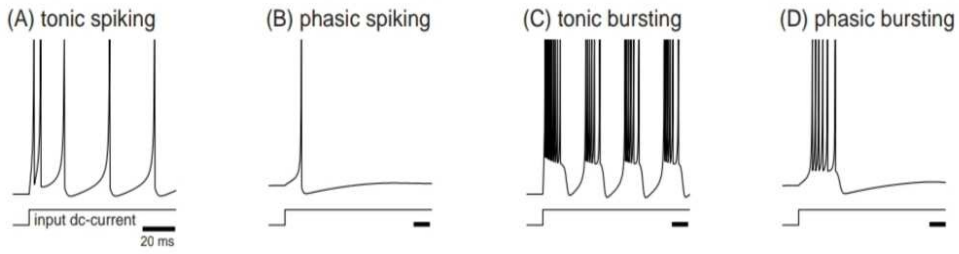

Figure 2.5: Various spiking and bursting patterns in response to a sustained depolarizing pulse(adapted from[45]).

2.2.2.2 Bursting

When neuron activity alternates between a quiescent state and repetitive spiking, it is termed as bursting. It is usually caused by a slow voltage or calcium dependent processes that can modulate fast spiking activity[44,45]. There are mainly two important bifurcations associated with bursting such as bifurcation of quiescent state that leads to repetitive spiking and bifurcation of a spiking attractor that leads to quiescence.

Sometimes neurons use rapid clusters of two or more action potentials, called bursts, as basic signaling events instead of simple spikes. Examples of tonic bursting and phasic bursting are shown in Figure 2.5(C) and Figure 2.5(D).

Some of the other commonly occurring firing patterns are shown in Figure 2.6

- Regular spiking (RS)

It is a tonic spiking with possible adapting frequency that present a stationary firing rate in response to a sustained depolarizing pulse[45]. This firing pattern is the most spread among excitatory neurons.

- Intrinsically bursting (IB)

Here neurons respond with bursts of action potential at the beginning of a strong depolarizing injection, followed by tonic spiking.

- Chattering (CH)

This corresponds to high frequency bursts with a relatively short interburst period. This behavior has mainly been observed in layer III Purkinje cell.

- Fast spiking (FS)

It is a high frequency tonic spiking with little adaptation, observed in inhibitory cells. Fast spiking cells exhibits irregular spiking when injected with weak current.

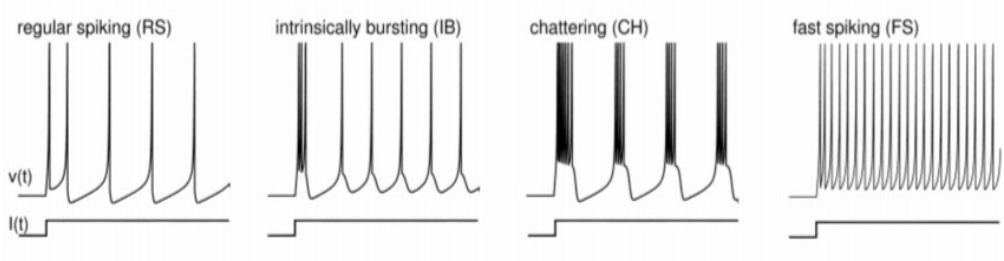

Figure 2.6: Firing patterns of regular spiking, Intrinsically bursting, Chattering and Fast spiking(adapted from[38])

2.2.2.3 Neuronal Excitability

Neuronal excitabilities behave as the basic dynamics related to the transitions between firing and resting states. These types of neuronal electronic activities play important roles for achieving biological functions of nervous systems such as information encoding, transmission and processing. In 1948,

Hodgkin[46] distinguished different firing frequency responses of resting state to external constant depolarization current simulations.

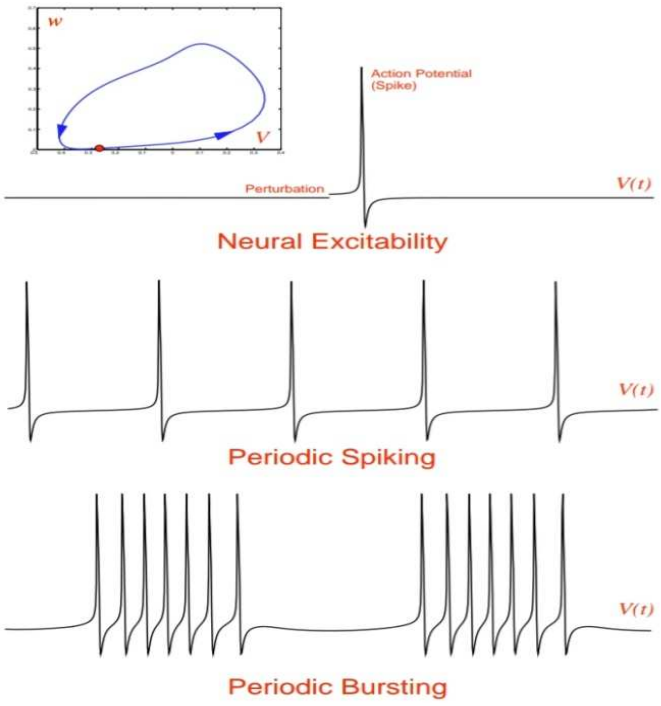

Figure 2.7: Neural excitability, periodic spiking and bursting (adapted from [38]).

There are different excitabilities according to the frequency of emerging firing. If the action potentials are generated with arbitrarily low frequency (5Hz-150 Hz), it is termed as Class 1 neural excitability. Here frequency increases with increase of current[47]. For Class 2 neural excitability the action potentials generated in a certain frequency band that is relatively insensitive to changes in the strength of applied current. Here firing frequency switches from 0 to a nearly fixed value (75 Hz-150 Hz).

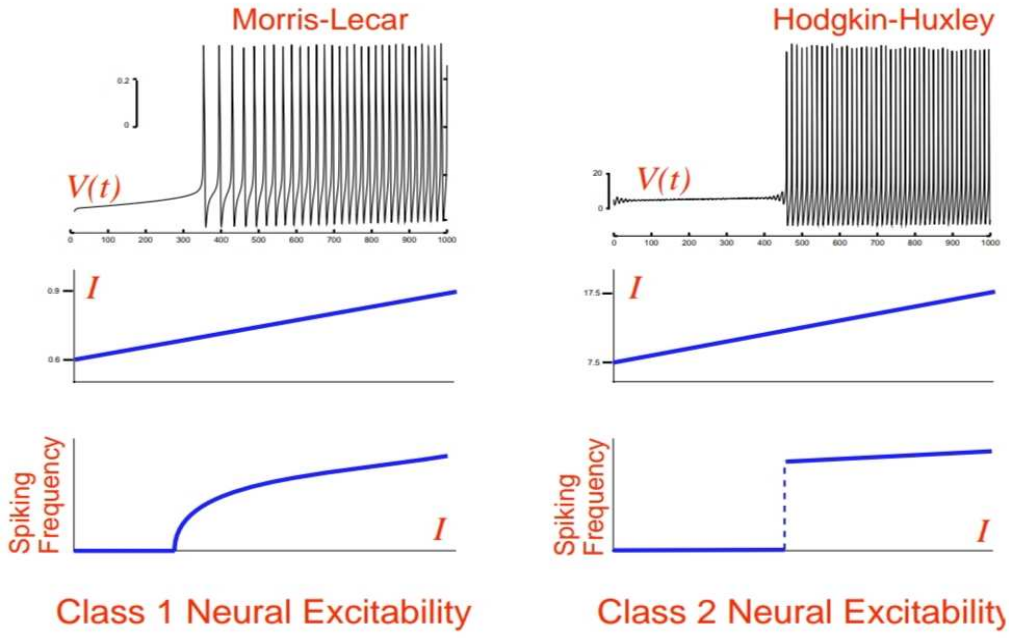

Figure 2.8: Transition from rest to repetitive spiking in Morris-Lecar and Hodgkin-Huxley models when the strength of applied current increases[47].

Class 1 and Class 2 neurons can also exhibit different phase and frequency responses, different coefficient of variations, or different histograms of interspike intervals to noise etc. Neuronal excitabilities can affect spatiotemporal behaviour of the nervous system. Pyramid neurons in hippocampus exhibits Class 1 excitability. Interneurons in the neocortical and entorhinal cortex manifest the excitability of Class 2.

Class 1 excitability corresponds to a resting state (stable equilibrium) changed to firing (limitcycle) through saddle node bifurcation as the depolarization current increases. The classes of spiking corresponding to bifurcations of the limit cycle combined with the classes of excitability help for understanding the dynamics of transitions between resting and firing states[48].

A fundamental property of the neurons is excitability illustrated in Figure 2.6. Small perturbation results in small departures from the equilibrium. It is denoted as postsynaptic potential. Larger perturbations are amplified by the neuron's intrinsic dynamics and cause initiation of the spike response. If a sufficiently strong current injected into the neuron, it will bring to a pace making mode and hence exhibits periodic spiking activity[38].

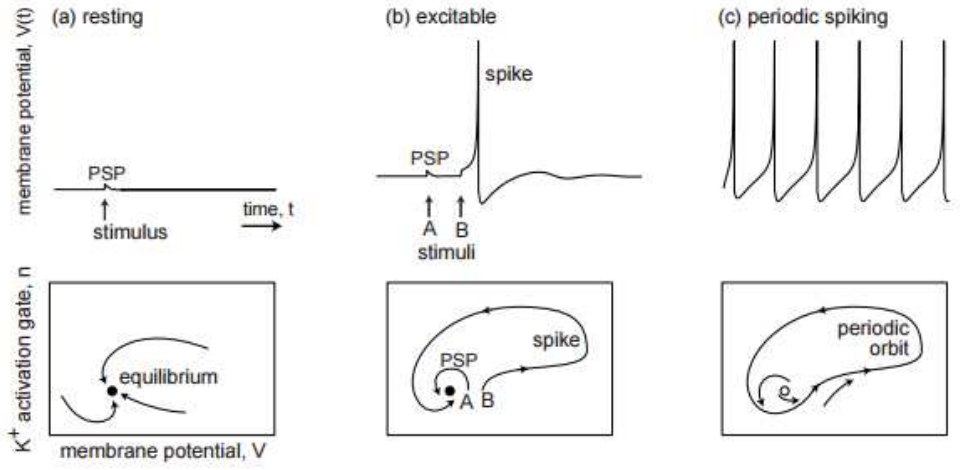

Figure 2.9: Resting, excitable, and periodic spiking activity corresponds to a stable equilibrium (a and b) or limit cycle (c), respectively (adapted from [39])**.**

The neuron can sustain quiescent state despite small disturbances and membrane noise. Then the corresponding equilibrium is termed as stable. The study of the phase portrait gives the overall qualitative description of dynamics. It depicts certain special trajectories (equilibriums, separatrices, limit cycles) which determine the topological behaviour of all the other trajectories in the phase space. In order to understand the dynamic mechanism such amplification, it is needed to consider the geometry of the phase portrait near the resting equilibrium. This is the region where the decision to fire or not to fire is made.

If the state of a neuron is given by a stable limit cycle in phase space. The corresponding phase space trajectory represents a stable periodic orbit. The electrophysiological details of the neuron helps to determine only the location, the shape, and the period of the limit cycle. The neuron can have periodic spiking activity as long as the limit cycle exists.

2.2.2.4 Bifurcations in neuron dynamics

Suppose, the control parameter is the current which is being injected to the neuron and its strength can be varied. Initially the neuron is at quiescence and as the strength of current is varied, the neuron exhibits tonic spiking (phase portrait corresponds to a limit cycle). So, there is some intermediate value of the injected current where this transition takes place. This transition corresponds to the bifurcation of the neuron dynamics (a qualitative change in the phase portrait). Neurons are excitable because they are near bifurcations from resting to spiking activity. So the type of the bifurcation determines the excitable properties of the neuron. The bifurcations of an equilibrium state leading to the transition from resting to periodic spiking behaviour in neurons. There are various types of Bifurcations, namely, Saddle-node bifurcation, Subcritical Andronov-Hopf bifurcation, Supercritical Andronov-Hopf bifurcation [49].

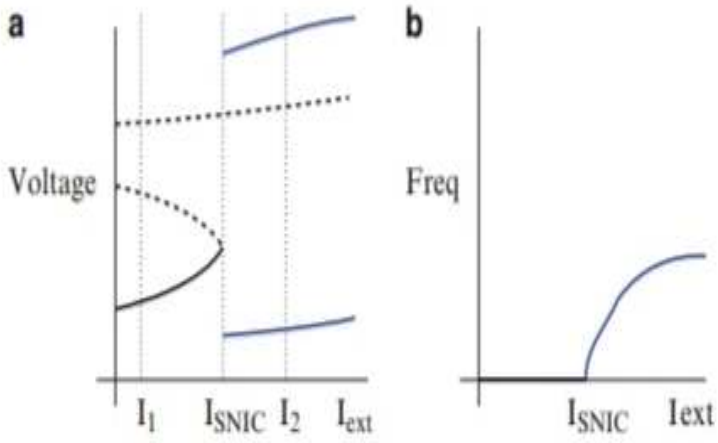

Figure 2.10: Saddle node bifurcation. (a) Stable and unstable solutions as a function of external current (b) Oscillations begin with arbitrarily low frequency (adapted from [41])

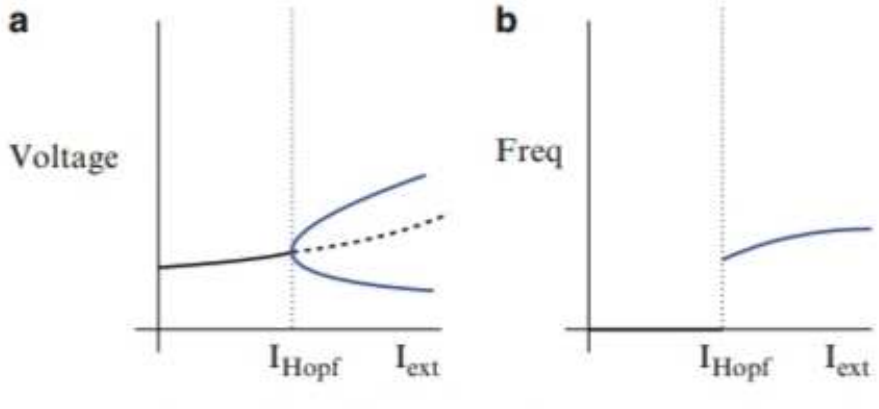

Figure 2.11: Hopf bifurcation. (a) Stable fixed point loses stability at supercritical hopf bifurcation point (b) Oscillations begin with frequency that is bounded from below but not equal to zero (adapted from [49]).

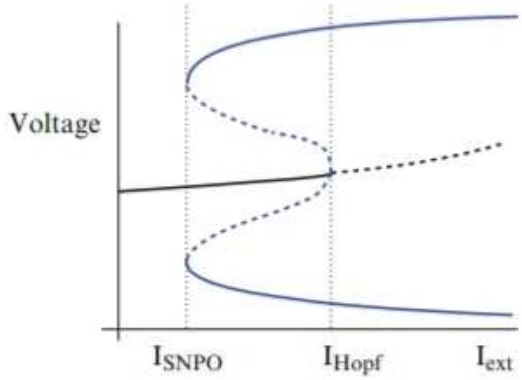

Figure 2.12: Subcritical Hopf bifurcation. (a) A single Stable fixed point loses stability at subcritical Hopf bifurcation point and branches of unstable periodic solutions are resulted. There is a region of bistability between $I_{SNPO}<I_{ext}<I_{Hope}$ (adapted from [49])

2.3 Neurons in brain

The neurons in the human nervous system can be divided into different classes; sensory neurons, motor neurons, interneurons and neurons in brain etc. Sensory neurons get information about what is going on inside and outside of the body and bring that information into central nervous system. Motor neurons get information from other neurons and convey commands to muscles, organs etc[50]. Interneurons connect one neuron to another and are found only in central nervous systems. In the brain, the distinction between the types of neurons is much more complex. Some of the brain neurons are involved in sensory processing like those in visual or auditory cortex and others are involved in motor processing – like those in the cerebellum or motor cortex. There are tens or hundreds of different neurons inside the sensory or motor regions. Researchers are trying to find out a way to classify the huge variety of neurons in the brain.

Mostly it is very difficult to define a neuron type. Neuron classification can be done depending on the type of neurotransmitter that a neuron uses. Some GABA neurons[42], for example, send their axon mostly to the cell bodies of other neurons; others prefer to target the dendrites. Each neurons show distinct behaviours in response to its electrical properties, shapes, genes expressed, projection patterns and receive different inputs. A single neuron model perform same function or suite of functions in the brain.

Researches[50] showed that neurons are discrete cells acting as metabolically distinct units communicating via specialized circuits and junctions. The main electrophysiological features of the neurons were obtained by the pioneering works of Hodgkin and Huxley[46]. Substantial early knowledge of neuron electrical activity came from experiments on the squid's giant axons [46]. As they are much larger than human neurons, but similar in nature, it was easier to study them with the technology of the first half of the twentieth century. This poor squid suffered pressure, stretch, injections of chemical substances and electrocutions, to record its axon's electrical activity by inserting electrodes into it. The accurate measurements obtained opened the way to the current neural science theory.

2.3.1 Dynamical and structural basis of brain activity

Brain research is one of the most important objectives of neuroscience which helps to understand the neuronal and cortical mechanisms underlying perceptual and cognitive functions. First influential brain theories such as localizationism [51] postulates that the brain is functionally segregated ie, the parts of the brain perform specific functions. This theory was motivated by Franz Joseph Gall’s theory of phrenology [51]. It is observed that specific regions in animals and humans is associated with particular brain functions and it led to the establishment of concept of functional segregation by the end of

nineteenth century. Functional brain imaging (eg. functional magnetic resonance imaging fMRI) confirmed that specific functions activate particular regions of brain. While many fMRI, human electroencephalography (EEG) and magneto encephalography (MEG) as well as animal cell recording studies put forward the idea that neuronal computations are distributed and engage a network of distributed brain areas[51]. This concept leads to the idea of functional integration. Perceptions, memories, and even emotions can be represented in a distributed manner. Functional connectivity is the statistical dependence on remote neurophysiologic events and can be assessed with simple coherence analysis of fMRI or electrophysiological time series[51]. Effective connectivity is defined as the influence of one system over another. Hence it can be concluded that global network dynamics over distributed brain areas can emerge from the local dynamics of each brain area. Conversely, global dynamics also can constrain local activity such that the whole system becomes self-organized. The implicit coupling between local and global scales induces a form of circular causality that characterize coupled complex self-organized system, like brain (e.g: Dynamics of neuronal populations within cortical areas are enslaved by large scale intercortical dynamics[49]).

2.3.1.1 Attractors and brain dynamics

Computational neuroscience tries to describe the dynamics of networks of neurons and synapses with realistic models. These models help to reproduce emergent properties in neurophysiology (Single and multiple cell recording, local field potentials, optical imaging, EEG, MEG, fMRI) and associated behaviour. The theoretical frame work, the attractor theory [49] helps to capture the neural computations inherent in cognitive functions. This theoretical frame work based on mathematical models is formulated at the level of neuronal spiking and synaptic activity.

Generally there are two main modeling approaches; bottom-up and top-down models. Bottom-up dynamical models start from a description of individual neurons and their synaptic connections. Using anatomical and physiological data, the particular pattern of connectivity in a circuit is reconstructed, taking into account the strength and polarity (excitatory or inhibitory) of the synaptic action. Synapses releasing a neurotransmitter brings the membrane potential of the postsynaptic neuron toward the threshold and the corresponding action potentials generated are said to be excitatory. Inhibitory synapses drive the membrane potential of postsynaptic neuron away from threshold and generate action potentials. Top-down dynamical models start with the analysis of those aspects of an animal's behaviour that are robust, reproducible and important for survival. Building such large-scale models is to determine the type of stimuli that elicit specific behaviours; this knowledge is then used to construct hypotheses about the dynamical principles that might be responsible for their organization.

For example local neuronal network model of integrate and fire [50] enables the study of spiking activity of single neuron and the effect of pharmacological agents on synaptic currents which is observed through fMRI and neurophysiological findings. Spike arriving at a given synapse provides input to the neuron which induces postsynaptic excitatory and inhibitory potentials.

Structural connectivity of the Macaque and the human cortex can be cited as an example for global network [51]. Here extrinsic connections between different cortical areas are specified by neuroanatomic matrix. These connections between a two distinct brain areas can be described by the density of synaptic connections between neurons in that area. Weight of inter areal connections is described by the coupling strength specified in the matrix. In

Macaque case, neuro anatomic matrix is obtained from CoCoMac database [49]. The connectivity of 40 cortical areas in one hemisphere of Macaque brain is obtained from the data base. In human case neuro anatomic information is obtained from diffusion weighted tensor imaging (DTI) and diffusion spectrum imaging (DSI) taractography [48].

2.4 Biological Neuron Models

Building dynamical models to study the neural basis of behaviour is one of the important issues in computational neuroscience. Specialized neurons transform environmental stimuli into neural code. This encoded information travels along specific pathways to the brain or central nervous system and combined with other information.

A biological neuronmodel represents the electrical properties of neuronal action potentials. The action potentials cause changes in electrical potential across cell membrane. It lasts for about one millisecond. Spiking neurons are the major signaling unit of the nervous system. It is observed that all cells of the nervous system do not produce the same types of spike. Cochlear hair cells, retinal receptor cells and retinal bipolar cells are some examples of cells which do not spike. Many artificial neuron models were proposed to model neurons in the nervous system to express the ion flows through the surface of membrane, to examine exactly how brain works and simulate the activities of the brain.

In 1943, the first neuron model[52] was proposed by McCullach and Pitts. Later the most successful and widely used neuron model, the Hodgkin-Huxley model is developed (1952) [46]. The ionic mechanism and electrical current on membrane surface were discussed in this model. After that, the FitzHugh–Nagumo neuron model, the simplified type of the Hodgkin– Huxley

neuron model, was proposed. In 1972, Nagumo and Sato [57] defined a neuron model and the weakly coupled Wilson–Cowan neuron model was defined in the same year. The Moris–Lecar neuron model was proposed in 1981 is a conductance based neuron model [49]. Later Hindmarsh–Rose(1984) [50] and Izhikevich (2003) [51] neuron models were also proposed. The studies based on the behaviour of the collective neurons rather than that of an individual neuron were proposed later. Since the biological information process and production of regular rhythmic activity are always related with the cooperative behaviour of neurons [48].

It is difficult to identify the interactions of the collective neurons in the living body except for some applications. Several alternative system approaches such as numerical modeling [52] and hardware implementations, which help to observe the fire patterns or synchronizations of neurons, have become crucial [53]. Hardware realizations are able to emulate the behaviour of an individual biological neuron or coupled neurons with real time adaptability. Furthermore, hardware realizations of neuron models can be used in practical applications such as bio-inspired robotic systems and CPGs (Central Pattern Generators) [53]. The software examinations of the biological neuron models can simulate the behaviour of the neurons[54]. Nowadays, Hindmarsh–Rose neuron model (H-R), which exhibits several fire patterns of the neuron are widely used in synchronization studies, due to their programmable and reconfigurable features.

2.4.1 Some commonly used neuron models

2.4.1.1 Hodgkin - Huxley Model

In 1952, Alan Hodgkin and Andrew Huxley was the first to study the bifurcation behaviour of the neuron. They developed a model system[46] quantifying the features of the giant squid axon, in Cambridge which

revolutionized the field of cellular biophysics. This eminent discovery was honoured with nobel prize in 1963.

This model gives an empirical kinetic description of ionic mechanisms in a neuron. It is based on Sodium, Potassium and leakage ion flow. An electrode is assumed to be inserted within the giant axon such that it has same potential that of intracellular component of the neuron (axoplasm)[55]. Another electrode is placed in the extracellular fluid (at zero volts). This set up thus measures the membrane potential as the difference in potential is determined with the help of an amplifier. This is then connected to a voltage clamp comparator along with a desired voltage (or command voltage), say V_c, which is set by the experimenter. As long as there is a difference signal given by $(V_m - V_c)$, generated by the amplifier, there is a current flowing into the axon through a current passing electrode and this will try to make both the potentials same. This injected current can be measured which essentially states that, corresponding to any change in the voltage across the membrane, ion channels open and close resulting in the flow of current. The current generated by those voltage gated ion channels are recordable.

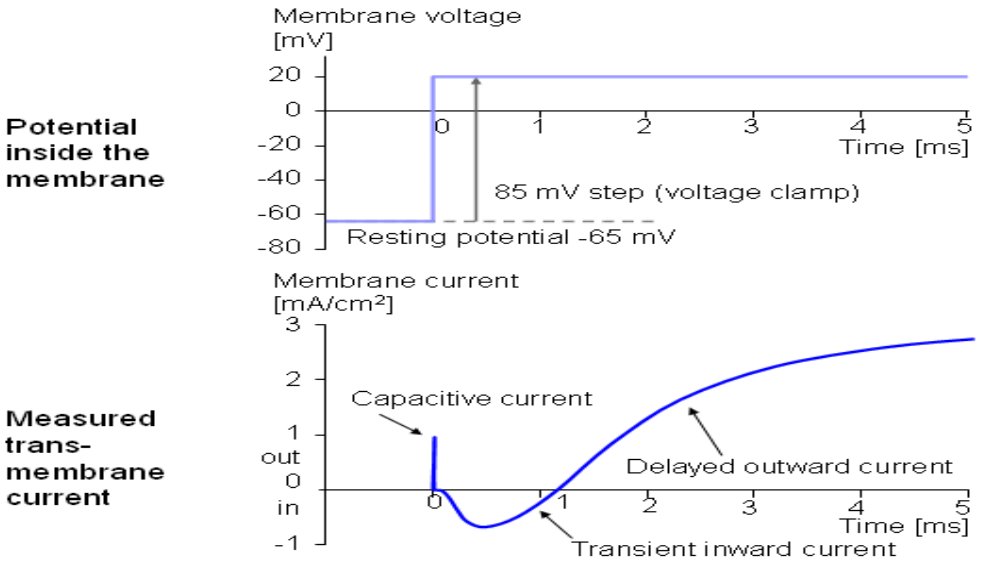

Figure 2.13: Time series of the membrane potential in the neuron(adapted from[45])**.**

The variation in the membrane potential leads to a change in the current through the ion channels. In the Figure 2.13, the resting potential is at -65 mV. When it is switched to 20 mV, there is a change in the charge separation and hence capacitive current flows. The capacitive current which is actually caused by the change in environment will have a sign opposite to the voltage perturbation applied and Once the new potential is reached, there is no more capacitive current [56]. Current flows so as to push the membrane potential back to the resting potential. Different ion channels open and close and a rapid inward and a delayed outward current are observed. This is because depolarization causes the transport of sodium ions. This inward current is known as sodium current. It is inactivated as time goes. The delayed outward current is caused by the Potassium ions and they don't show any decrease or inactivation in axons. The current flow is greater for depolarization than that for hyper polarization [56].

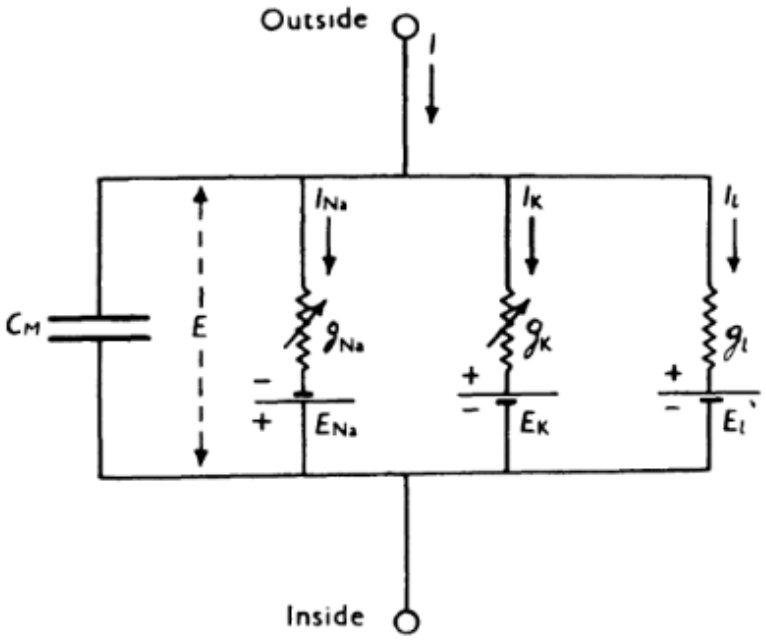

Figure 2.14: Equivalent circuit representation for the Hodgkin-Huxley model (adapted from [45]).

The nonlinear differential equations representing Hodgkin-Huxley model (H-H model) is as follows

$$-C\frac{dV}{dt} = m^3 h\bar{g}_{Na}\big(V - E(Na)\big) + n^4\bar{g}_K\big(V - E(K)\big) + \bar{g}_L\big(V - E(L)\big) - I$$

$$\frac{dn}{dt} = \alpha_n(1-n) - \beta_n n$$

$$\frac{dm}{dt} = \alpha_m(1-m) - \beta_m m$$

$$\frac{dh}{dt} = \alpha_h(1-h) - \beta_h h \qquad (2.1)$$

C represents the membrane capacity, V the total membrane potential, m the sodium activation variable and h the Potassium activation variable. $\bar{g}_{Na}\, is$ the maximum sodium conductance and $\bar{g}_K$is the maximum Potassium conductance. $E(K)$ represents the Potassium equilibrium potential, $\bar{g}_L$ maximum leakage conductance and $E(L)$ represents the leakage equilibrium potential. I gives the external current, α_i represents gate inactivation rate ($i = m, n, h$), and β_i gives the gate activation rate ($i = m, n, h$).

2.4.1.2 Fitzhugh – Nagumo Model

The Hodgkin–Huxley (H-H) model[46] of the nerve impulse made up of four coupled nonlinear differential equations. Because of the complexity of the equations, it is difficult to use them in simulations of interactions in small neural networks. Hodgkin-Huxley model can mimic all the behaviours of neuron spiking. But due to its high dimensionality it is difficult to achieve analytical solutions. Only numerical solution can be found for each specific conditions. Thus second-order differential equation of the model which can predict the main properties such as the frequency–current relationship.

Fitzhugh[52] introduced a second-order model of the nerve impulse. It helps for the prediction of an action potential duration. The dynamics of the slow sodium and potassium ions in H-H model i.e., the gating variables: n and $h$are replaced by an effective current $w(t)$ in Fitzhugh – Nagumo(FHN) model[57]. The fast dynamics of sodium ion across the neurons in H-H model is replaced by $v(t)$ [59].

The FHN model is expressed as,

$$\frac{dv}{dt} = v - \frac{1}{3}v^3 - w + I_{ext}$$

$$\frac{dw}{dt} = \varphi(v + a - bw) \tag{2.2}$$

where, v is the rate of change of the neuron membrane potential from its equilibrium due to the fast ion dynamics with time. w is the recovery variable for the neuron membrane potential which deals with slow diffusive ion currents in the neuron. These two variables represent the state of the system at any instant. The equation for the recovery variable shows that, it depends on the departure of the membrane potential from its equilibrium value v , and it decays at a constant rate 'b'. I_{ext} is the external stimulus or the external current given to the neuron. a, b and φ are constants, where typically $0 < a < 1, \varphi > 0, b > 0$. Parameters can be chosen as $a = 0.7, b = 0.8$, $\varphi = 0.08$.

With $\varphi > 0$, the origin in the system is an unstable fixed point surrounded by a globally stable limit cycle. It is the only parameter that can change the behaviour of the neuron around the threshold. Also, decreasing φ decreases spike rise and fall times. Finally, the behaviour around and below threshold is influenced by φ. For certain parameter values, the solution demonstrates a slow collection and fast release of the potential. This kind of behaviour is often labeled as 'integrate and fire'. However, in biological systems, a resting phase is required for the neurons after firing. Tonic spiking with FHN can be generated withs appropriate parameter values.

2.4.1.3 Hindmarsh-Rose Model

FitzHugh-Nagumo model is the simplification of the Hodgkin-Huxley model for neurons. It came with many drawbacks. The FHN model reduced the complexity of the neuron models. Self-sustained chaotic dynamics was not observed with FHN model. The most essential characteristics of neurons such as bursting could not be observed. FHN model consists of only a few parameters. It is difficult to adapt this model to neurons with specific properties.

The problem with FHN model is that those equations do not provide a very realistic description of the rapid firing of the neuron [57]. They do not give a reasonable frequency–current relationship. The FHN model, which is the simplified version of H-H model, with only two dimensions was introduced so that its global behaviour can be easily studied in a phase plane. However, this model could explain only the generation and propagation of action potentials with only the Sodium and Potassium channels. Elucidation of the rhythm of spike train seems to be difficult with FHN model. More channels with slower kinetics have to be introduced to understand more about the underlying mechanisms. Hence, the FHN model was modified to give the Hindmarsh-Rose model which is a three dimensional model for neuron with rapid firing. In particular, it shows bursting behaviour and chaos.

The Hindmarsh-Rose (H-R) model for neurons was developed by J. L. Hindmarsh and R. M. Rose to allow for rapid firing or bursting in neurons. The Hindmarsh-Rose neuron model is a simplified model of the Hodgkin-Huxley model and a modification of the FitzHugh-Nagumo model [57]. The Hindmarsh-Rose model differs in many ways from FitzHugh-Nagumo model in terms of topology of the phase space, the threshold for spikes, the way the spike trains are created and how bursting is shut off [14].

H-R model of neuronal activity is used to study the spiking-bursting behaviour of the membrane potential. A chain of action potentials emitted by a single neuron is called a spike train; a sequence of stereotyped events which occur at regular or irregular intervals [58]. The bursting behaviour of the neurons, characterized by the transition of a neuron from resting phase to a recurring firing state, relies on the slow adaptation variable $z(t)$ [58]. This means that the adaptation variable was added to the existing model to terminate the firing. Each burst will have a definite number of spikes unless they are in

the chaotic regime. This model is based on the global behaviour of the neuron. Despite being simpler with less governing equations and coefficients, the model is accurate to neurons seen in biology and was created to accurately follow the bursting seen in mollusks [58]. The membrane potential is represented by the variable, $x(t)$. It is written in dimensionless units. There are two more variables, $y(t)$ and $z(t)$ which denotes the transport of ions across the membrane through the ion channels. Thus, at any instant, the state of the system is represented by these time dependent state variables. The transport of sodium and potassium ions is made through fast ion channels and its rate is measured by $y(t)$, which is called the spiking variable. The transport of other ions is made through slow channels represented by $z(t)$ which is called the bursting variable (slow adaptation variable).

The Hindmarsh–Rose model has the mathematical form of a system of three nonlinear ordinary differential equations used to represent pulse propagation in neurons

$$\dot{x} = y - ax^3 + bx^2 - z + I_{ext}$$

$$\dot{y} = c - dx^2 - y$$

$$\dot{z} = r(s(x - x_e) - z \tag{2.3}$$

Here, $x(t)$represents the membrane potential and it considered as a natural output of the cell. Also $y(t)$and $z(t)$are recovery and adaptation variables, which account for fast and slow ion currents respectively. I_{ext} represents the external stimuli or the applied current. We choose the parameters as $a = 1$, $b = 3, c = 1, d = 5, r = 0.005$, $s = 4, x_e = -\frac{8}{5}$ so that the rich phenomena like bursting and spiking are observed.

The responses of this model to a current, largely depends on the values of μ and b. The parameter 'μ' controls the speed of variation of the slow variable z(t). This helps to analyse how efficiently the slow variables are exchanging the ions. It is not possible by the FitzHugh-Nagumo model. In the presence of spiking and bursting behaviour, it can determine the spiking frequency and the number of spikes per burst. Here x_e sets the resting potential of the system. The parameter 'b' allows one to switch between bursting and spiking behaviour of the neutrons and thus affects the qualitative behaviour of the neurons. The model could successfully display regular bursting, chaotic bursting and post inhibitory rebound. Generally speaking, three modes of operation can be distinguished in the full Hindmarsh- Rose model:

1. Quiescent
2. Spiking
3. Bursting

The quiescent mode corresponds to the absence of stable cycles. Spiking means the continuous generation of action potential, either regular or irregular but with no clear formation of packets of spikes. Bursting on the contrary means that action potentials arrive in clear bursts, separated by clear, regular or irregular silent periods. These can be illustrated using the figure below.

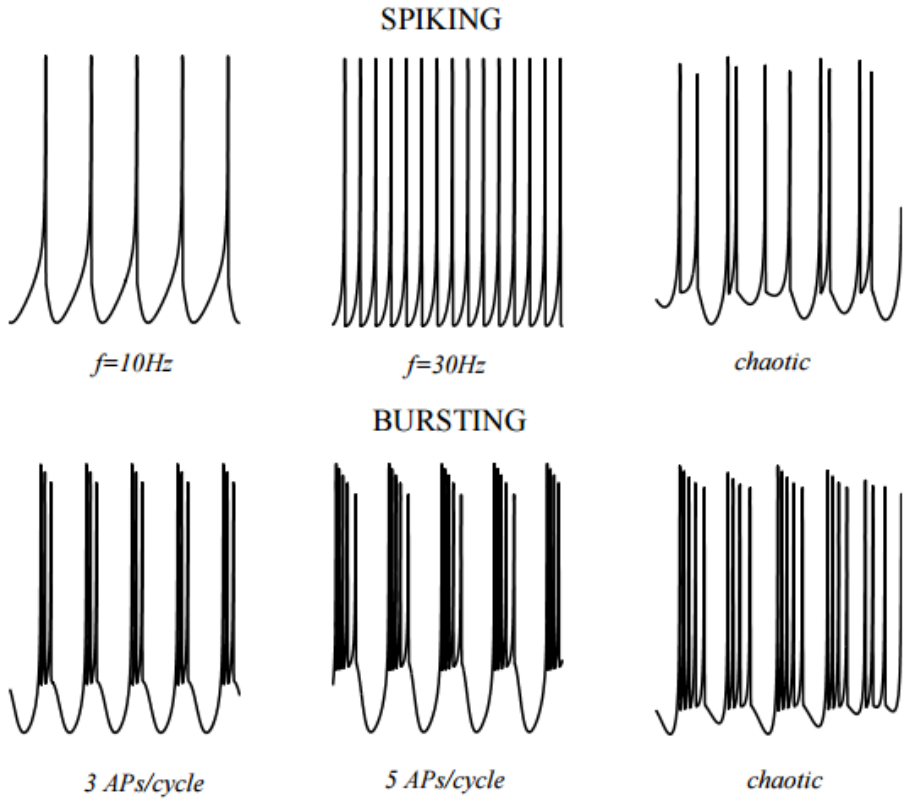

Figure 2.15: Different modes of operation in Hindmarsh- Rose model (adapted from [56]).

2.4.1.4 Neuron model with Josephson Junction

Josephson Junctions are two superconductors separated by thin insulating barrier. Here phase difference of electron across the barrier controls the electrical properties including voltage and current across the junction**.** Voltage developed above critical current is

$$V = \left(\frac{\varphi_0}{2\pi}\right)\frac{d\varphi}{dt} \text{ where } \varphi_0 = \frac{h}{e} \tag{2.4}$$

Current through the circuit can be represented as

$$i = \ddot{\varphi} + \Gamma\dot{\varphi} + sin\varphi \tag{2.5}$$

Where Γ is a damping parameter which depends on resistance and capacitance.

The superconducting circuits containing Josephson Junctions can model many characteristics of biologically realistic models such as action potentials, firing threshold and refractory periods.

Basic circuit of JJ neuron (Figure 2.14) involves two Josephson Junctions connected in a loop. The individual junctions behave like ion channels. One corresponds to depolarizing current such as Sodium(Na^+) and other to a hyperpolarizing Potassium(K^+) current[59]. It is possible for the enhancement of model by inclusion of a third junction. It could allow for behaviours such as bursting that require at least three currents.

The JJ neuron uses rapid single flux quantum technology. Here single chip can model up to N=10000 neurons. Here simulated action potential lasts about 50 ps.

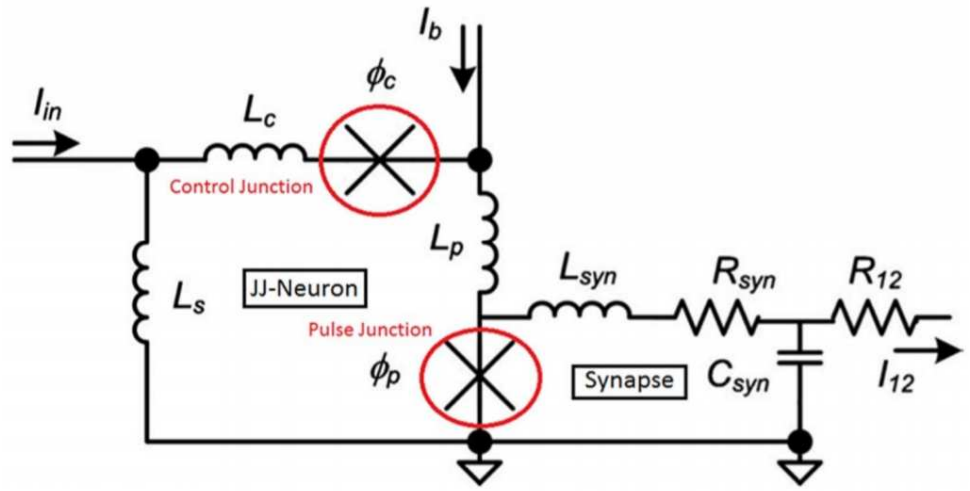

Figure 2.16: Circuit diagram of JJ neuron connected to a model chemical synapse (adapted from [54]). Many synapses could connect to a single JJ Neuron.

Table 2.1: Biological equivalents of the JJ model

JJ- Neuron	Biological equivalent
Flux $\phi = \lambda(\phi_p + \phi_c)$	Membrane Potential
Pulse voltage v_p	Na^+ currentI_{Na}
Control Voltage v_c	K^+ current I_K
Input current I_{in}	Synapse current ,I_{syn}

The dimensionless model of resistive–capacitive–inductive-shunted Josephson Junctioncan be described by

$$\dot{x_1} = \frac{1}{\beta_c}[I - g(x_1)x_1 - \sin(x_2) - x_3]$$

$$\dot{x_2} = x_1$$

$$\dot{x_3} = \frac{1}{\beta_L}(x_1 - x_3) \quad (2.6)$$

The $g(x_1)$ denotes the correlation between voltage and current of Josephson Junction.

$$g(x) = \begin{cases} 0.366\, x_1 < 2.9 \\ 0.0661 x_1 \geq 2.9 \end{cases} \quad (2.7)$$

The voltage, phase difference and induction current of Josephson Junction are represented by $\dot{x_1}$, $\dot{x_2}$ and $\dot{x_3}$ respectively. I is the external forcing DC current and the constants β_c and β_L are the mapped parameters from the circuit equation.

2.5 Noise in neurons

Neuronal noise designates random influences on the transmembrane voltage of single neurons. It can influence the transmission and integration of signals from other neurons and can alter the firing activity of neurons in isolation. Highly nonlinear operations can be performed by neurons. These operations involve high gain amplifications and feedback. Hence small biochemical and electrochemical fluctuations [61] can change whole cell responses. If the membrane potential is near the firing threshold, then the corresponding action potential is highly sensitive to noise[62].

It is possible to detect and transmit weak periodic signals with threshold systems. This can be enhanced by presence of certain noise[63]. This process of enhancing certain level of noise is known as stochastic resonance. There are various sources of noise in neurons. Noise accumulates on each neuron due to randomness in the cellular machinery. At the biochemical and biophysical level there are so many stochastic processes in neurons. Some of the sources of noise in neurons are mainly due to protein production, degradation, opening and closing of ion channels, fusing of synaptic vesicles, diffusion and binding of signaling molecules to receptors etc [64].

Large part of the noise experienced by a cortical neuron is mainly due to the intensive and random excitation of synaptic sites. It has been observed from in vivo recordings of cortical neurons in awake [65] and anesthetized animals that a spontaneous activity exists and that the related spike process can be considered as Poisson. The origin of irregularities is still poorly known. Gerstner and Kistler [66] had shown that we can distinguish between intrinsic noise sources that generate stochastic behaviour at the level of the neuronal dynamics and extrinsic sources arising from network effects and synaptic transmission.

A permanent noise source is the thermal noise linked with discrete nature of electric charge carriers. Fluctuations linked with this phenomenon are however of minor importance compared to other noise sources in neurons. The finite number of ion channels is another noise source. Most of the ion channels have only two states: they are open or closed. The electrical conductivity of a patch of membrane is proportional to the number of open ion channels. The conductivity therefore fluctuates and so does the potential. Noise is also due to signal transmission and network effects (extrinsic noise). Typical examples are synaptic transmission failures and randomness of excitatory and inhibitory connections. The global networks effects where there is random excitatory or inhibitory connectivity can produce highly irregular spikes trains even in the absence of noise.

2.5.1 White Gaussian Noise

White noise is a random signal with equal intensity at different frequencies. It has uniform power distribution across the frequency band for the information system. In discrete time white noise is a discrete signal whose samples are regarded as uncorrelated random variables with zero mean and finite variance.

If each sample follows a normal distribution with zero mean, then the signal is said to be additive white Gaussian noise. Additive white Gaussian noise[67] is used in information theory in order to mimic the effect of many random processes in nature. The Gaussian noise follows a normal distribution.

The idea of white noise refers that it has uniform power across the frequency band for information system. Gaussian white noise is a stationary and ergodic random processes. It follows a normal distribution in the time domain with average time domain value of zero.

The generalized correlation function of white noise can be represented as

$$X(t) = \sigma^2 \delta(t) \tag{2.8}$$

Where σ^2 is a positive constant and $\delta(t)$ is the delta function.

White noise is applied in describing random disturbances with small correlation period. It can be represented in spectral decomposition as

$$X(t) = \int_{-\infty}^{+\infty} e^{i\lambda t}\, dz(\lambda) \tag{2.9}$$

The elementary vibrations $e^{i\lambda t} dz(\lambda)$, on an average, follows same intensity at all frequencies λ.

The average squared amplitude is

$$E|dz(\lambda)|^2 = \frac{\sigma^2}{2\pi} d\lambda \; -\infty < \lambda < \infty \tag{2.10}$$

In practical application white noise follows the form

$$X(t) = \sum_k \delta(t - \tau_k) \tag{2.11}$$

Here k varies between $-\infty$ and $+\infty$ and $\tau_{-1}, \tau_0, \tau_1, \ldots \ldots$ form a Poisson process. $X(t)$ also can be represented as generalized derivative of Poisson processes $\eta(t)$

$$Y(t) = \int_{-\infty}^{+\infty} w(t,s)X(s)ds = \int_{-\infty}^{+\infty} w(t,s)d\eta(s) = \sum_k w(t,\tau_k) \tag{2.12}$$

Corresponding average value of squared amplitude is

$$E|dz(\lambda)|^2 = \frac{a}{2\pi} d\lambda \tag{2.13}$$

2.5.2 L*è*vy Noise

Gaussian noise cannot incorporate large bursts that typically occurring in real experiments. L*è*vy processes represents the motion of a point whose successive displacements are random and independent in nature. One of the main feature of simple L*è*vy noise models is its large jump. The skewness parameter enables L*è*vy noise to produce an asymmetric noise distribution, which takes a key role on phenomena that transitions between stable points occur frequently in a noisy field[68,70]. Gaussian white noise hardly induce this type of translations due to its symmetric distribution. Hence L*è*vy distribution is an appropriate choice when one considers realistic models with pulse phenomena in various systems[69].

Let ξ denotes the time dependent L*è*vy noise and obeys the probability density function $L_{\alpha,\beta}(\xi;\sigma,\mu)$, whose characteristic function is represented by[68]

$$\Phi(k) = \int_{-\infty}^{+\infty} d\xi e^{ik\xi} L_{\alpha,\beta}(\xi;\sigma,\mu) \tag{2.14}$$

Therefore, for $\alpha \in (0,1)\ U\ (0,2)$

$$\Phi(k) = \exp\left[i\mu k - \sigma^k|k^\alpha|\left(1 - i\beta sgn(k)\tan\left(\frac{\pi\alpha}{2}\right)\right)\right] \tag{2.15}$$

and for $\alpha = 1$,

$$\Phi(k) = \exp\left[i\mu k - \sigma|k|\left(1 + i\beta sgn(k)\frac{\pi}{2}\ ln|k|\right)\right] \tag{2.16}$$

Here $\alpha \in (0,2)$is known as the characeristic exponent and it denotes the stability index that describes an asymptotic power law of the Lévy distribution. The constant β $(\beta \in [-1,1])$ is the asymmetry or skewness parameter.

σ ($\sigma \in (0, \infty)$)is the scale parameter and $\mu(\mu \in$ R) is the mean parameter. The noise intensity is denoted as $D = \sigma^{\alpha}$ and hence the Lévy process can also be represented as $L_{\alpha,\beta}(\xi; D, \mu)$. When α = 0.5, the stable distribution is called α-stable Lévy distribution.

Chapter 3
Nonlinear Feedback Coupling in Hindmarsh –Rose Neurons

Chapter 3

Nonlinear Feedback Coupling in Hindmarsh –Rose Neurons

3.1 Introduction

The nonlinear dynamics of a neuron can generate deterministic chaos under some conditions[83]. Networks of coupled dynamical systems exhibit many interesting behaviours such as spatio-temporal chaos, pattern formation and synchronization. Such networks can be used to model a large variety of biological and physical systems.

The coupling schemes for different neurons such as dynamical coupling, time delay feedback coupling, conjugate coupling, diffusive coupling[84], nonlinear coupling [85], Memristor coupling [86], repulsive mean field interaction, damping effect by an environment[87] etc. can be applied to study amplitude death, oscillation death and various other dynamical evolutions of neuron systems. Coupling between same variables of two or more non-linear systems may lead to synchronization. This has been observed in many physical[88], chemical[89], ecological[90], and biological systems[91]. This phenomenon has found many applications in cryptography and in secure communications. Also recent works have shown that the coupling of nonlinear elements can invoke interesting phenomena, such as hysteresis, phase locking, phase shifting, phase flip, amplitude death [92] and oscillation death [93].

Neural synchrony is believed to be an important mechanism underlying many phenomena in the human brain, including the formation of neuronal assemblies[94]. In the brain, synchronization is often associated with epileptic form of behaviour[95]. The theoretical and experimental studies on chaotic neural dynamics helps to understand higher functions of brain such as

adaptation, perception, episodic memory, learning, awareness, intentionality, and thought [83]. The studies of dynamical behaviour of neurons are relevant in this context.

Further, recent studies [87] show that when an indirect feedback coupling through an environment or an external system is applied to neurons there is a tendency for anti-synchronization, amplitude death, in phase and out of phase synchronization[96] etc.

Oscillation quenching in the form of amplitude death (AD) and oscillation death (OD) are known to appear in oscillatory systems under different coupling schemes. This emergent behaviour in coupled oscillators occurs when they drive each other to a stable equilibrium. In the case of AD, all the coupled oscillators are stabilized to one equilibrium state which may be the origin or any other fixed point. But the coupled systems are stabilized to multiple equilibrium states in the case of OD. This strange phenomenon was, at first, explained as an effect of large parameter mismatch[97] on coupled oscillatory systems. Later, AD was also observed in two identical oscillators when a critical propagation delay [98] is introduced in the coupling.

Synchronization of two nonlinear oscillator systems when coupled through a memristor like nano scale devices is also an interesting research area[99]. Recently its applications on neuromorphic computing, device modeling, signal processing etc. are reported[100-105]. It is possible to emulate short term synaptic dynamics with memristive devices where memristor have full potential for building biophysically realistic neural processing systems[106]. When memristor function as a novel neuro-fuzzy computing system[107] it can be used for creating artificial brain. The mechanism underlying the emergence of synchronization between two memristor-coupled Hindmarsh–Rose oscillatory neural cells is also interest of study.

In the present chapter the model of neurons described by Hindmarsh-Rose (H-R) system is examined with various linear and nonlinear coupling schemes. The H-R model is a well-known model that describes the action potentials[108]. In nervous systems neuron encoding, transferring and integrating information are realized by a series of action potentials [109]. This model equation of H-R neuron describes actually a nonlinear dynamical system which demonstrates the pulse propagation in neurons, and is very important from biophysical perspectives[109]. Here the coupling strength summarizes information distribution between neurons.

Linear indirect synaptic coupling of the H-R neurons and the coupling of the form of nonlinear cubic feedback are anlaysed in this chapter. The coupling between two neurons using different memristor as electrical synapse is also examined. The scope of synchronization, anti-phase synchronization, amplitude death, oscillation death, and near death rare spikes etc. are also studied. The work also focuses on the stability of different coupled systems. The simulation results of different coupling schemes in H-R neurons show many interesting dynamical characteristics of coupled neuron cells.

It is shown that linear coupling, nonlinear feedback coupling and memristor based coupling establish a pathway to amplitude death and oscillation death. Amplitude response /death and phase resetting are analyzed in the present work which is having much importance in the study of brain cells. Our work shows possibilities of anti-phase synchronization with linear synaptic coupling, nonlinear cubic feedback coupling and with unidirectional cubic flux controlled memristor coupling. The quadratic flux controlled memristor coupling shows many interesting dynamics like near death rare spikes. Near Death Experiences (NDEs) are found to occur as a result of neurobiological

alterations in the brain**.** Cognitive, emotional and transcendental elements comprise NDEs[110].

The study of stability is always a central task for nonlinear differential systems. Here the general linear stability analysis[87] for the dynamics of nonlinear feedback, cubic flux controlled memristor, quadratic flux controlled memristor and exponential flux controlled memristor is done. The values of Lyapunov Exponent (LE) are also computed for the proposed couplings. The neural systems certainly involve non-linear mechanisms, so the unpredictable and complex behaviour of neural systems can be measured by the computation of Lyapunov Exponents. If physiological signals have at least one positive Lyapunov Exponent, they reflect an unstable and unpredictable system and are used to define deterministic chaos[111]. The largest LE value close to 1, indicate chaotic behaviour. From our plots it is clear that among the memristor couplings H-R neurons coupled with cubic flux controlled memristor exhibits more chaotic nature. In neural systems this value falls due to relaxed situations in the brain[111]. This suggests that when subjects are exposed to external sound or reflexologic stimuli, the brain goes into more relaxed state.

3.2 Model and scheme

Hindmarsh –Rose neuron (H-R neuron) model is chosen to study the spiking-bursting behaviour neurons[87]. This model is very important to analyse biophysical perspectives of neuronal systems.

The dynamical equation of three-variable H-R neuron can be represented as

$$\dot{x}_1 = x_2 - ax_1^3 + bx_1^2 + I_{ext} - x_3$$
$$\dot{x}_2 = c - dx_1^2 - x_2$$
$$\dot{x}_3 = r\left(s\left(x_1 - x_0\right) - x_3\right) \tag{3.1}$$

The variable x_1 represents the membrane potential of a neuron and the variables x_2 and x_3 are related ion currents across the membrane. Here parameters are chosen as a=1, b=3, d=5, r = 0.006, s=4, c=1, I_{ext}=3.00, k=1.6. The parameters of the system are chosen such that the individual neurons are in the bursting state.

3.3 Linear coupling in H-R neurons

3.3.1 Indirect-synaptic coupled H-R neurons

Hindmarsh-Rose system model of neurons is described by the equations, which are subjected to linear-synaptic and indirect coupled equations. Here we take two neurons with excitatory synaptic coupling and an indirect coupling is introduced between them[87].

$$\dot{x}_1 = x_2 - ax_1^3 + bx_1^2 + I_{ext} - x_3 + \varepsilon u + \omega_2 \frac{V_r - x_1}{1 + \exp\left(-\lambda\left(x_4 - \theta\right)\right)}$$
$$\dot{x}_2 = c - dx_1^2 + x_2$$
$$\dot{x}_3 = r\left(s\left(x_1 - x_0\right) - x_3\right)$$
$$\dot{x}_4 = x_5 - ax_4^3 + bx_4^2 + I_{ext} - x_6 + \varepsilon u + \omega_2 \frac{V_r - x_4}{1 + \exp\left(-\lambda\left(x_1 - \theta\right)\right)} \tag{3.2}$$
$$\dot{x}_5 = c - dx_4^2 + x_5$$
$$\dot{x}_6 = r\left(s\left(x_4 - x_0\right) - x_6\right)$$
$$\dot{u} = -ku - \frac{\varepsilon}{2}\sum_{i=1,4} x_i$$

x_1, x_2 and x_3 represents membrane potential and related fast and slow ion current variables for the first neuron and x_4, x_5 and x_6 are corresponding variables of second neuron. V_r represents the action potential. The parameter values are chosen as a=1, b=3, d=5, r=0.006, s=4, c=1, I_{ext}=3.05, k=1.6. The parameters of the system are chosen such that the individual neurons are in the bursting state. Here the synaptic coupling is given by the term $\omega_2 \frac{V_r - x_1}{1+exp(-\lambda(x_4-\theta))}$ and indirect coupling is achieved by an environment. The last equation which governs the dynamics of u represents the active feed back from both the systems through the environment[87].

There are excitatory or inhibitory synaptic coupling depending upon whether the synapse is fast or slow[112]. Direct synapses are activated as soon as a membrane potential crosses the threshold value while the effect of indirect synapse is to introduce a delay from the time one oscillator jumps up until the time the other feels the synaptic input.

The time series analysis and corresponding synchronization, antiphase synchronization and amplitude death plots are examined in section 3.3.1.1.

3.3.1.1 Time series plots for linear indirect synaptic coupling

The effects of synaptic coupling on the time series behaviour of neurons are examined. The chaotic behaviour of indirect synaptic coupled neurons depends on the specific values of parameters in the H-R neuron equation.

Synchronization

Synchronization behaviour of two linear indirect synaptic coupled H-R neurons is shown through time series analysis. Here for sufficiently large value

of one coupling parameter (ω_2), bursts of both neurons become synchronized as shown in Figure 3.1.

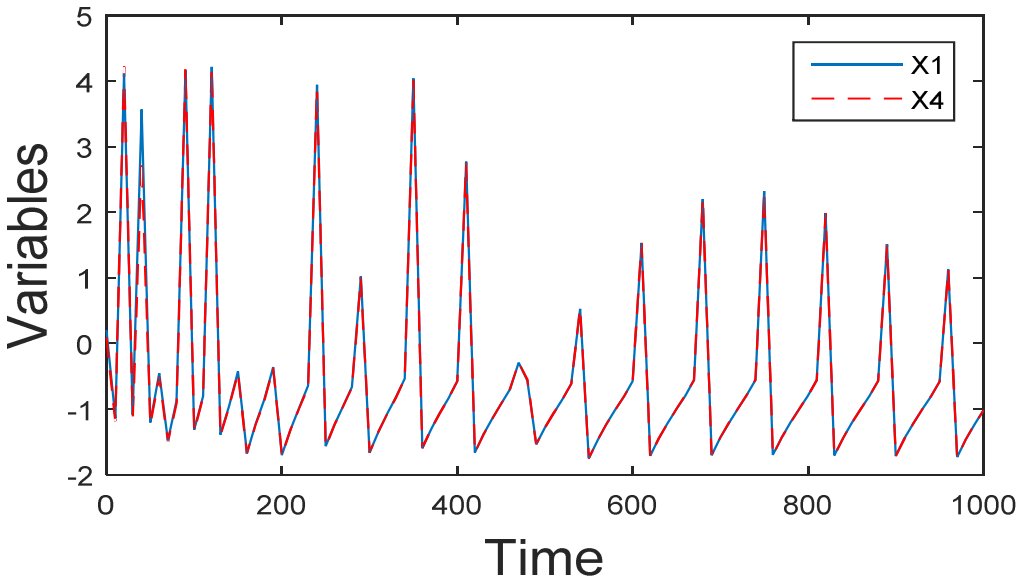

Figure 3.1: Time series of the first variables ($x_1 and\ x_4$) of indirect and synaptically coupled neurons show synchronization. At $\varepsilon = 0, \omega_2 = 1$, the synchronization behaviour of two neurons is established.

Anti-phase synchronization

Anti-phase synchronization property of linear indirect synaptic coupled neurons (Figure3.2) is shown through time series analysis. Here one of parameter is of low value and other is of high value.

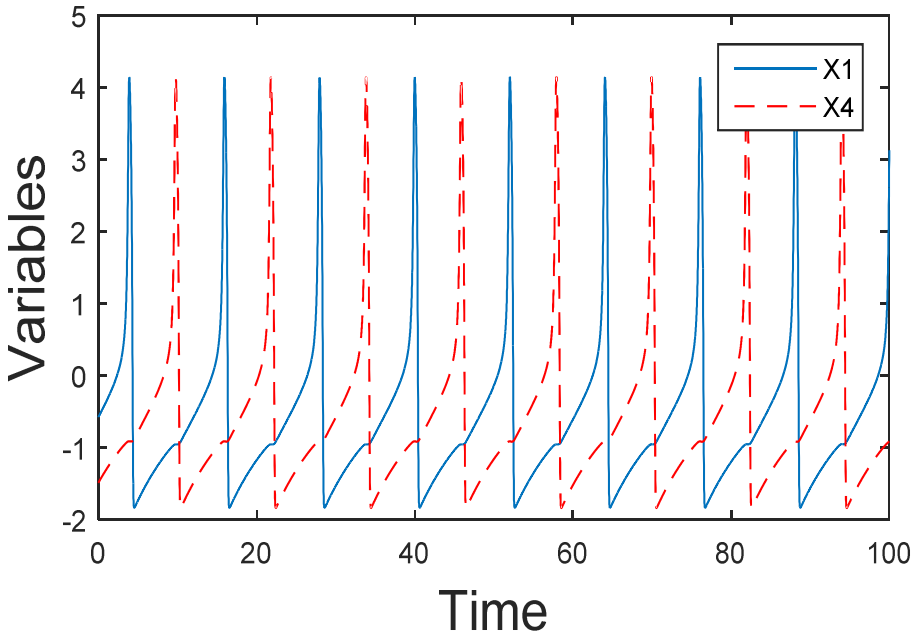

Figure 3.2: Time series of indirect and synaptic coupled neurons exhibits anti-phase synchronization for the values of coupling strengths $\varepsilon = 1$and $\omega_2 = 0$.

Amplitude death

For higher values of coupling parameters, amplitude death of indirect synaptic coupled neurons is established through time series analysis of $x_1$and x_4 as shown in Figure 3.3. Here oscillation of two neurons comes to a common steady state condition.

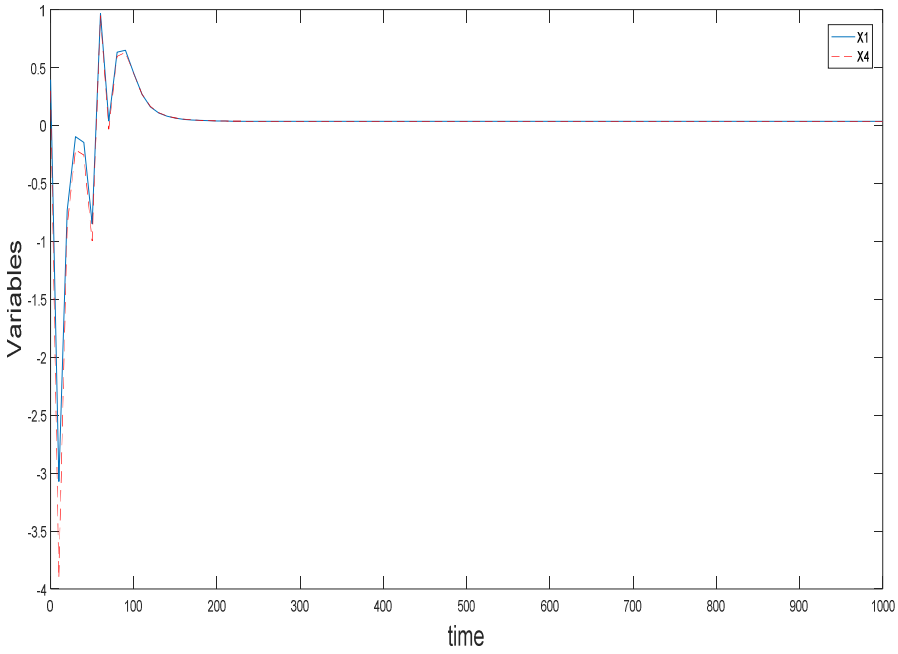

Figure 3.3: Time series plots of indirect and synaptic coupled H-R neurons evolves into amplitude death condition for higher values of both of the coupling/ control parameters $\varepsilon \; and \; \omega_2$.

We have also identified the regions of amplitude death, synchronization and anti-phase synchronization in the two neuron system for linear, indirect synaptic coupling for various values of coupling parameters (Figure 3.4). The regions are identified by correlation analysis[87]where synchronization, anti-phase synchronization and amplitude death are found to emerge in. When one of the control or coupling parameter is set as high value, synchronization or anti-phase synchronization regions are obtained.

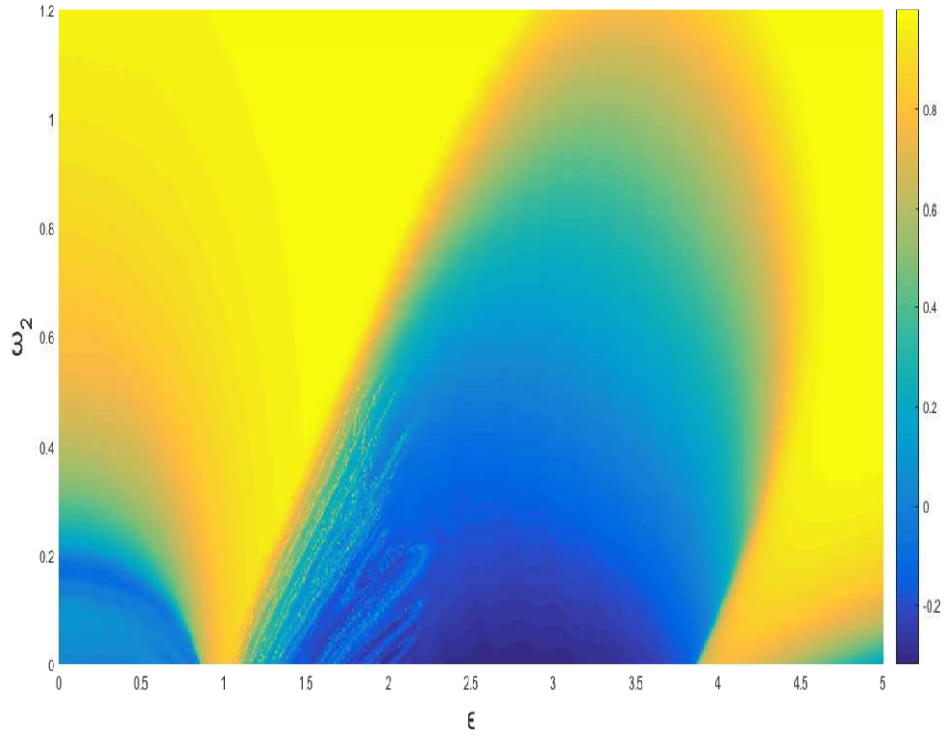

Figure 3.4: Amplitude death, synchronization and anti-phasesynchronization regions through $\varepsilon - \omega_2$ plot**.** Regions are found by varying coupling strengths. Parameter range is selected as ε= [0:0.5:5] and ω_2 = [0:0.2:1.2]. Synchronization and anti-phase synchronization regions obtained are depicted through yellow and dark blue color in the above plot. For higher values of control parameters amplitude death behaviour is set in, which is shown by light green region in the figure.

Due to rigorous mathematical calculations, stability analysis of synaptic coupled H-R neuron is not done.

3.3.1.2 Lyapunov Exponent plot for synaptic coupled H-R neurons

Here we studied dynamics of synaptic coupled system through Lyapunov Exponent (LE) plot as shown in Figure 3.5. The increased LE value

reflects greater sensitivity to initial conditions and characterizes unpredictable variations, while low value indicate the regularity of the system.

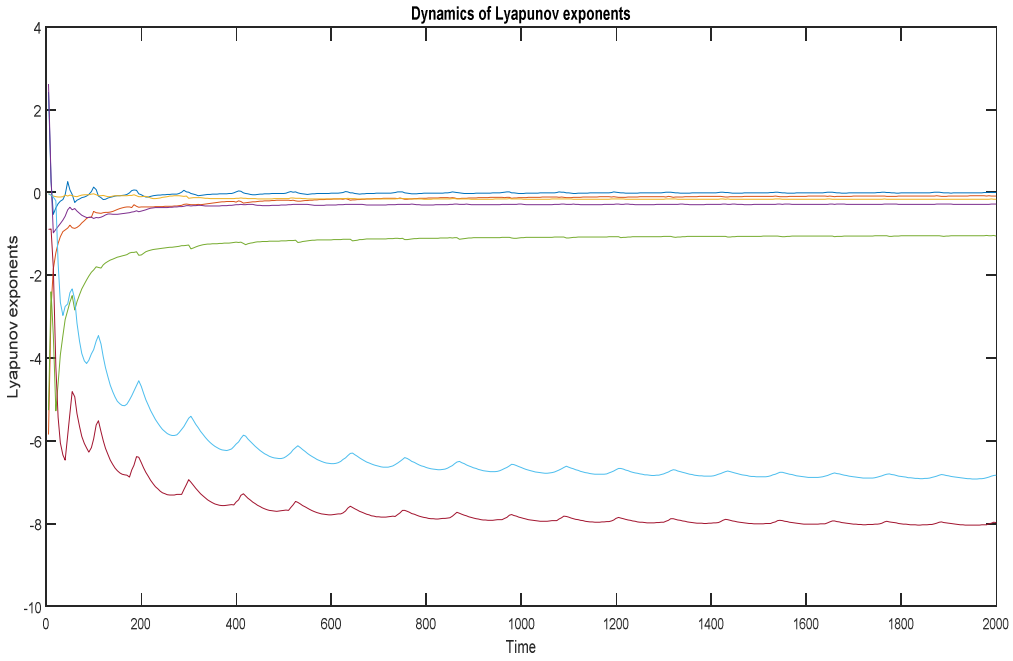

Figure 3.5: Lyapunov Exponent plot for linear synaptic coupled H-R neurons.

3.4 Nonlinear feedback coupling in H-R neurons

In this section the dynamical behaviour of two H-R neurons is examined where cubic nonlinear coupling is adopted. The excitability in neuron based excitable cells is most often associated with the presence of a cubic nonlinearity[113] in the relevant system of differential equations. When the nonlinear coupling feedback term of cubic order is added to the differential equation representing dynamical evolution of first variable of H-R model, the two neurons do not achieve full synchronization. But when a quadratic form of membrane potential is added to the differential equation representing the

behaviour of fast current variable x_2 or x_5 [113], the behaviour of dynamics exhibits an interesting behaviour. Adding cubic power of membrane potentials to neuron model helps to understand the anharmonicity in the neural systems. It is found that the coupling strengths decide the evolution of the system.

In H-R neuron, the recovery variable which is the current variable x_2 is influenced by the outward flow of Potassium ions immediately after the discharge of action potentials. The Potassium ion current slows down the returning of membrane potential to the threshold value and it also reduces frequency of repeating discharge [113]. It also allows a delay between excitable simulate and action discharge. So introduction of the quadratic form of membrane voltage between two neurons results in a coupling feedback into the flow of Potassium ions. This means a change of Potassium ion concentration affects modulation with respect to the burst interval of H-R neurons which in turn may affect chaotic synchronization of two neurons [113].

Consider the nonlinear feedback coupled H-R neurons

$$\begin{aligned}
\dot{x}_1 &= x_2 - ax_1^3 + bx_1^2 + I_{ext} - x_3 - \varepsilon\left(x_1^3 - x_4^3\right) \\
\dot{x}_2 &= c - dx_1^2 - x_2 + \omega_2\left(x_1^2 - x_4^2\right) \\
\dot{x}_3 &= r\left(s\left(x_1 - x_0\right) - x_3\right) \\
\dot{x}_4 &= x_5 - ax_4^3 + bx_4^2 + I_{ext} - x_6 - \varepsilon\left(x_1^3 - x_4^3\right) \\
\dot{x}_5 &= c - dx_4^2 - x_5 + \omega_2\left(x_4^2 - x_1^2\right) \\
\dot{x}_6 &= r\left(s\left(x_4 - x_0\right) - x_6\right)
\end{aligned} \tag{3.3}$$

Here the membrane potential of first neuron and the related ion currents across the membrane are represented by the variables $x_{1,}x_2 and\ x_3$. Parameters a, b, c, d, r, s and I_{ext} are chosen as a=1, b=3, d=5, c=1 r =0.006, s=4, I_{ext}=3.05 and initial condition of the system is chosen such that $[x_1, x_2, x_3, x_4, x_5, x_6\ ]$ are

assigned the values [0.3, 0.3, 3.0, 0.2, 0.35, 3.2] where ε and ω_2 are coupling parameters. Here $\varepsilon\left(x_1^3 - x_4^3\right)$ represents nonlinear feedback of cubic order. By varying the value of coupling strength various dynamics of chaotic neurons are analysed.

3.4.1. Linear stability analysis

We present an analysis of stability of the steady state of two H-R neurons coupled by non-linear cubic feedback coupling.

$$\dot{x}_1 = f(x_1) + \varepsilon({x_1}^3 - {x_4}^3)$$

$$\dot{x}_2 = f(x_2) + \omega_2({x_1}^2 - {x_4}^2)$$

$$\dot{x}_4 = f(x_4) + \varepsilon({x_1}^3 - {x_4}^3)$$

$$\dot{x}_5 = f(x_5) + \omega_2({x_4}^2 - {x_1}^2) \qquad (3.4)$$

Here ε and ω_2 are coupling parameters. Let $\bar{x}_1$, $\bar{x}_2$, $\bar{x}_4$, $\bar{x}_5$be the steady state of the system, then $f(x_1, \bar{x}_1)$=0, $f(x_2, \bar{x}_2)$=0, $f(x_4, \bar{x}_4)$=0 and $f(x_5, \bar{x}_5)$=0.

Let $\eta_1, \eta_{2,}, \eta_4, \eta_{5,}$ be the inifinitesimal perturbations of the system. As $\eta_1, \eta_{2,}, \eta_4, \eta_5$ grows $x_1, x_{2,} x_4$, $and x_5$ move away from steady state and if these values of decay to zero, the variable values of $x_1, x_2, x_4, and x_5$ move towards steady state.

To obtain stability of the steady state of systems, we write variational equations formed by linearizing above equations.

$$\dot{\eta}_1 = \dot{x}_1 = f(\bar{x}_1 + \eta_1) \qquad (3.5)$$

Using Taylor expansion and neglecting higher order terms,

$$\dot{\eta}_1 = \eta_1 f'(x_1, \bar{x}_1) \tag{3.6}$$

From equation (3.4) and (3.6)we get

$$\dot{\eta}_1 = f'(x_1)\eta_1 + \varepsilon(\eta_1^3 - \eta_4^3) \tag{3.7a}$$

$$\dot{\eta}_4 = f'(x_4)\eta_4 + \varepsilon(\eta_1^3 - \eta_4^3) \tag{3.7b}$$

Let the synchronization and antisynchronization tendencies are expressed through the variables $\eta_{syn}$and η_{anti} respectively. Then

$\eta_{syn} = \eta_1 - \eta_4$ and $\eta_{anti} = \eta_1 + \eta_4$

$\dot{\eta}_{syn} = \dot{\eta}_1 - \dot{\eta}_4$

$$\dot{\eta}_{anti} = \dot{\eta}_1 + \dot{\eta}_4 \tag{3.8}$$

So condition for synchronization is obtained as

$$\dot{\eta}_{syn} = \left[\frac{f'(x_1)+f'(x_4)}{2}\right]\eta_{syn} + \left[\frac{f'(x_1)-f'(x_4)}{2}\right]\eta_{anti} + \varepsilon(\eta_1^3 - \eta_4^3 - \eta_1^3 - \eta_4^3) \tag{3.9}$$

Considering the time average value of $f'(x_1)\ and f'(x_4)$ are approximately same and are replaced by effective constant value τ, the equation changes as

$$\dot{\eta}_{syn} = \tau\, \eta_{syn} \tag{3.10}$$

From equation (3.10), it is clear that cubic order feedback alone doesn't give a complete synchronization.

Similarly for other set of variables condition becomes

$\dot{\eta}_{syn} = \dot{\eta}_2 - \dot{\eta}_5$

$$= \tau\, \eta_{syn} + 2\omega_2(\eta_1^2 - \eta_4^2) \tag{3.11}$$

From equation (3.11), it is clear that synchronization is achieved through the term $2\omega_2(\eta_1^2 - \eta_4^2)$. This is in agreement with numerical analysis of the coupling scheme.

Anti-synchronization properties are obtained for the system through the same analysis described above.

$$\dot{\eta}_{anti} = \dot{\eta}_1 + \dot{\eta}_4$$

$$= \tau\, \eta_{anti} + 2\varepsilon(\eta_1^3 - \eta_4^3)$$

$$= \tau\, \eta_{anti} + 2\varepsilon.\eta_{syn}(\eta_1^2 + \eta_1\eta_4 + \eta_4^2) \quad (3.12)$$

Second term in the above equation leads to antisynchronization.

Similarly, for other set variables,

$$\dot{\eta}_{anti} = \dot{\eta}_2 + \dot{\eta}_5$$

$$= \tau\, \eta_{anti} \quad (3.13)$$

From equation (3.12) and (3.13) Jacobian matrix is written as

$$J = \begin{pmatrix} \tau & 0 \\ 2\varepsilon(\eta_1^2 + \eta_1\eta_4 + \eta_4^2) & \tau \end{pmatrix} \quad (3.14)$$

Jacobin value for equations (3.7) and (3.10) is also calculated as above and Eigen values obtained may be real which is positive or negative and corresponding fixed point is of stable node or unstable node.

Eigen value of the above equation can be obtained as

$$\lambda = \tau \mp \sqrt{\tau^2 + 8\varepsilon\tau(\eta_1^3 - \eta_4^3)} \quad (3.15)$$

Antisynchronization and Synchronization tendencies are effective when the corresponding, Lyapunov Exponents, i.e., real parts of the eigen values are negative. So condition for stability is obtained as $\eta_1^3 > \eta_4^3$.

3.4.2 Time series plot of coupled neurons with cubic order feed back

Synchronization

Synchronization of two nonlinear cubic feedback coupled H-R neurons are shown through time series analysis. As nonlinear coupling replaces linear coupling, the synchronization pattern given in Figure 3.1 changes to behavior shown in Figure 3.6 which shows synchronization of first variables for Iext=3.05. The bursting behavior for synchronization exhibited by the H-R system is an additional feature shown by the presence of nonlinear coupling.

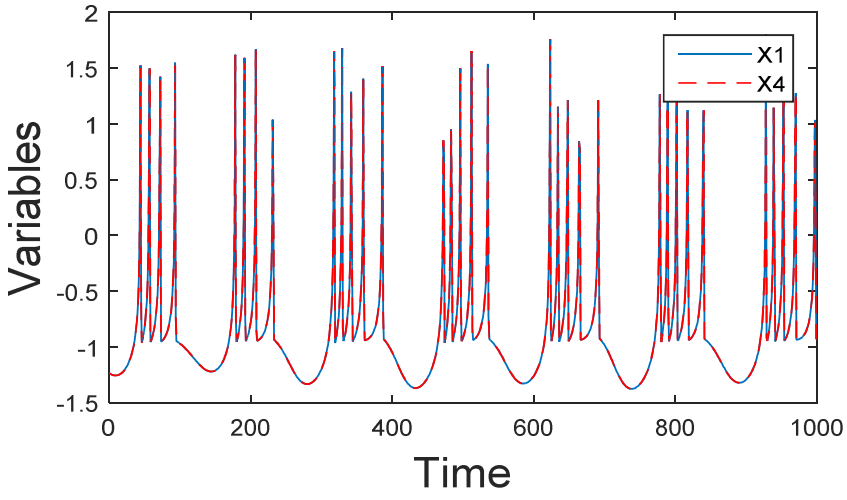

Figure 3.6: Time series plots of first variables show synchronization of coupled neurons. Bursting synchronization of neurons with nonlinear feedback in cubic order are obtained for $\varepsilon = 1, \omega_2$=1, I_{ext}= 3.05.

Anti-phase synchronization

The anti-phase synchronization of nonlinear cubic feedback coupled neurons is established through time series analysis for certain values of coupling parameters and current. Here first variables of two coupled H-R neurons are showing anti-phase properties, which are depicted through blue and red colour as shown in Figure 3.7. The plot is obtained for the parameter values $\varepsilon = 0, \omega_2$=0.001, I_{ext}= 3.00.

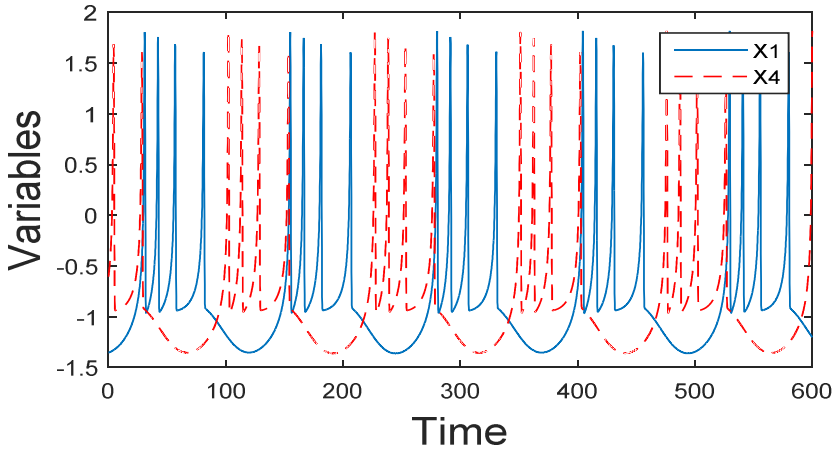

Figure 3.7: Time series plots of first variables shows anti-phase synchronization of coupled neurons with cubic non linear feedback with parameter values $\mathcal{E} = 0, \omega_2 = 0.001, I_{ext} = 3.00$.

The regions of synchronization, anti phase synchronization and amplitude death for different ranges of control parameters are depicted through Figure 3.8. Here control or coupling parameters are selected in the range ε= [0:0.5:5] and ω_2 = [0: 0.2:1.6].

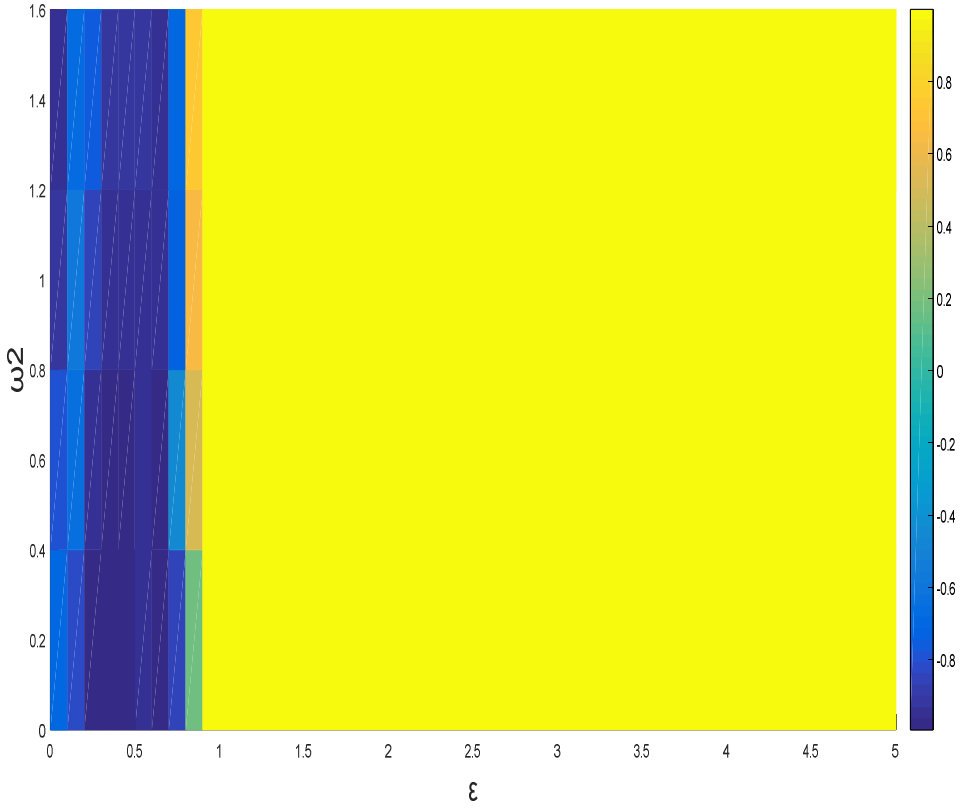

Figure 3.8: Anti phase synchronization, synchronization and amplitude death of cubic feedback coupled neurons are examined through $\varepsilon - \omega_2$ plot. When the value of ε = [0.9:0.5:5] and =[0:0.5:1.6] synchronization regions are observed and is shown by yellow color in the figure.For the range of ε = [0:0.5:0.7] and [0:0.5:1.6],dark blue region shows ant-synchronization. Also for the values of ε = [0.75:0.5:0.89] and [0:0.5:0.4], amplitude death is observed, depicted by light green.

3.4.3 Lyapunov exponent plot for nonlinear cubic feedback coupling in H-R neurons

The behaviour of nonlinear cubic feedback coupled H-R neuron is analysed through Lyapunov Exponent (LE) plot which is found to exhibit similar behaviour as in Figure 3.5. Here the low LE values indicate regularity of

the coupling method. Largest LE is obtained in the range -1.1834 to -1.1832. It is in agreement with synchronization stability of this system observed by Fang and etal.[107].

3.5. Memristor based coupling in neurons

In 1971, Leon Chua postulated the fourth basic circuit element memristor[114, 115] and established a missing constitutive relationship between the electrical charge and the magnetic flux. Using Lewis Carroll's portmanteau naming technique[116], Chua named this hypothetical nonlinear device as memristor (memory + resistor). It demonstrated the hysteresis property of the ferromagnetic core memory and also the dissipative characteristics of a resistor. Clearly, in such devices, the nonlinear resistance can be memorized indefinitely by controlling the flow of the electrical charge or the magnetic flux[117].

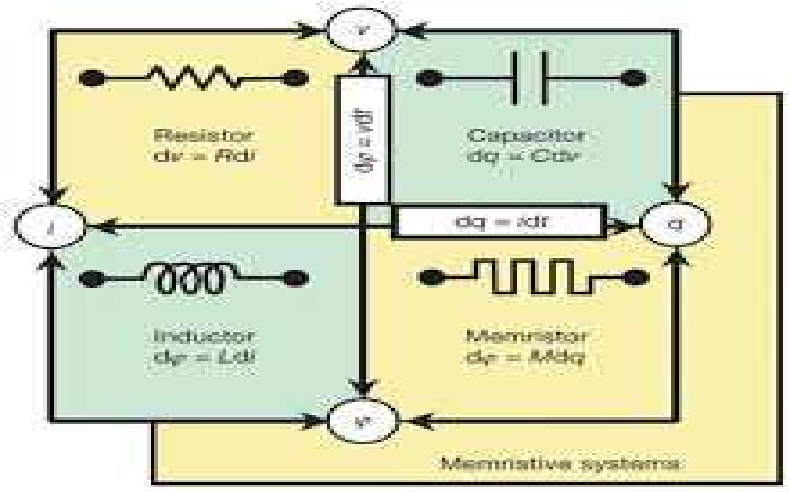

Figure 3.9: Comparison of resistor, capacitor, inductor and memristor

Memristor are nano scale devices. Although memristor and memristive systems have been introduced a long time ago by Chua, applications of them

have developed recently after the invention of the nano–scale HP memristor [118].

A memristor consists of a variable resistance and has two terminals. In DRAM a memristor can replace the capacitor which can store one bit of data. Then this memory is not volatile, has no leakage power which at the same time is more stable. Also in comparison with flash memory, this memory has improved speed and scalability. A memristor can also connect electric charge to magnetic flux. As its resistive value is retained it can increase flow of current in one direction and can decrease flow of current in the opposite direction.

Memristor finds improved applications[119] in logic circuits and in digital memory. In neuromorphic systems they can act as basic building blocks where they behave like biological synapses. Neurons and synapses act as electronic systems. Besides being at the basis of next-generation ultra dense non-volatile memories, a nano scale memristor also has the potential to reproduce the behaviour of a biological synapse. As in a living creature the weight of a synapse is adapted by the ionic flow through it, so the conductance of a memristor is adjusted by the flux across or the charge through it depending on its controlling source[86].

The proposed memristor are having cubic nonlinearity which is represented by $q(\phi)=k_1\phi+k_3\phi^3$. It is a smooth continous cubic functionand corresponding memductance is $W(\phi)=k_1+3k_3\phi^2$. It is used as a memristive coupling term and will act as a artifical synapse between coupled neuron cells. Hence they are responsible for chaotic dynamics in the system.

In this section two Hindmarsh-Rose neurons are considered, coupled via a memristive device mimicking a biological synapse. The investigation is done

on how the dynamics of the memristive element may influence the synchronization and other interesting properties.

3.5.1 Memristor controlled by cubic order flux

Flux controlled memristor is used to emulate the excitatory and inhibitory synaptic connection between the neurons[86]. It is used as a memristive coupling term and will act as a artifical synapse between coupled neuron cells.

Consider the memristive mutual coupled H-R equations as below

$$\begin{aligned}
\dot{x}_1 &= x_2 - ax_1^3 + bx_1^2 + I_{ext} - x_3 - (\alpha + \beta u^2)(x_1 - x_4) \\
\dot{x}_2 &= c - dx_1^2 - x_2 \\
\dot{x}_3 &= r(s(x_1 - x_0) - x_3) \\
\dot{x}_4 &= x_5 - ax_4^3 + bx_4^2 + I_{ext} - x_6 - (\alpha + \beta u^2)(x_4 - x_1) \\
\dot{x}_5 &= c - dx_4^2 - x_5 \\
\dot{x}_6 &= r(s(x_4 - x_0) - x_6) \\
\dot{u} &= x_1 - x_4
\end{aligned} \tag{3.13}$$

The variable x_1 represents the membrane potential of a neuron and the variables x_2 and x_3 are related ion currents across the membrane. Where and x_4 gives the coupling between the neurons achieved through memristor.u is flux variable due to memristor. Here the memductance term $(\alpha + \beta u^2)$ function as cubic flux controlled memristive term and act as coupling synapse between two neurons.

3.5.1.1. Linear stability analysis of cubic flux controlled memristor coupling

We present the analysis of stability of the steady state of two H-R neurons coupled by cubic flux controlled memristor.

$$\dot{x}_1 = f(x_1) - c(\propto + \beta u^2)(x_1 - x_4)$$

$$\dot{x}_4 = f(x_4) + c(\propto + \beta u^2)(x_1 - x_4)$$

$$\dot{u} = (x_1 - x_4) \tag{3.14}$$

Here $\propto$ and β are coupling parameters and c is a constant. Let $\bar{x}_1, \bar{x}_4, \bar{u}$ be the steady state of the system, then $f(x_1, \bar{x}_1)$=0, $f(x_4, \bar{x}_4)$=0 and $f(u, \bar{u}) = 0$.

Let η_1, η_4, u be the infinitesimal perturbations of the system. As η_1, η_4, z grows $x_1, x_4 \; and \; u$ move away from steady state, if these values decay to zero $x_1, x_4 \; and \; u$ move towards steady state.

To obtain stability of the steady state of two systems, we write variational equations formed by linearizing equation as below.

$$\dot{\eta}_1 = \dot{x}_1 = f(\bar{x}_1 + \eta_1)$$

Using Taylor expansion and neglecting higher order terms,

$$\dot{\eta}_1 = \eta_1 f'(x_1, \bar{x}_1)$$

$$\dot{\eta}_1 = f'(x_1)\eta_1 - c(\alpha + \beta u^2)(x_1 - x_4)$$

$$\dot{\eta}_4 = f'(x_4)\eta_4 + c(\alpha + \beta u^2)(x_1 - x_4) \tag{3.15}$$

Let the synchronization and antisynchronization tendencies are expressed through the variables η_{syn} and η_{anti}respectively.

Then

$\eta_{syn} = \eta_1 - \eta_4$ and $\eta_{anti} = \eta_1 + \eta_4$ (3.16 a)

$\dot{\eta}_{syn} = \dot{\eta}_1 - \dot{\eta}_4$ (3.16b)

$\dot{\eta}_{anti} = \dot{\eta}_1 + \dot{\eta}_4$ (3.16c)

From equation (3.14) equation (3.16 a) changes as

$\dot{\eta}_{syn} = \left[\frac{f'(x_1)+f'(x_4)}{2}\right]\eta_{syn} + \left[\frac{f'(x_1)-f'(x_4)}{2}\right]\eta_{anti} - 2c(\alpha + \beta u^2)\eta_{syn}$ (3.17)

Considering the time average value of $f'(x_1)\ and f'(x_4)$are approximately same and replaced by effective constant value τ, equation changes as

$\dot{\eta}_{syn} = \tau\,\eta_{syn}$-$2c(\alpha + \beta u^2)\eta_{syn}$ (3.18.a)

Similarly we get,

$\dot{\eta}_{anti} = \tau\,\eta_{anti}$ (3.18.b)

$\dot{u}$=$c\eta_{syn}$ (3.18.c)

From equation (3.18 a) Lyapunov Exponent is obtained as

$\lambda = \tau - 2c(\alpha + \beta u^2)$ (3.19)

The synchronization and anti synchronization tendencies effective when corresponding Lyapunov Exponents, i..e, real part of eigenvalues are negative. So condition for stability is given as below.

$$\beta > \frac{\tau}{2cu^2} - \alpha \qquad (3.20.)$$

These synchronization conditions are compatible with the numerical evaluation. Also the antisynchronization properties are not exactly observed for memristor coupled systems .It is also evident from the equation (3.18.b).

3.5.1.2 Time series plot of coupled neurons with cubic flux controlled memristor

Bidirectional coupling

In bidirectional coupling both neurons are influenced by a memristor of cubic order flux. Synchronization and amplitude death behaviour are exhibited by the system as described below.

Synchronization behaviour in bidirectional coupling

Synchronization of H-R neurons coupled by cubic flux controlled memristor shows chaotic bursting synchronization for the parameters a=1, b=3, d=5, c=1, α=0.05, β=0.5 and I_{ext}=3. Time series plots of first variables x_1 and x_4 shows synchronization pattern where the number of spikes per burst is irregular. The dynamics exhibited is very similar to that of coupled neurons with cubic order feed back and it is shown in Figure 3.6.

Amplitude death

As the values of α, β and current are changed, time series plots of cubic flux controlled memristor coupled H-R neurons shows the amplitude death state

as shown in Figure 3.10. Here first variables of coupled H-R neurons comes to a common stady state which was unstable other wise.The parameter values are set as α=0.005, β= 0, I_{ext}=3 for obtaining the plot.

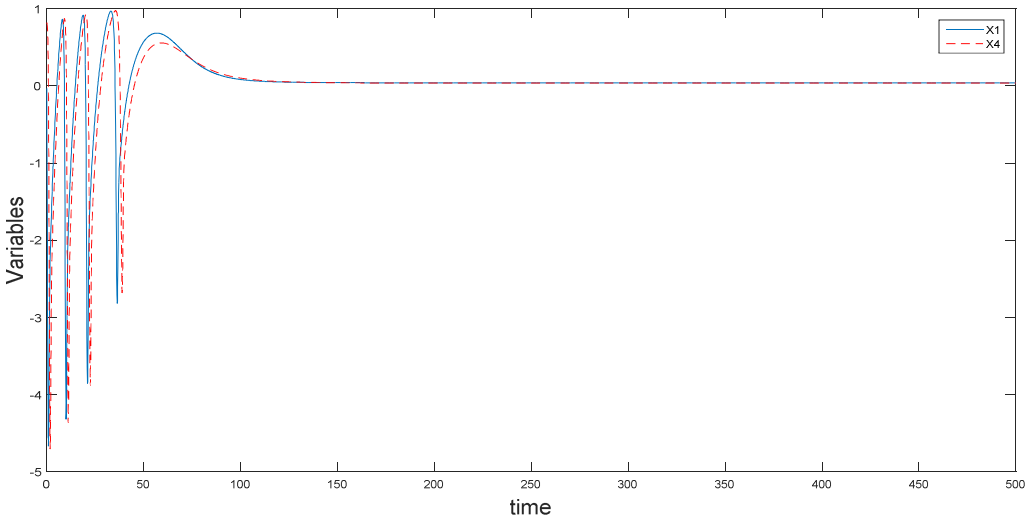

Figure 3.10: Time series plots of first variables $x_1 and x_4$of cubic flux controlled memristor shows amplitude death state. When the parameter values are set as α=0.005, β= 0, I_{ext}=3 amplitude death states of neurons are emerging out.

Unidirectional coupling

In unidirectional coupling only one neuron is triggered by a memristor of cubic order flux while the other neuron is not influenced by coupling. In the scenario represented by equation (3.13), as the bidirectional coupling is replaced with unidirectional coupling of cubic flux controlled memristor, the x_1 variable (the membrane potential of first neuron) is not infulenced by the term $(\alpha+\beta u^2)(x_1-x_4)$. The dynamics observed are shown through Figure 3.10-Figure 3.13.

Synchronization behaviour in unidirectional coupling

Synchronization pattern of two H-R neurons coupled with unidirectional cubic flux controlled memristor is shown in Figure 3.11 through time series analysis. Here bursting synchronization of bidirectional coupling is replaced by the tonic spiking in unidirectional coupling. As the neuron is stimulated, the inhibitory ion currents will dominate the stimulating current and corresponding membrane potential will decrease. Persistence of this activity leads to tonic spiking. The plot is obtained for the parameter values I_{ext} =2.8, α =0.001, and β=0.02.

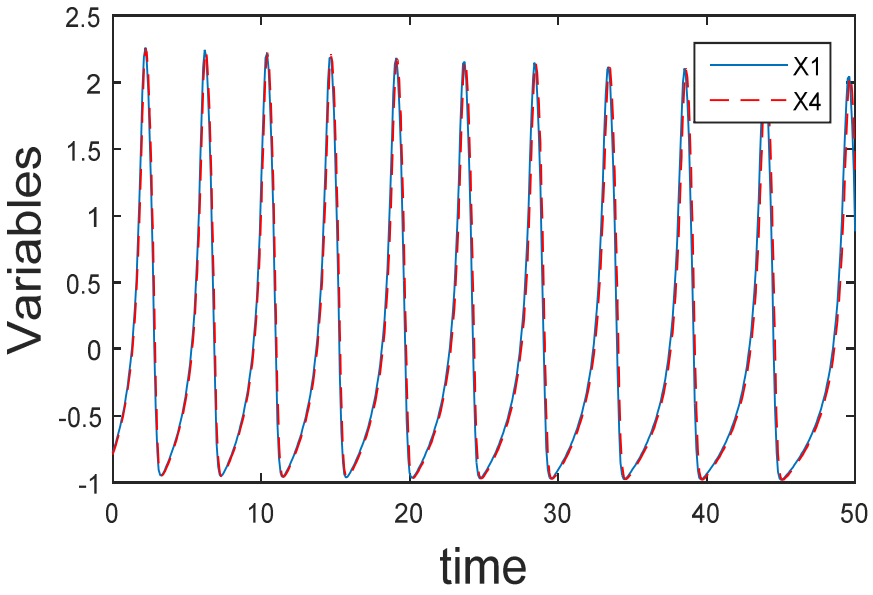

Figure 3.11: Time series plots of first variables $x_1 and\ x_4$shows synchronization pattern in unidirectional coupled cubic flux controlled memristor. The parameters are chosen as I_{ext} =2.8, α=0.001, and β=0.02 for obtaining tonic synchronization pattern of neurons.

Tonic spiking of one neuron and the inactive state of the other neuron in unidirectional coupling

Time series analysis of two H-R neurons coupled with unidirectional cubic flux controlled memristor leads to tonic spiking of the neuron which is coupled with and inactive or death state of the uncoupled neuron as shown in Figure 3.12.

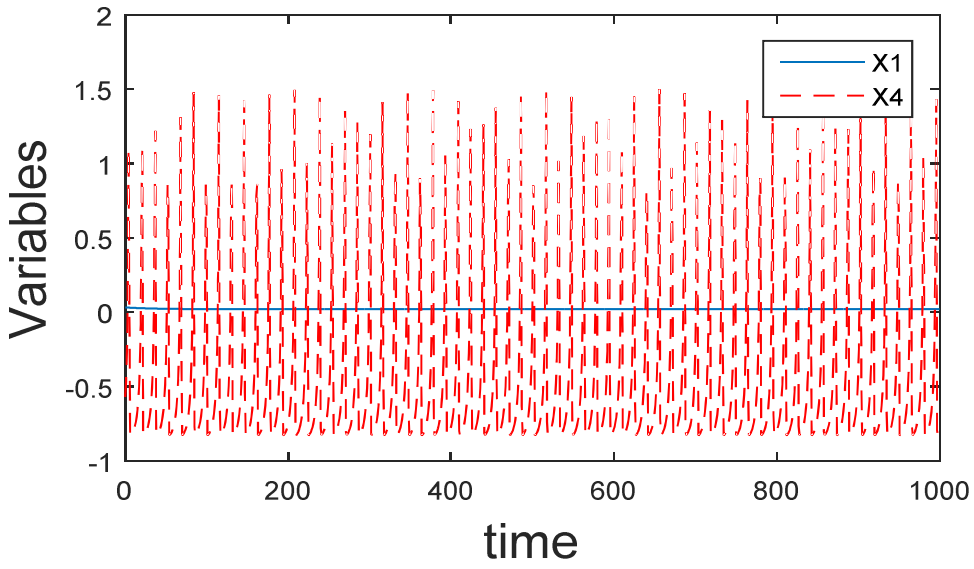

Figure 3.12: Time series plots of first variables x_1 *and* $x_4$of the two coupled neurons. Here the coupling is unidirectional through flux controlled memristor. With parameter values d=2.82, I_{ext} =4, α=1,and β=0.01 tonic spiking is shown up for one neuron and inactive or death state is exhibited by the uncoupled neuron.

Bursting and death of neuron

As the parameters are changed, the tonic spiking give way to bursting for the coupled neuron while the uncoupled neuron remains in the resting state for two H-R neurons coupled with unidirectional cubic flux controlled

memristor. The dynamics is established through time series plots (Figure 3.13) for the parameter values I_{ext} =5, α= 0.02 and β=0.

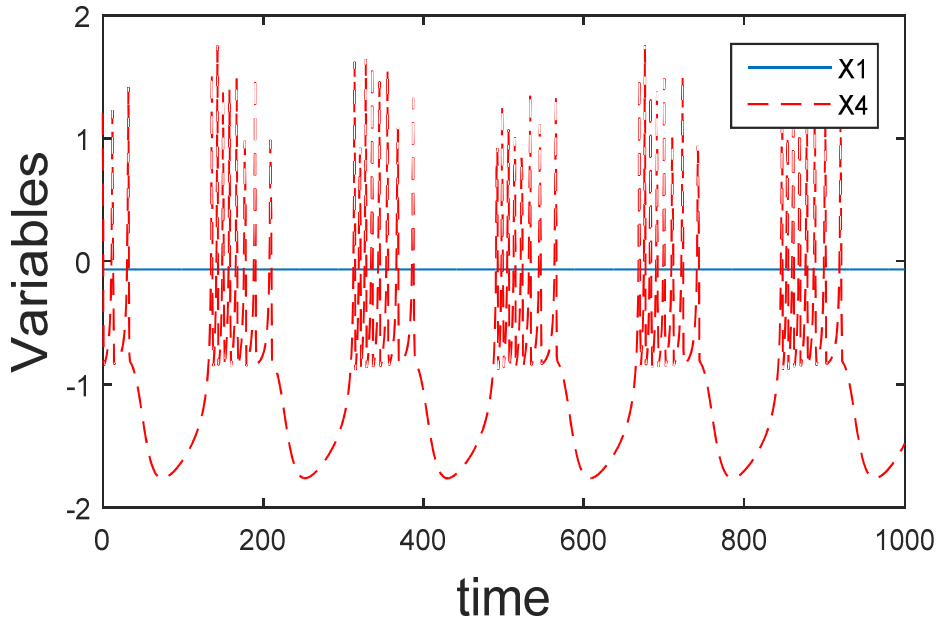

Figure 3.13: Time evolution of first variables x_1 *and* x_4 for unidirectional coupled cubic flux controlled memristor. As the parameter is changed to I_{ext} =5, α=0.02 and β=0, coupled neuron exhibits the bursting but the other neuron seems to be inactive.

Anti-phase dynamics

For still other parameter values it is interesting to report anti phase synchronization of two H-R neurons with unidirectional coupled cubic flux controlled memristor as shown in Figure 3.14. Here bursting behaviour of two neurons shows anti phase dynamics. To obtain the desired plot, parameter values are set as I_{ext} =2.8, α =0.02, and β=0.3.

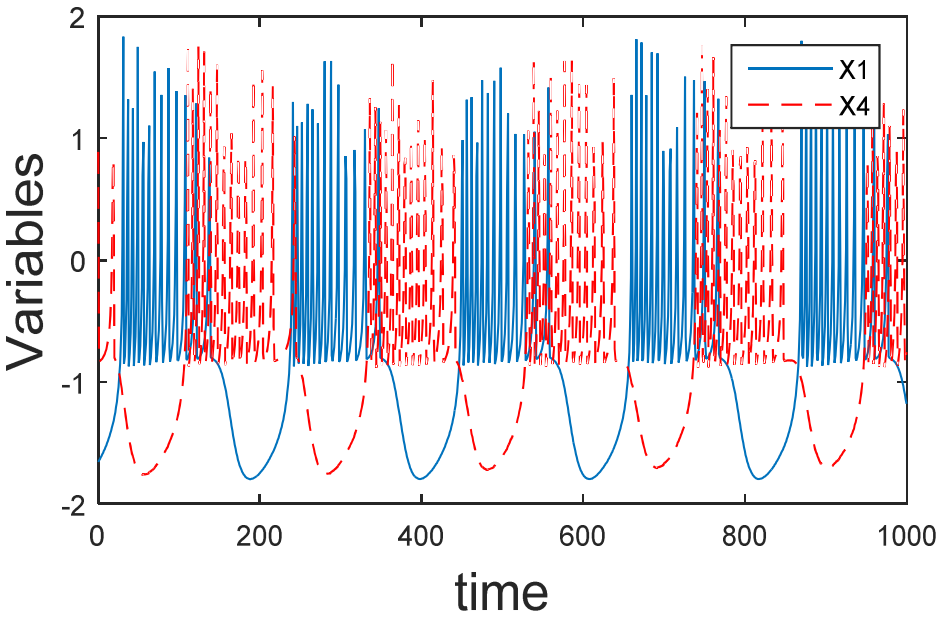

Figure 3.14: Time series plots of first variables x_1 $and x_4$shows anti phase synchronization in unidirectional coupled by cubic flux controlled memristor. Anti-phase dynamics obtained above has some similarity with that of time series plot of Firing pattern of autapic neuron[114]. Parameters are chosen as I_{ext} =2.8, α=0.02, and β=0.3.

3.5.1.3 Lyapunov exponent plot

The dynamics of Lyapunov Exponents for H-R neurons coupled with cubic flux controlled memristor is shown in Figure 3.15. It is observed that largest LE value is close to 1 (0.9727). Positive value of LE's obtained due to coupling having much importance. For arterial blood pressure time series, ocular aberration dynamics of human eye etc. shows positive Lyapunov Exponents. So our coupling scheme can be referred to some neural base system analysis.

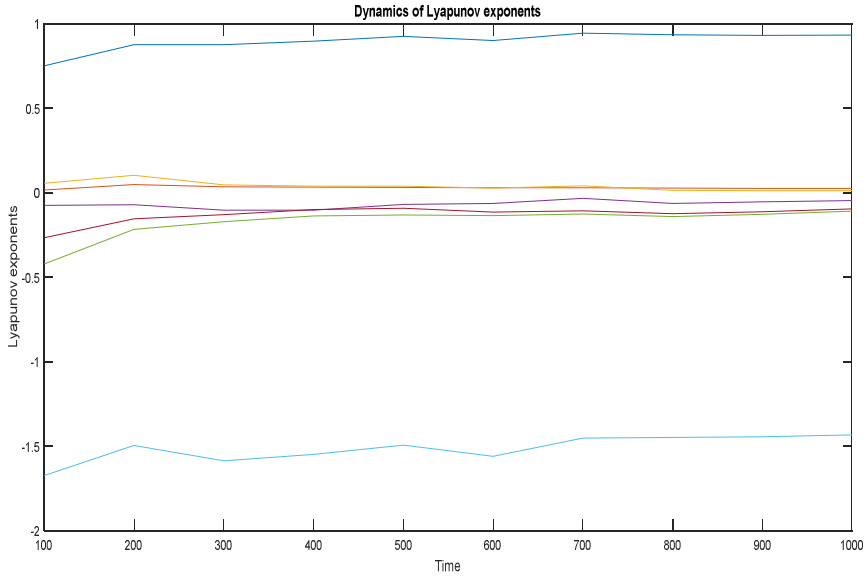

Figure 3.15: Lyapunov Exponent plot for cubic flux controlled memristor coupled with H-R neurons.

3.5.2 Memristor controlled by quadratic flux

The properties of memristor controlled by quadratic flux with varying coupling strengths and external currents are studied. For the quadratic flux-controlled memristor [121] studied in this section, the memristance can be expressed as:

$$M(\phi)=\alpha\phi^2+\beta\phi+\gamma \tag{3.21}$$

We can see that, $M(\phi)$ is linear flux-controlled as $\alpha=0$. Memristor of this type has been researched widely, so we focus on the influence of quadratic type coupling in H-R neuron. The term $M(\phi)=\alpha\phi^2+\beta\phi+\gamma$ act as quadratic memristive function.

$$
\begin{aligned}
\dot{x}_1 &= x_2 - ax_1^3 + bx_1^2 + I_{ext} - x_3 - \left(\alpha\phi^2 + \beta\phi + \gamma\right)\left(x_1 - x_4\right) \\
\dot{x}_2 &= c - dx_1^2 - x_2 \\
\dot{x}_3 &= r\left(s\left(x_1 - x_0\right) - x_3\right) \\
\dot{x}_4 &= x_5 - ax_4^3 + bx_4^2 + I_{ext} - x_6 - \left(\alpha\phi^2 + \beta\phi + \gamma\right)\left(x_4 - x_1\right) \\
\dot{x}_5 &= c - dx_4^2 - x_5 \\
\dot{x}_6 &= r\left(s\left(x_4 - x_0\right) - x_6\right) \\
\dot{u} &= x_1 - x_4
\end{aligned}
\tag{3.22}
$$

The variable x_1 represents the membrane potential of a neuron and the variables x_2 and x_3 are related ion currents across the membrane for first neuron. Here parameters are taken as a=1, b=3, d=5, c=1, d=2.84, r=0.005, s=4 and k=1.

3.5.2.1 Linear stability analysis

As in section 3.5.1, we can do linear stability analysis of quadratic flux controlled memristor. Then the condition for stability in quadratic flux controlled memristor is obtained as

$$\beta > \left(\frac{\tau - A}{2C\varphi} - \alpha\varphi\right) \tag{3.23}$$

3.5.2.2 Phase portrait and time series plots of memristor coupled neurons controlled by quadratic flux

Synchronization

Synchronization of two H-R neurons coupled with quadratic flux controlled memristor is shown through the $x_2 - x_5$ plot. Parameter values are selected as I_{ext} =2, α=2, β=1 and γ=1. Here two neurons behave in the same way and full synchronization is achieved as shown in Figure 3.16.

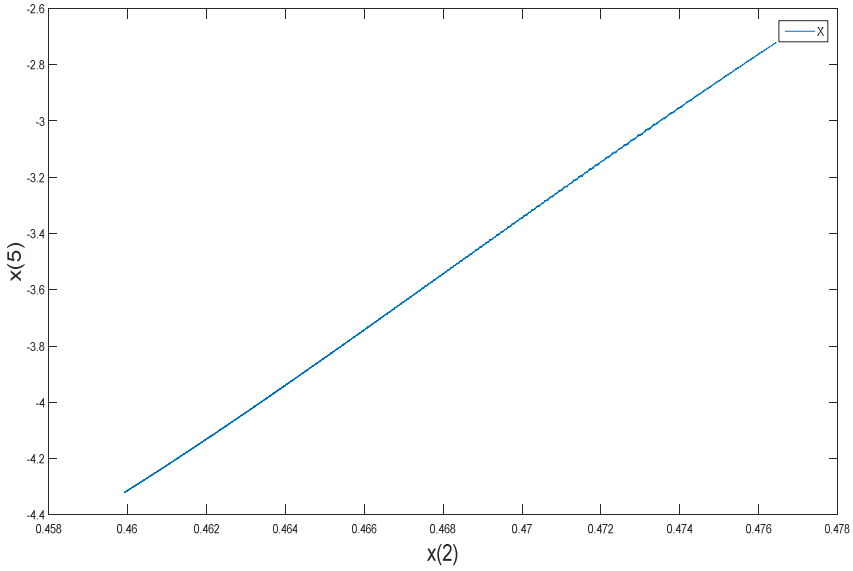

Figure 3.16: Phase portrait of second variables x_2 *and* $x_5$shows synchronization pattern of memristor controlled by quadratic flux. Synchronization is observed for the parameters I_{ext} =2, α =2, β=1 and γ=1.

Oscillation death

Time series of two variables x_1 and x_4 of H-R neurons coupled with quadratic flux controlled memristor shows oscillation death for the parameter values I_{ext} =1.4, α=1, β=0 and γ=1. The coupled two neurons takes a stable rest state as depicted in Figure. 3.17.

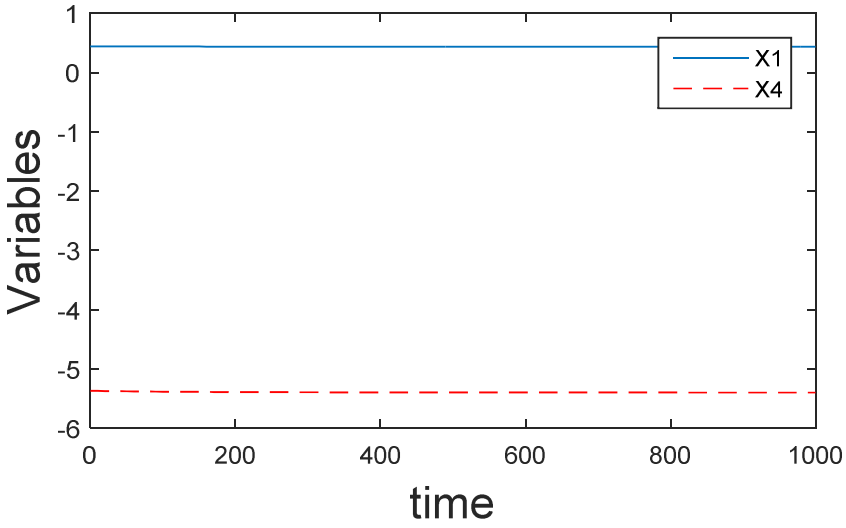

Figure 3.17: Time series plots of first variables x_1 and x_4 of neurons with quadratic flux controlled memristor. With parameter values I_{ext} =1.4, α=1, β=0 and γ=1 oscillation deaths of neurons which are controlled by memristor having quadratic flux are shown.

Near death spikes

For someparameter values an interesting dynamics is exhibited by the H-R neurons which are coupled via quadratic flux controlled memristor. Rare spikes are observed with time variation of variables of two neurons before death (Near Death rare Spikes [122–124]). Experimentally it is observed that moments before death, the patients experiences a burst in brain wave activity, with the spikes occuring simultaneously for two coupled neurons and with approximately of same intensity and duration around the time slot 125 which is shown in Figure 3.18.

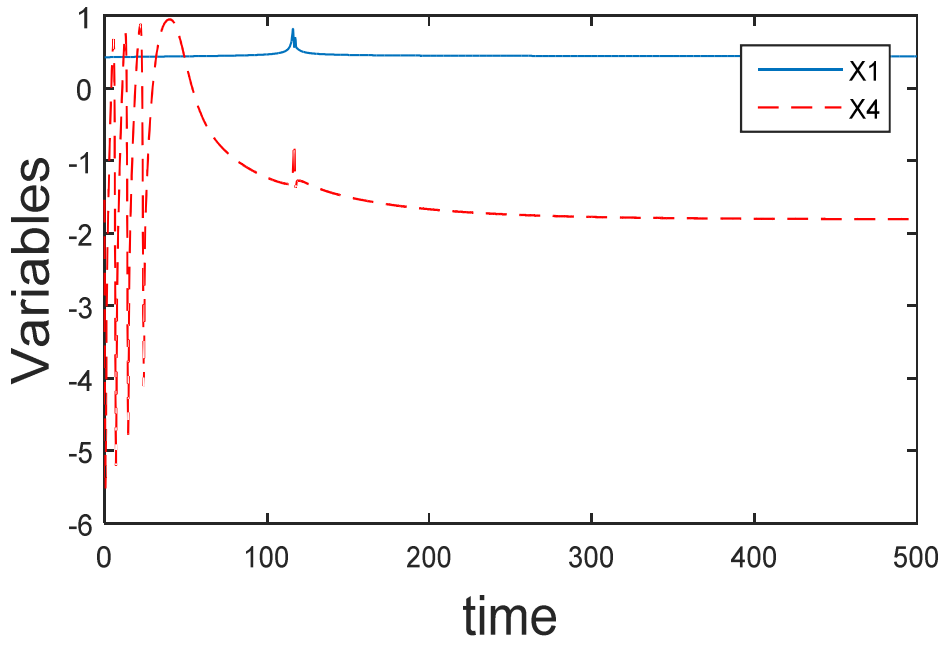

Figure 3.17: Time series plots of first variables x_1 and x_4 of neurons with quadratic flux controlled Memristor. Dynamics obtained for parameter values I_{ext} =4, α=5, β=1, γ=0 and I_{ext} =3, α=2, β=1, γ=0 shows phenomena like near death rare spikes.

The near death spikes are supported by experimental observation [122–124]. Experimentalists implanted several electrodes across the brains of nine rats to measure their brain waves rhythmic pulses of neural activity depending on their frequency. The rats were sedated with anesthetic, and then killed with either by a lethal injection that stopped their hearts, or a fatal dose of carbon dioxide, after the hearts have stopped, most of these brainwaves weakened with time. But one set, the low-gamma waves produced when neurons fire between 25-55 times per second, became stronger for a brief period. The activity in different parts of their brains also became more synchronized. Their low-gamma waves, in particular, became synchronized when they were in their near-death state than when they were anaesthetized or awake [122–124].

3.5.2.3 Lyapunov exponent plot

Lyapunov exponent plot for H-R neurons coupled with quadratic flux controlled memristor dynamics is shown through Figure 3.19. Sensitivity to initial condition of systems and its regularity are examined through plot.

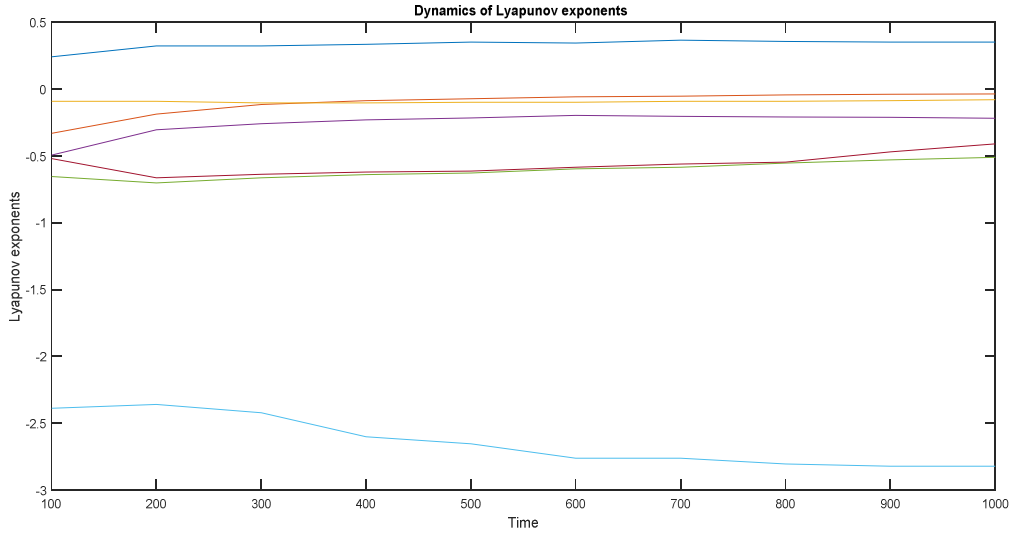

Figure 3.19: Lyapunov exponent plot for quadratic flux controlled memristor coupled with H-R neurons.

3.5.3 Memristor controlled by exponential flux

The cubic flux controlled memristor have limitations in situations which demand a larger current[125] and not compatible with terminal voltage fluctuations. Here the memductance or Memristance always keep increasing or decreasing until polarity of voltages or current reverses. The proposed exponential model obeys stable variation law of the memductance (memristance) under various excitation voltages[125] and hence this model

meet large current situations. So the memristor controlled by exponential flux is chosen for coupling parameter.

A novel model of the flux-controlled memristor is selected as below

$$q(\phi) = kb\left(a^{bq} - 1\right) \tag{3.23}$$

Where $a \rangle 0$, and kb $a \rangle 0$. Then, the memductance function of this memristor can be given by

$$W\ (\phi) = a^{bq} kb \ln a \tag{3.24}$$

When $b \langle 0$, above equation model is a decremented flux-controlled memristor, that is, it's Memductance is monotonically decreasing (increasing) when the supply voltage is positive (negative). On the contrary, when $b \rangle 0$, equation presents an incremental flux-controlled memristor.

Consider the exponential flux controlled H-R model equations as

$$\begin{aligned}
\dot{x}_1 &= x_2 - x_1^3 + bx_1^2 + I_{ext} - x_3 - a^{bq} kb \ln a\left(x_1 - x_4\right) \\
\dot{x}_2 &= c - dx_1^2 - x_2 \\
\dot{x}_3 &= r\left(s\left(x_1 - x_0\right) - x_3\right) \\
\dot{x}_4 &= x_5 - x_4^3 + bx_4^2 + I_{ext} - x_6 - a^{bq} kb \ln a\left(x_4 - x_1\right) \\
\dot{x}_2 &= c - dx_4^2 - x_5 \\
\dot{x}_3 &= r\left(s\left(x_4 - x_0\right) - x_6\right) \\
\dot{u} &= x_1 - x_4
\end{aligned} \tag{3.25}$$

The variable x_1 represents membrane potential of a neuron and the variables x_2 and x_3 are related ion currents across the membrane for first

neuron. The term $a^{bq} kb \ln a$ is a function that act as exponential flux controlled memristor. The parameters take values b=3, c=1, d=5, r=0.005, a=e, b=50log(0.5), k=10. With the variation of external current various dynamics are obtained as in Figure. 3.14-Figure.3.17.

3.5.3.1 Linear stability analysis

For exponentially flux controlled memristor coupling with H-R neurons, the condition for stability is found to be

$$\tau < 2a^{bq} kblna \tag{3.26}$$

For decrimental flux controlled memristor (b<0) the condition for stability is reversed.

3.5.3.2 Phase portrait and time series plot of memristor coupled neurons controlled by exponential flux

Synchronization

Phase portrait plots of second variables x_2 and x_5 of two H-R neurons coupled with exponential flux controlled memristor shows synchronization similar to that of quadratic flux controlled memristor (Figure.3.15).

Response to external current

The response of membrane potential of two coupled neurons with respect to time is examined in detail which is shown in Figure. 3. 20. When the external current is set to I_{ext} = 3, the neuron is stimulated and the membrane potential will change. Initially due to stimulating ionic currents, the membrane potential will increase. After a certain point, the inhibitory ionic currents will dominate the stimulating currents and the membrane potential will decrease

which Results in a spike which represents action potential. If this behaviour is persistent, then it is called tonic spiking.

(a)

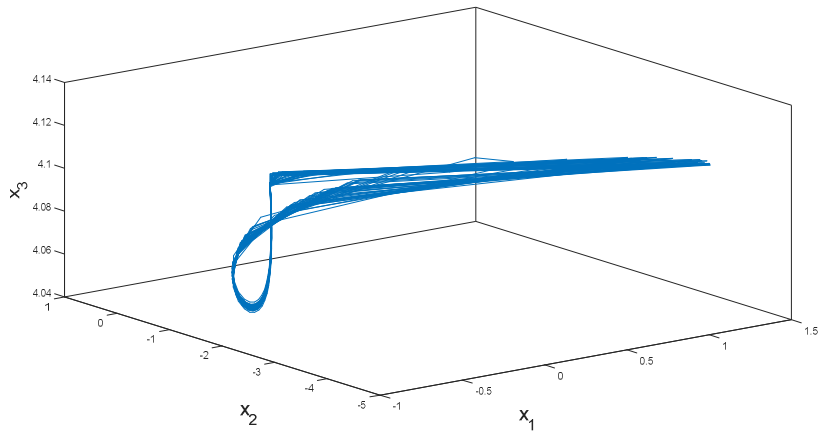

(b)

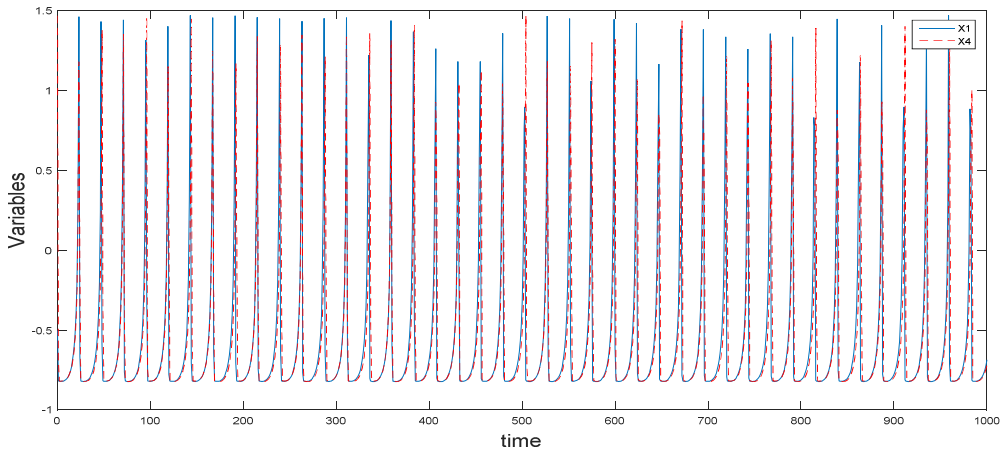

Figure 3.20: (a) Three dimensional x_1, x_2, x_3plot shows dynamics of the system. **(b)** Time series plots of first variables x_1 *and* x_4 of neurons which are coupled through a memristor controlled by exponential flux. When external current is set to I_{ext} = 3, tonic spike synchronization of neurons are obtained.

Bursting synchronization

As the external current is changed bursting synchronization is resulted in and the corresponding phase space plot of two H-R neurons coupled with exponential flux controlled memristor shows (Figure 3.21) interesting dynamics.

(a)

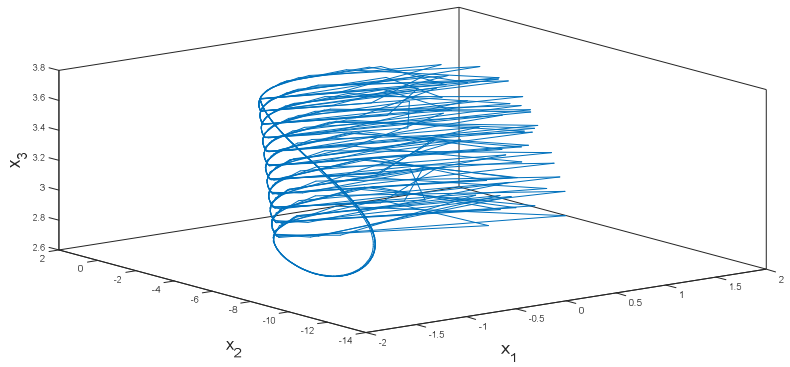

(b)

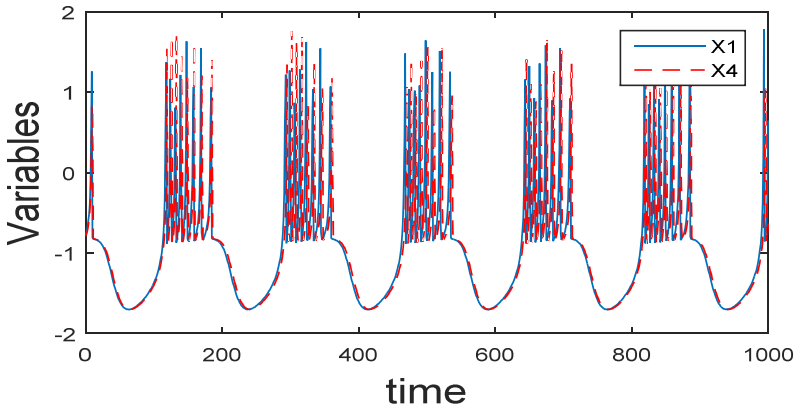

Figure 3.21: (a) Dynamical behaviour of system shown through three dimensional x_1, x_2, x_3 plot. (b)Time series plot of first variables $x_1 and\ x_4$ shows bursting synchronization of neurons where coupling is due to memristor which is controlled by exponentially varying flux and here external current is set to I_{ext}=4.

Oscillation death

Time series plots of first variables x_1 and x_4 of two H-R neurons coupled with exponential flux controlled memristor shows oscillation death for certain parameter values. If the parameter values a, b, d and Iext are chosen as a=1, b=0.01, d=2.82, and I_{ext}=3.8, the two neurons approach a stable rest state as in the case of quadratic flux controlled Memristor as shown inFigure3.16.

3.5.3.3 Lyapunov exponent plot

Dynamics of Lyapunov Exponent of H-R neurons coupled with exponential flux controlled memristor is shown in Figure 3.22. Higher value reflects greater sensitivity and low value shows regularity. Largest LE values are in range -1.0457 to -1.0456.

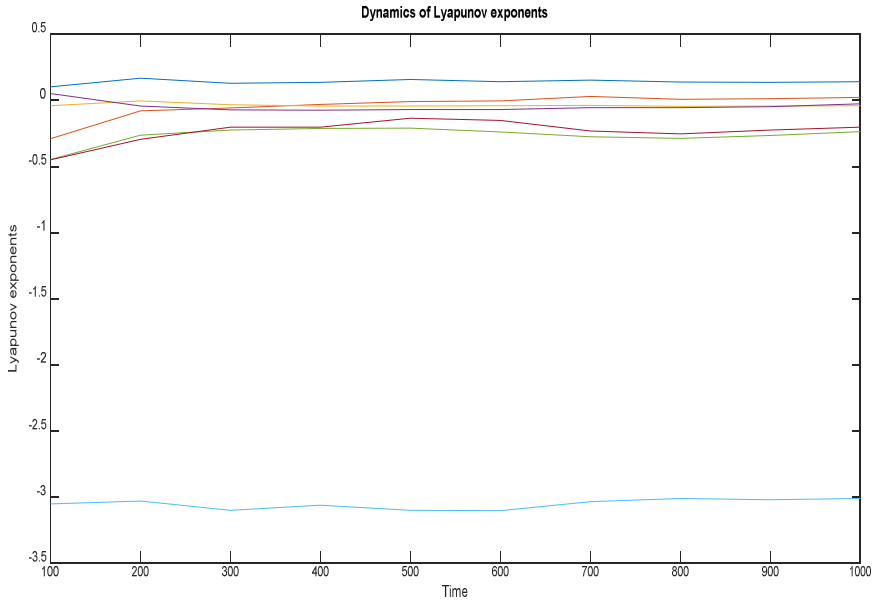

Figure 3.22: Lyapunov Exponent plot for exponentially flux controlled memristor coupled with H-R neurons.

Among different memristor coupling, cubic flux controlled memristor coupling in H-R neurons shows more chaotic behaviour since it has largest Lyapunov value is close to one.

3.6. Summary

The present work describes the possibilities of linear and nonlinear coupling in neurons. It has implications for the analysis and characterization of neuronal interactions.

Linear models of effective connectivity in brain assume that the multiple inputs to a brain region are linearly separable. This assumption does not allow activity-dependent connections that are expressed in one context which is not reflected in the other. This problem is overcome by adopting nonlinear models that include nonlinear interactions among inputs. These interactions can be considered as a context- or activity-dependent modulation of the influence that one region exerts over another [126].

The present work establishes the fact that indirect synaptic coupling dynamics of H-R neurons exhibits the properties like synchronization, anti phase synchronization and amplitude death. As feedback coupling is varying in a cubic order, synchronization and antisynchronization regions are observed.

Different memristor based couplings are also taken in to account. Both bidirectional and unidirectional coupling of cubic flux controlled Memristor in H-R neurons are examined. Mutual coupling of two neurons governed by H-R equations exhibits the properties of synchronization in tonic spiking and bursting. It also exhibits the property of amplitude death for certain values of coupling parameters. The unidirectional coupling shows tonic spiking or

bursting for one of the neurons and death like phenomenon for the uncoupled neuron depending upon the coupling coefficient and external current.

Memristor coupling of quadratic order shows the behaviour of synchronization, oscillation death and other interesting dynamics like near death rare spikes for the neurons. Memristor controlled by exponential flux also showed the synchronization and oscillation death but near death rare spikes are found to be absent.

We have done the general stability analysis for various couplings in H-R neurons. Lyapunov Exponent plots are also examined in each case. It is observed that among different Memristor based coupling, cubic flux controlled Memristor shows more chaotic nature.

The present work is on the effect of different coupling schemes in biological neuron model. The rich dynamical behaviour exhibited by the coupled systems depends upon system parameter values. We also intend to extend the work to latest developments in the field of Memristor, such as Spintronic memristor, and to its potential applications in neuromorphic circuits.

Chapter 4
Influence of Memristor and Noise on H-R neurons

Chapter 4
Influence of Memristor and Noise on H-R neurons

4.1. Introduction

When noise and external electromagnetic radiation is imposed on the neuronal model, it can influence mode transition of electric activities and synchronization pattern formation. In the present chapter improved Hindmarsh Rose neuron model (H-R neuron) is selected and the electrical activity of the neuron model under the influence of quadratic and exponential flux controlled memristor is analysed. Different neuronal responses towards noise which acts as the control parameter are studied. The Hamilton energy is computed and the stability analysis for the system is performed. Hence the work gives a pathway to understand influence of electromagnetic flux on the overall activity of neurons and it is established that it introduces high nonlinearity to the neuron model.

The role of electrical activity of neurons for neuroprotection [127] is an emergent research field. When neuron is exposed to electromagnetic radiation, the effect of radiation could be described by an equivalent current in neuronal loop [128] and the corresponding electrical activities could be detected. Experimental studies of complex electrical activities in cardiac tissues with electromagnetic induction are reported which say that these activities causes spiral waves, encounter breakup and turbulence in electrical activities [129].

Nowadays the electromagnetic induction studies [130] on neuronal networks are carried out where memristor is used to describe the memory effect which remembers the magnetic flux across the membrane of neurons or cells. Memristors (memory+ resistors) are nano scale devices, where the nonlinear resistance can be memorized indefinitely by controlling the flow of the

electrical charge or the magnetic flux[131,132]. The non –volatile memory property of a memristor is a consequence of state dependent ohms law. So it affects the potential difference and may lead to a structural change due to the supplied electrical energy[133]. The 'on' state is represented by a memory function. A conservation function gives the time-varying resistance which represents the 'off' state[133]. It can be used as a synapse in hardware of artificial neural networks. The magnetic effect due to memristor is similar to that of atomic scale magnetic susceptibility exhibited by NMR spectroscopy and of MRI imaging[134]. Memristive neural network studies help to integrate information in different functionally specialized regions of brain. Further, the neuronal synchronization helps to encode information in brain through different coherent states which arise through temporal patterns of neural activity and it emulates even an optical illusion [135,136].

Recent studies of coupled networks under electromagnetic induction show that the synchronization of neurons also causes enlargement of frequency spectrum and self-induction effect[137]. When external electromagnetic radiation is imposed on the Fitzhugh–Nagumo neuron model[138,65], it helps to detect the mode transition of electrical activities in a myocardial cell.

Noise also can influence and enhance the synchronization pattern formation in excitable systems[139]. The local magnetic flux density due to neurons is very much less than that of the Earth's magnetic field. So the surrounding noise always becomes comparable to neuronal magnetic signal. The influence of noise can be studied by changing its frequency or intensity[140]. It is also reported [141] that information processing due to synchrony can be modulated by noise.

Energy is an important parameter which influences the normal behaviour of brain and its usage mainly depends on the rate of variation of

action potential and also on the fraction used by brain for signaling activity. Various studies [142-144] are done on metabolic energy for neural activity, energy efficient neural codes, collective behaviour of biological oscillators and its energy cost. It is reported that the energy is much dependent on the mode of electrical activities instead of the external forcing currents directly and a smaller energy occurs under bursting states[145]. The study helps to understand the onset of epilepsy (bursting synchronization induced epilepsy makes energy release). The calculation of Hamilton energy of the neuron systems based on Helmholtz's theorem can explain neurobiological energy states[146]. It is also observed that an event based minimum energy input is desirable clinically for brain simulation treatment of neurological diseases (like Parkinson's disease)[147]. The delayed response of Hamilton energy to external forcing currents confirms that neuron contributes to energy coding[148,149]. These results prompt for further investigation on energy problems in neuronal network.

Bifurcation analysis[150] of H-R neuron helps to understand the relationship between neural firing patterns which are induced by corresponding modulations in potassium channel of neuron model. Huaguan Gu and et al.[151] experimentally demonstrated the bifurcations from bursting to spiking state predicted by theoretical models. The effect of external forcing current on electrical activities of neuron can be predicted with bifurcation diagram[152]. Transverse Lyapunov Exponent plot[153] confirms synchronization stability. Also to determine the neuro-computational properties of cell, bifurcation analysis is important.

The Hindmarsh-Rose model with fractional order[154] can give an explanation to dynamical properties of neuronal electric activities. It is observed that autapse-modulated neuron model and the time- varying electromagnetic

field can modulate the membrane potential of neuron and even the time delay in autapse can suppress the bursting in neuronal behaviour[155]. Recent studies [156] show that field coupling is also an effective way to contribute towards electromagnetic induction on neurons, when synaptic coupling is not available. Lulu Lu and et al. [152] have examined the mode selection in neural activities and has done the corresponding bifurcation analysis under high and low frequency current to study electromagnetic induction of four-variable H-R model with cubic flux controlled memristor. Also, studies of Mengyan Ge and et al [157] showed that for a magnetic flux driven neuron model, different responses in electrical activities are resulted in under periodic frequency of electromagnetic radiation and in the presence of Gaussian white noise.

Studies of S.R. Hudson and et al. [158] have identified that the quadratic flux minimizing surfaces can be constructed for toroidal magnetic fields. The memory based quadratic and exponential flux induction can influence conductance in channels including channel blocking [159]. Also, studies[160] show that mathematical model can interpret the experimental observation of exponential variation of fluxes which permit to evaluate the extent to which the membrane is affected by external flux. Under these contexts it seems to be relevant to examine influence of quadratic and exponential flux controlled memristor on neurons.

In section 4.3 the influence of quadratic flux based memristor on the electric activities properties of improved H-R model is analysed. The dynamics is examined for periodic and non periodicforcing current. Bifurcation diagram of Inter spike interval versus current and the corresponding Lyapunov Exponent for the system is plotted. In Section 4.5, the effect of noise on electromagnetic induction of neuron is examined. Section 4.6 gives the energy of improved H-R model under quadratic flux and the corresponding numerical analysis. In

Section 4.7, the study is extended on coupled neurons under quadratic and exponential flux and the Transverse Lyapunov exponent plot for coupled neurons under quadratic flux is also analysed.

The studies exhibit the highly interesting rich phenomena such as transitions from the rest state to the firing state and from the spiking state to the bursting states in the four variable H-R neuron models with these different flux based memristors. Also, the states exhibit tonic spiking and oscillation deaths under various external conditions. When noise is added to the neuronal model the suppression of these activities is achieved. The mode transitions exhibited are different from that of improved H-R neuron model with cubic flux controlled memristor in the presence of Gaussian white noise [157,161].

Numerical analysis of Hamilton energy also supports the different transistions in electrical modes. The energy exhibits discontinuous behaviour with respect to the variation of external current. Bifurcation analysis of Inter spike Interval (ISI) versus current also shows difference in behaviour when compared to that of ordinary H-R neuron model and improved H-R neuron model with cubic flux based electromagnetic induction[130]. The irregularity in the behaviour of neurons is also examined through Lyapunov Exponent plot[162].

For coupled neurons, synchronization behaviour of neurons under quadratic flux and noise shows periodic, chaotic and tonic type patterns. The quiescent state and subsequent suppression of oscillations are observed for high values of noise intensity and coupling strength. For exponential flux under noise, the synchronization pattern leads to oscillation death.

4.2. Model and Scheme

The general H-R model in an isolated neuron has been extended to an improved model of four variables[73,130]. The new variable φ incorporate magnetic flux. Hence this model can be effective to detect the effect of electromagnetic radiation by applying external magnetic flux associated with electromagnetic field on the dynamical equation for magnetic flux. The neuron model is made to interact with memristor. The memristor magnetic flux is due to the flux arising from the ions.

The four –variable H-R neuron model with memristor can be written as

$$\dot{x}_1 = x_2 - ax_1^3 + bx_2^2 - x_3 + I_{ext} - k\rho(\varphi)x_1$$

$$\dot{x}_2 = c - dx_1^2 - x_2$$

$$\dot{x}_3 = r\big(s(x_1 - x_0)\big) - x_3$$

$$\dot{\varphi} = k_1 x_1 - k_2\varphi \tag{4.1}$$

Here the variables $x_1, x_2 and\ x_3$ represent the membrane potential, slow current recovery variable and adaption current for first neuron and $x_4, x_5 and\ x_6$ represents corresponding variables for second neuron. The important electrical signal in neurons arises from a big voltage change (of the order of many millivolts) which is termed as action potential or membrane potential (spikes)and it occurs in less than a second for neuron[163]. The parameter values are selected as $a = 1, b = 3, c = 1, d = 5, s = 4, r = 0.006, x_0 = -1.6$. External forcing current is represented by the term I_{ext} and the magnetic flux across the membrane is denoted by the fourth variable φ. The memductance corresponding to the charge $q(\varphi)$ is given by $\rho(\varphi)$. Relation among induced

current, flux and memristor can be understood by Faraday's law of electromagnetic induction[140] as given below.

$$i = \frac{dq(\varphi)}{dt} = \frac{dq(\varphi)}{d\varphi}\frac{d\varphi}{dt} = \rho(\varphi)V = k\rho(\varphi)x_1 \quad (4.2)$$

Here $k_1 x_1$denotes the changes in magnetic flux induced by membrane potential and $k_2\varphi$ represents the leakage of magnetic flux. Also the interaction between membrane potential and magnetic flux is represented by the variables k and k_2. The effect of electromagnetic induction and corresponding modes of electrical activities with memristor could be examined by finding the influence of the magnetic flux on membrane. Also the term $k\rho(\varphi)x_1$denotes induced current and it causes the variation in magnetic flux which in turn generates Faradic current.

4.3 Electric activities in H-R neuron

Different modes in electrical activities are studied with the help of time series of membrane potential of neuron. Studies on Bifurcation diagram of Inter spike Interval, Lyapunov Exponent, variation of Hamilton energy with external simulation and synchronization are done for the in the respective neuron models. Synchronization behaviour on coupled neurons is also examined.

4.3.1 Electrical activities in an improved H-R neuron under electromagnetic induction without noise

In this section the study is done on a four variable H-R neuron model which is made to interact with quadratic flux controlled memristor. The memductance corresponding to the charge $q(\varphi)$is given by the derivative of q with respect to the flux [130,155]. It is appropriate to incorporate the quadratic term dependence for the charge [164] and hence the corresponding

memductance after scaling will be $\alpha\varphi^2 + \beta\varphi + \gamma$. It is observed that Memductance can affect the conduction of electrons [133] and this term can act as the influencing magnetic flux on membrane potential of the selected neuron.

4.3.1.1 Time Series behaviour under external non periodic current

The time series of membrane potential of a neuron is studied under different external forcing current and parameter values. Different electric modes are observed for different external currents. The other parameters are chosen as $k = 0.4, k_1$=1, k_2=0.5,$\alpha = 0.1, \beta = 0.02, \gamma = 0.2$. It is observed that the electrical activity selects different discharge modes under suitable parameter values. The plots are shown through Figure 4.1(a)-Figure 4.1(c). It is observed that the quiescent states[165,166] become broadened for the behaviour of the membrane potential as the value of external current increases. Also for higher values of external current, the system settles down to oscillation death[130] after a short time [Figure 4.1(c)].

(a)

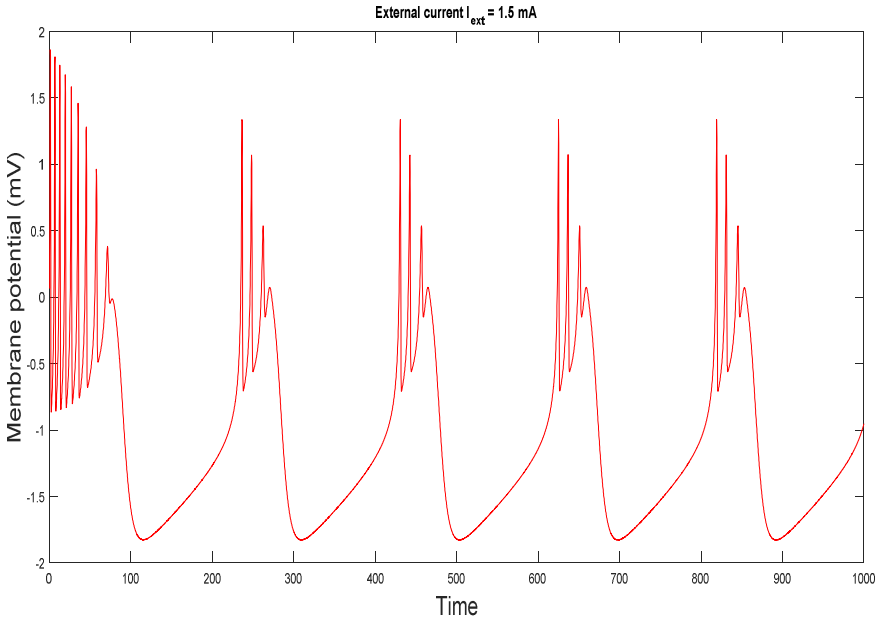

(b)

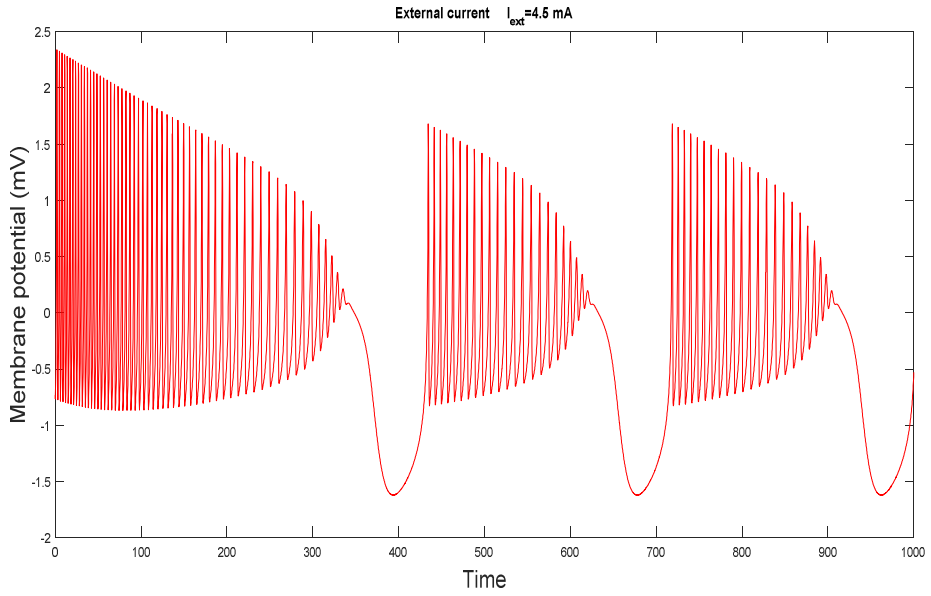

(c)

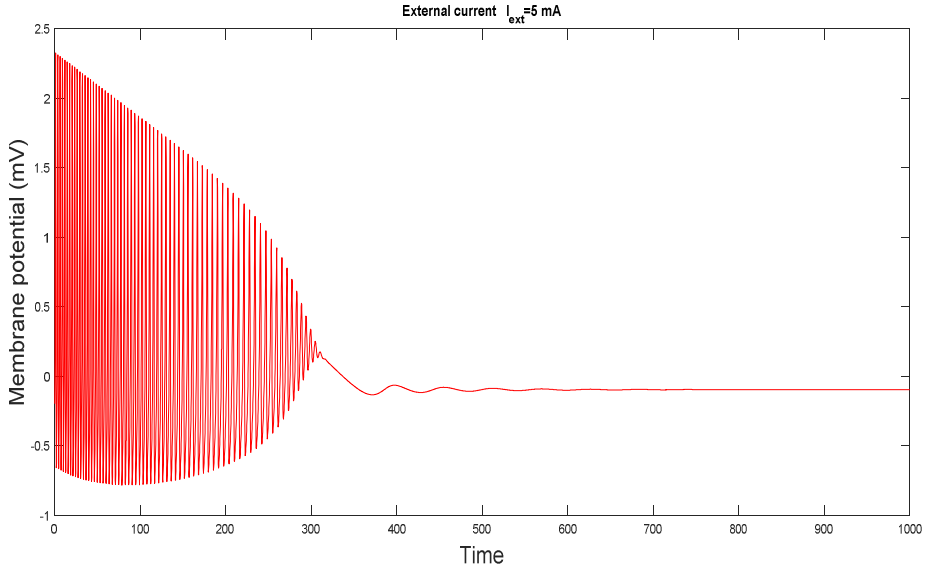

Figure 4.1: Variation of action potential with time is plotted for I_{ext}=1.5, 4.5and 5mA respectively. It is clear from the figure that for high values of external current, the system changes from quiescent state to oscillation suppression behaviour.

The results of simulations are summarized in Table 4. 1.

Table 4.1: Different types of dynamics of four-variable H-R neuron with quadratic flux under external non periodic current

External non periodic current	Dynamics
I_{ext}= 1.5	Quiescent state
I_{ext}=4.5	Quiescent state broadens
I_{ext}=5.5	Oscillation death

4.3.1.2 Behaviour under external periodic current

To study the influence of periodic external current on neuronal electrical activities, periodic current $I_{ext} = A\,cos\omega t$ is applied to the system and the dynamics is analysed. From the plots it is clear that as external periodic current increases, the action potential shows enhanced quiescent states for the spiking activities and for a higher value of current the neuron system exhibits tonic oscillations in contrast to the suppression of activities observed with the nonperiodic external current described in the previous section. The states can be observed by choosing appropriate parameter valuesas $k = 1, k_1 = 0.9,$ $k_2 = 0.5, \alpha = 0.4, \beta = 0.02, and\ \gamma = 0.2.$

(a)

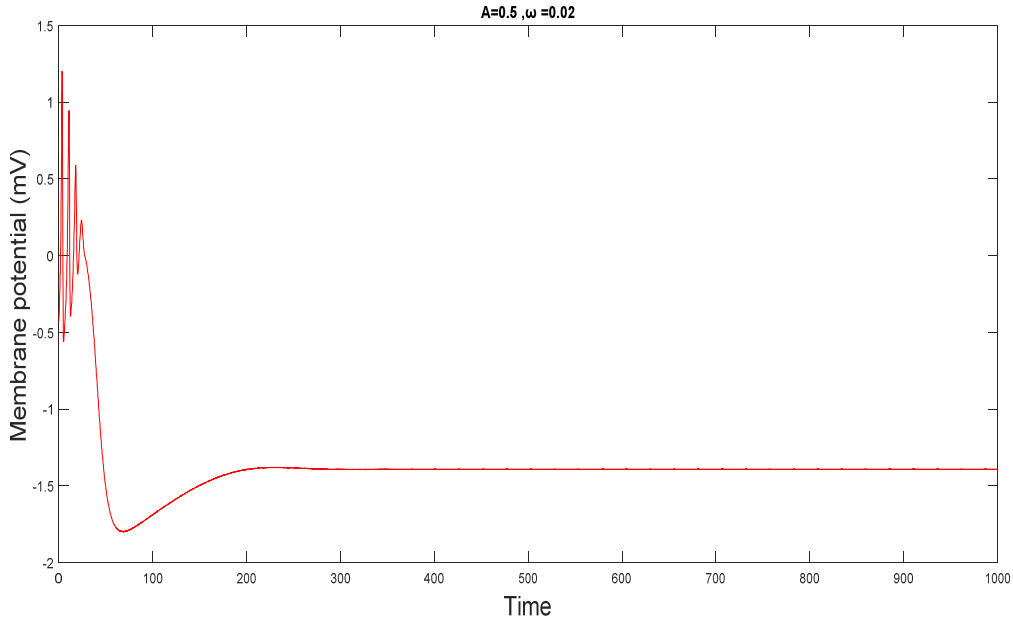
A=0.5 ,ω =0.02
Membrane potential (mV)
Time
1.5
1
0.5
0
-0.5
-1
-1.5
-2
0
100
200
300
400
500
600
700
800
900
1000

(b)

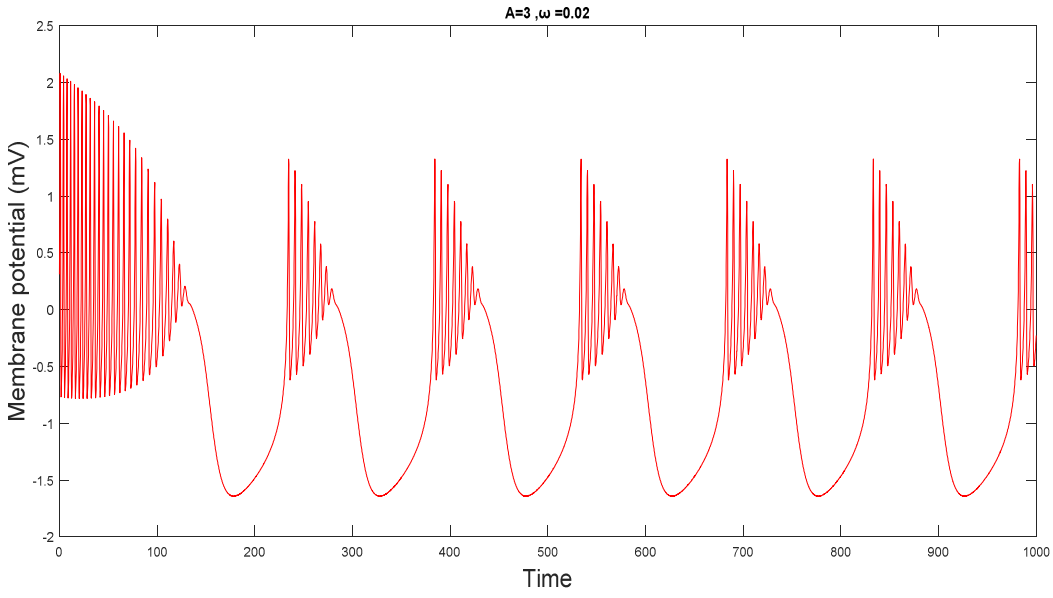
A=3 ,ω =0.02
Membrane potential (mV)
Time
2.5
2
1.5
1
0.5
0
-0.5
-1
-1.5
-2
0
100
200
300
400
500
600
700
800
900
1000

(c)

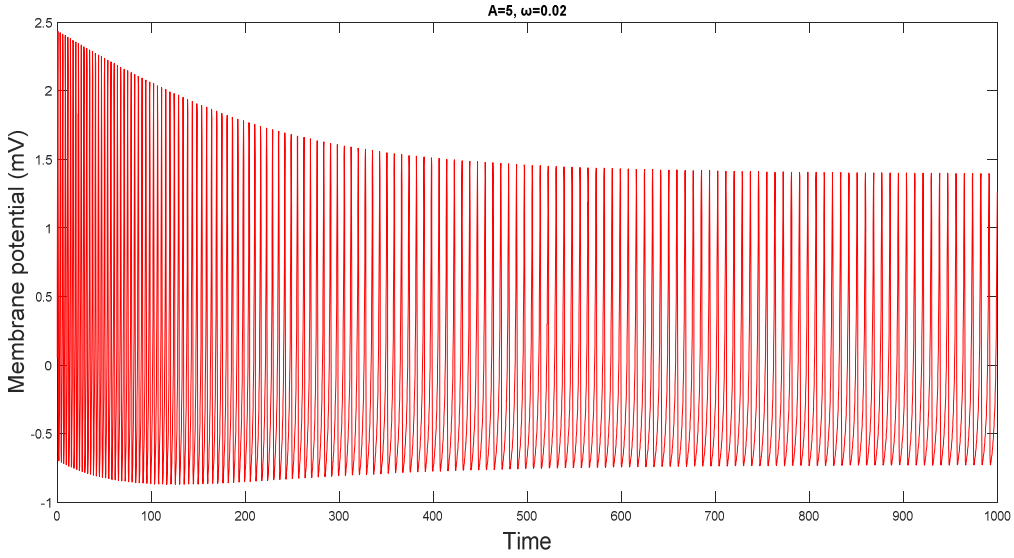

Figure 4.2: Influence of periodic current on membrane potential is shown in figure. Figures are plotted for (a) A=0.5, ω=0.02, (b) A=3, ω=0.02 and (c) A=5, ω=0.02 respectively. The behaviour of membrane potential gets changed through quiescent spiking states to tonic behaviour as the external periodic current becomes high.

The results are summarized in Table 4.2.

Table 4.2: Dynamics of for-variable H-R neuron with quadratic flux under external periodic current

External periodic current	Dynamics
A =0.5 , ω =0.02	Quiescent state
A=1.5 , ω=0.02	Quiescent state broadens
A=3 , ω =0.02	Tonic spiking

4.3.1.3 Bifurcation diagram of Inter Spike interval versus external current

To study the electrical behaviour of neurons, it is important to analyse pattern of spikes. The complex bifurcation structures in H-R neuron model [151] mainly help to understand the mechanisms used by the neurons to encode information and its rapid response to stimuli. So bifurcation plot of Inter Spike Interval (ISI) versus current is important in this respect.

Bifurcation diagram of Inter Spike Interval (ISI) versus current of improved H-R neuron model under the influence of quadratic memristor flux is as shown in Figure 4.3. Here the pattern of spikes depends on intrinsic property of neurons, nature of input to neurons and on network of interactions.

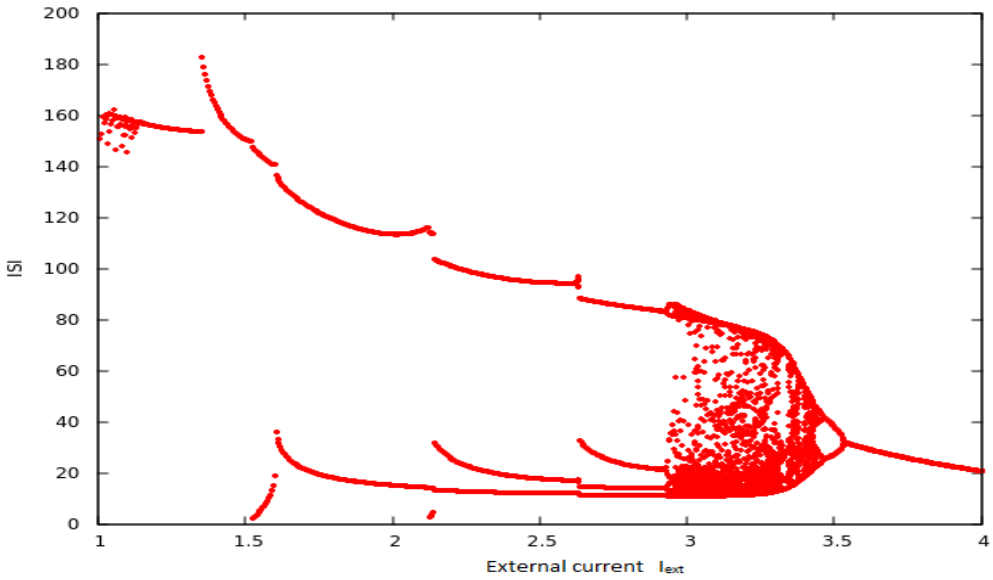

Figure 4.3: Bifurcation diagram of Inter Spike Interval (ISI) versus current for four variable H-R neuron with quadratic flux controlled memristor

On Comparing with the study of bifurcation diagram of cubic flux based improved H-R model [152, 157], it is observed that for improved H-R neuron model with quadratic flux memristor, bifurcation diagram of Inter Spike

Interval (ISI)versus external forcing current is more dense exhibiting the possibility of higher number of periods and hence of more complexity.

4.3.1.4 Lyapunov Exponents versus External current

The dynamics and hence the anisotropy due to the effect of electromagnetic radiation on neurons are observed through Lyapunov Exponent plot (Figure 4.4**)**. Here variation of Lyapunov Exponent versus external current is plotted which establishes the chaotic nature of the system.

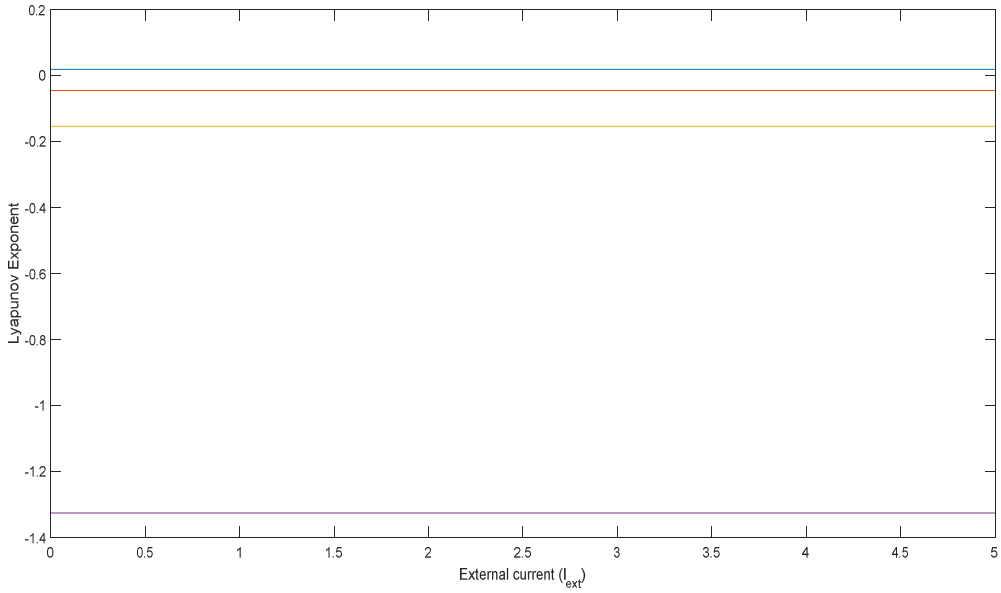

Figure 4.4: Dynamics of Lyapunov Exponent versus parameter for improved H-R neuron model with quadratic flux controlled memristor.

4.4 Effect of noise on electromagnetic induction of neurons

Noise can affect the transmission of periodic signals by nonlinear systems. Studies show[167] that external noise sources can influence neuronal

systems and hence the important parameters like intensity and correlation time of noise can play remarkable role in transmission of signals among the neurons.

Here noise term is added to the fourth variable of equation (4.1). So the fourth term changes to $\dot{\varphi}=k_1x_1-k_2\varphi+\xi(t)$. The parameter values are selected as given in Section 4.2.The irregularity of electromagnetic radiation is represented by Gaussian white noise term$\xi(t)$[167]. Here $\langle\xi(t)\rangle$=0, $\langle\xi(t)\xi(t')\rangle$= $2D_0\delta(t-t')$ where $D_o$represents the noise intensity.

$$\dot{x}_1 = x_2 - ax_1^3 + bx_2^2 - x_3 + I_{ext} - k\rho(\varphi)x_1$$

$$\dot{x}_2 = c - dx_1^2 - x_2$$

$$\dot{x}_3 = r\big(s(x_1 - x_0)\big) - x_3$$

$$\dot{\varphi}=k_1x_1-k_2\varphi+\xi(t) \qquad (4.3)$$

4.4.1 Influence of Noise under external periodic and non periodic currents

Noise term is introduced as given in equation (4.3) keeping all the other parameters the same. For non periodic current, the variation of membrane potential with time exhibits the same dynamics as that of noiseless system [Figure 4.1(a)-Figure 4.1(b)]. But the magnitude of external current needed to achieve suppression of oscillation gets reduced compared to that of the system without noise [Figure 4.1(c)] and also it occurs at an earlier time. The Figure 4.5 illustrates the dynamics.

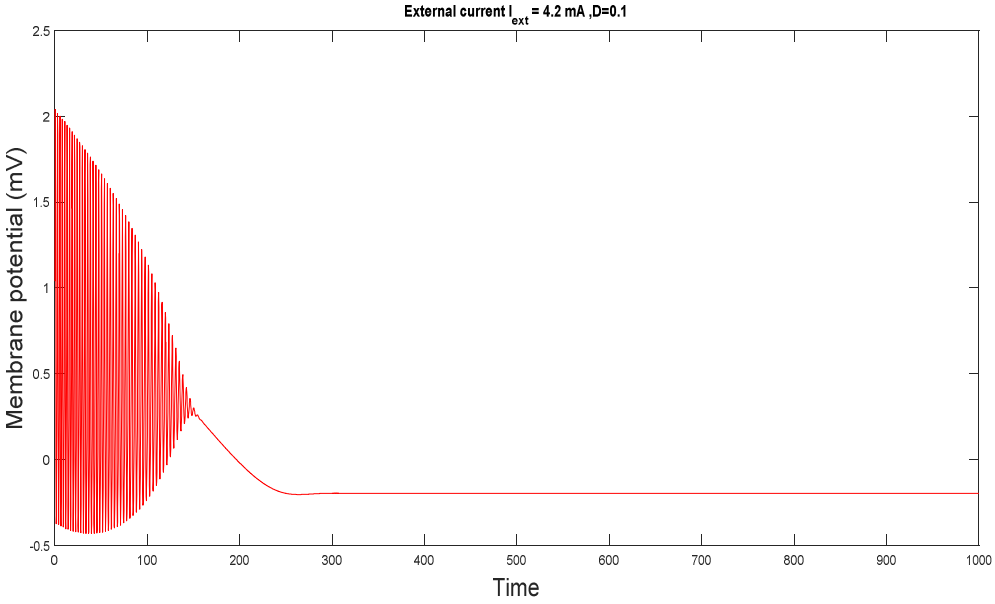

Figure 4.5: The variation of action potential under non periodic current and noise. It is observed that when $I_{ext} = 4.2$ mA and for noise intensity $\boldsymbol{D_0}$=0.1 suppression of oscillation takes place. The same behaviour persists for higher values of noise.

As the current is changed to the periodic one, for amplitude A=1.6 the oscillations are resulted in Figure 4.6. Further for the amplitude and frequency A=3 and ω=0.02 respectively, the addition of noise leads to tonic type behaviour similar to Figure 4.2c instead of quiescent states exhibited in Figure 4.2(a). So it is important that in contrast to the behaviour of the system in noiseless background the effect of noise in the presence of periodic current inhibits the quiescent behaviour for low values of amplitude of external current. The system exhibits the tonic type oscillation in the presence of noise as time progresses. But the presence of noise did not alter the time series plot for the values A=0.5, ω=0.02 and A=5, ω=0.02 Figure 4. 2(a) and Figure 4. 2 (c).

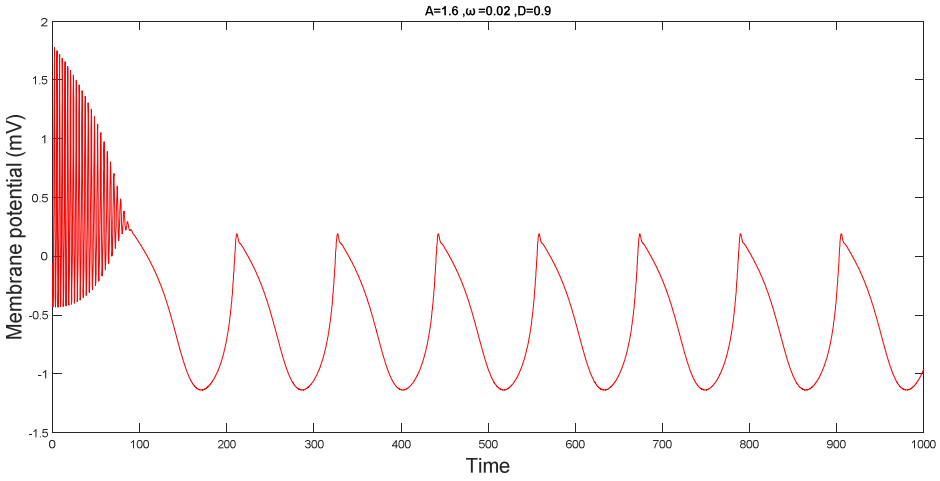

Figure 4.6: The variation of action potential under the influence periodic current and noise. It is observed that when A=1.6, ω=0.02 and noise intensity D_0=0.9, the quiescent state later on changes to oscillations.

4.5. Energy for improved H-R neuron model under the influence of quadratic memristor flux.

Hamilton energy can be calculated on chaotic neural systems with different types of attractors[168]. The energy modulation helps to control chaos in various systems. The negative feedback in energy can suppress the phase space and oscillating behaviours and it in turn can control the chaotic and periodic oscillators. So the calculation and analysis of Hamilton energy in neuronal chaotic and hyper chaotic systems are relevant in this context.

Based on the Helmholtz theorem, the Hamilton energy is calculated. It helps to discern the energy dependence on the mode selection of the electric activities of neuron. Here the statistical Hamilton energy[168] is calculated and it can be used to find out the relation among action potential, transition of electric activities of neurons in terms of external forcing and energy. According to Helmholtz theorem, the dynamical equations for neuron can be treated as

velocity vector field [169] and this can include sum of two vector fields. These vector fields represent the dissipative and conservative fields. So the system can be represented as sum of two sub-vector fields as shown below

$$f(r) = f_d(r) + f_c(r) \tag{4.4}$$

So the dynamical system given by equation (4.1) can be represented written as

$$\begin{pmatrix} \dot{x_1} \\ \dot{x_2} \\ \dot{x_3} \\ \varphi \end{pmatrix} = [\, J(x_1, x_2, x_3, \varphi) + R(x_1, x_2, x_3, \varphi)]\nabla H$$

$$= f_c(x_1, x_2, x_3, \varphi) + f_d(x_1, x_2, x_3, \varphi) \tag{4.5}$$

where$(x_1, x_2, x_3, \varphi\ )$ and $R(x_1, x_2, x_3, \varphi)$ represent skew symmetric matrix which satisfies the Jacobi's closure condition.

So $f_c(x_1, x_2, x_3) = \quad J(x_1, x_2, x_3, \varphi)\nabla H$

$$= \begin{pmatrix} x_2 - x_3 + I_{ext} - \varphi \\ c - dx_1^2 \\ r\big(s(x_1 - x_0)\big) \\ k_2 x_1 \end{pmatrix} \tag{4.6}$$

and

$$f_d(x_1, x_2, x_3, \varphi) = \begin{pmatrix} -ax_1^3 + bx_1^2 - k\rho(\varphi)x_1 + \varphi \\ -x_2 \\ -rx_3 \\ -k_3\varphi \end{pmatrix} \tag{4.7}$$

The general hamilton energy function H is defined by the criterion

$\nabla H^T f_c(x_1, x_2, x_3, \varphi)$=0

$$\nabla H^T f_d(x_1, x_2, x_3, \varphi) = \frac{dH}{dt} = \dot{H} \tag{4.8}$$

So energy can be obtained by substituting equation (4.6) and (4.7) in equation (4.8) and can be written as

$$(x_2 - x_3 + I_{ext} - \varphi)\frac{\partial H}{\partial x_1} + (c - dx_1^2)\frac{\partial H}{\partial x_2} + rs(x_1 - x_0)\frac{\partial H}{\partial x_3} + k_2 x_1 \frac{\partial H}{\partial \varphi} = 0$$

Solution of above equation can be written as

$$H = \frac{2}{3}dx_1^3 - 2cx_1 + rs(x_1 - x_0)^2 + (x_2 - x_3 + I_{ext} - \varphi)^2 + k_2 x_1^2 \tag{4.9}$$

Hence time variation of Hamilton energy is given by

$$\dot{H} = 2dx_1^2\dot{x}_1 - 2c\dot{x}_1 + 2rs(x_1 - x_0)\dot{x}_1 + 2(x_2 - x_3 + I_{ext} - \varphi)(\dot{x}_2 - \dot{x}_3 - \dot{\varphi}) + 2k_2\dot{x}_1 x_1 \tag{4.10}$$

On substituting the values of $\dot{x}_1, \dot{x}_2, \dot{x}_3$ and $\dot{\varphi}$ in the above equation and rearranging the terms we get derivative of energy as

$$\dot{H} = 2dx_1^2(x_2 - ax_1^3 + bx_1^2 - x_3 + I_{ext} - k_1\rho(\varphi)x_1) - 2c(x_2 - ax_1^3 + bx_1^2 - x_3 + I_{ext} - k_1\rho(\varphi)x_1) + 2rs(x_1 - x_0)(x_2 - ax_1^3 + bx_1^2 - x_3 + I_{ext} - k_1\rho(\varphi)x_1) + 2(x_2 - x_3 + I_{ext} - \varphi)(c - dx_1{}^2 - x_2 - rs(x_1 - x_0) + rx_3 - k_2 x_1 + k_3\varphi) \tag{4.11}$$

Again on rearranging the terms in equation(4.11) we get

$$\dot{H} = 2dx_1^2 - 2c + 2rs(x_1 + 1.6) + 2k_2 x_1(-ax_1^3 + bx_1^2 - k_1\rho(\varphi)x_1 + \varphi) + 2(x_2 - x_3 + I_{ext} - \varphi)(-x_2) - 2(x_2 - x_3 + I_{ext} - \varphi) + (-rx_3) - 2(x_2 - x_3 + I_{ext} - \varphi)(-k_3\varphi) = \nabla H^T f_d \tag{4.12}$$

The energy function in neuron shows distinct dependence on external forcing current I_{ext} and the action potential x_1 and thus discharge states are obtained. So the Hamilton energy gives the fluctuation of energy function associated with external forcing. This explains why the neuron can give appropriate response to external forcing which supplies continuous energy for neurons.

Numerical analysis of system is also done (Figure 4.7). The variation of Hamilton energy with external forcing current shows discontinuity in behaviours [170].

(a)

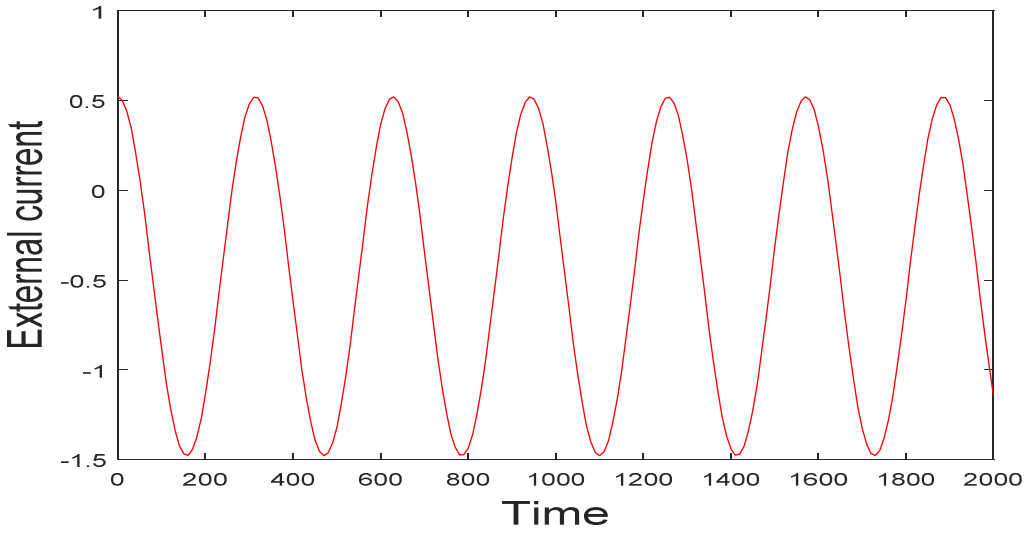

(b)

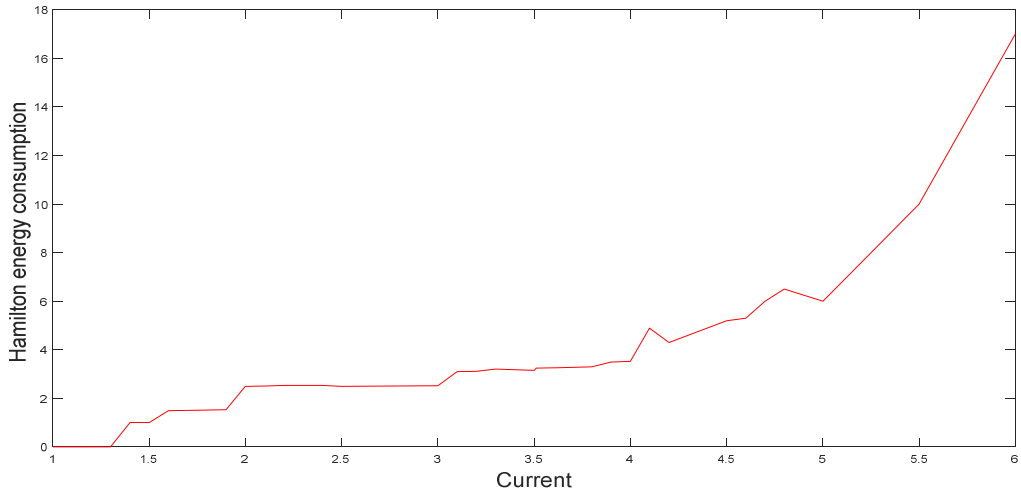

Figure 4.7: (a) External current variation with time **(b)**Variation of average of Hamilton energy with respect to current. Here low value of current gives quiescent state and high value of current leads to tonic type transitions

The plot for the variation of average value of Hamilton energy with current shows a plateau for low values of current which explains the presence of the quiescent state[169,170] in Figure 4.2a. For increased current its behaviour get changed through its irregularity and for values high values of external current high frequency tonic type transitions are obtained. To be specific, when amplitude of external current increases beyond 5mA, the Hamilton energy increases linearly and hence the appearance of tonic spiking described in section 4.2.1 is justified.

4.6. Synchronization under electromagnetic induction and noise

4.6.1 Quadratic flux controlled memristor for coupled neurons

It is possible to control the activity of neurons by magnetic forces which in turn control the flow of ions into specifically targeted cells[171].Here coupling is introduced to modified four variable H-R neuron models where quadratic flux controlled memristor based electromagnetic radiation is present.

$$\dot{x}_1 = x_2 - ax_1^3 + bx_2^2 - x_3 + I_{ext} - k\rho(\varphi_1)x_1 + g(x_4 - x_1)$$

$$\dot{x}_2 = c - dx_1^2 - x_2$$

$$\dot{x}_3 = r\big(s(x_1 - x_0)\big) - x_3$$

$$\dot{\varphi}=k_1x_1 - k_2\varphi_1 + \xi(t)$$

$$\dot{x}_4 = x_5 - ax_4^3 + bx_5^2 - x_6 + I_{ext} - k\rho(\varphi_2)x_4 + g(x_1 - x_4)$$

$$\dot{x}_5 = c - dx_4^2 - x_5$$

$$\dot{x}_6= r\big(s(x_5 - x_o)\big) - x_5$$

$$\dot{\varphi}=k_1x_4 - k_2\varphi_2+\xi(t) \qquad (4.13)$$

Here $x_1, x_2, x_3$and I_{ext} represent the membrane potential, slow current associated with the recovery variable, adaptation current term and external forcing current respectively for the first neuron. Similarly $x_4, x_5,$ and x_6 represent the corresponding variables for the second neuron. The parameter values are selected as a=1, b=3, c=1, d=5, r=0.006, s=4, x_0=-1.6.

The memristance of quadratic flux controlled memristor is represented by $\rho(\varphi)= \alpha\varphi^2 + \beta\varphi + \gamma$. Since this term is associated with the memory it is

used for estimating the effect of feedback regulation on membrane potential when corresponding magnetic flux is changed. The term g represents the coupling intensity between the neurons. Here the irregularity of electromagnetic radiation is represented by Gaussian white noise term $\xi(t)$. It is found that the synchronization degree depends on the coupling intensity and the intensity of external electromagnetic radiation.

Time series plots of membrane potentials (x_1 and x_4) for coupled H-R neurons (Figure 4.8) confirm the synchronization pattern. Here the parameter values are$k$=0.4, k_1=0.8, k_2=0.5, D_o=0.6, α=0.02, β=0.1, γ=0.1, g=1. Depending upon the parameter values and external forcing current I_{ext}, various synchronization phenomena are observed. As the value of external current increases the dynamical behaviours such as periodic, chaotic and tonic type synchronizations are observed.

(a)

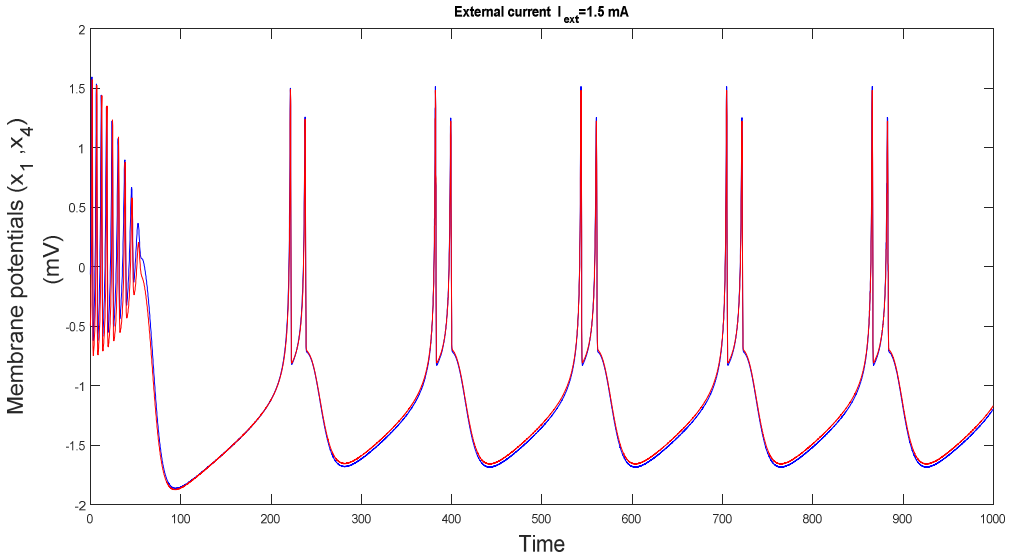

(b)

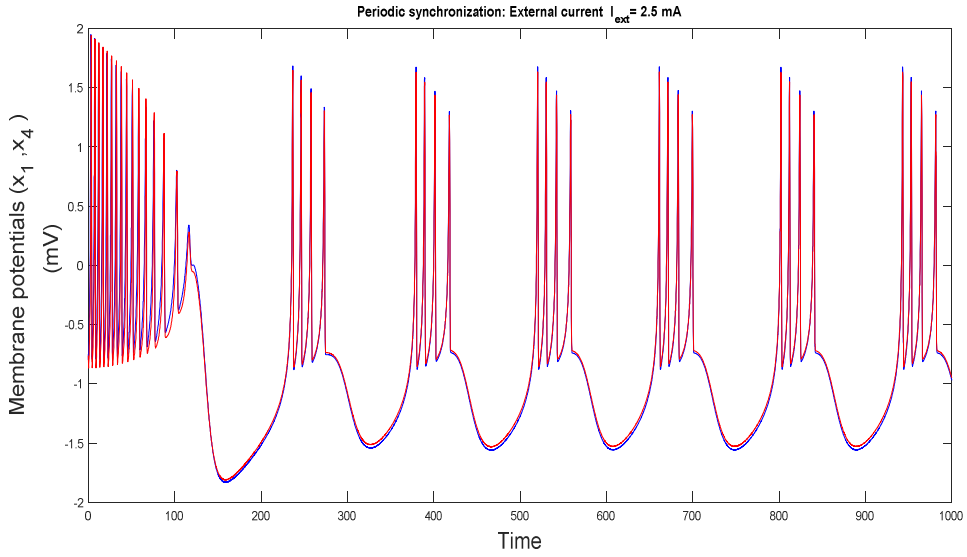
Periodic synchronization: External current I_{ext}= 2.5 mA
Membrane potentials (x_1, x_4) (mV)
Time

(c)

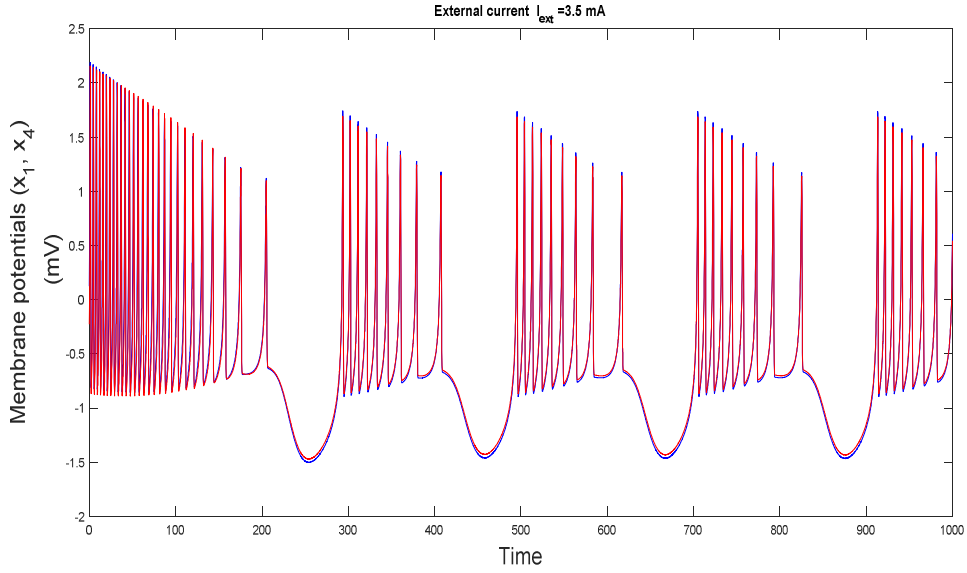
External current I_{ext} =3.5 mA
Membrane potentials (x_1, x_4) (mV)
Time

(d)

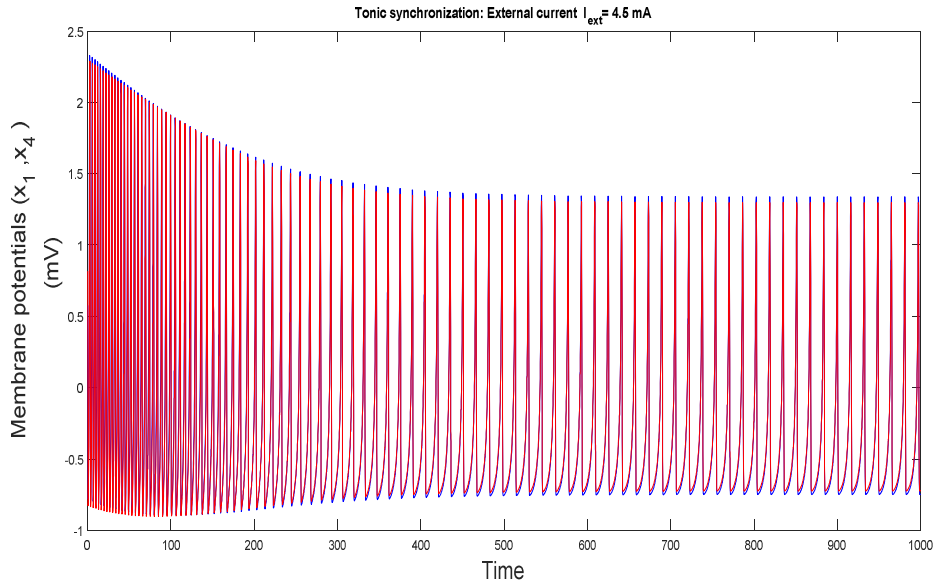

Figure 4.8: Time series for membrane potentials for the two coupled neurons are plotted for different external forcing current. For I_{ext}=1.5, 2.5, 3.5, and 4.5 mA the synchronization behaviour of the system of neurons changes through periodic, chaotic and finally through tonic type synchronization.

In a similar way by keeping the external current fixed as I_{ext} =3.5 mA and changing the coupling parameter and noise intensity as (a)g=0, D=0, (b)g=1, D=0 and (c) g=1 and D=0.9 various patterns are observed. When there is no influence of coupling (g=0) and with no noise intensity (D=0), the two different neurons behave independently as it must be[Figure 4.9(a)]. The behaviour is retained with the case where the noise intensity is raised to maximum [same behaviour as that of Figure 4.9(a)]. But as the two neurons are coupled, for high value of coupling strength and in absence of noise intensity, synchronization of the system takes place. [Figure 4.9(b)]. Finally quiescent state and subsequent suppression of oscillation effects are observed for appropriate high values of noise intensity and coupling strength [Figure 4.9(c)].

(a)

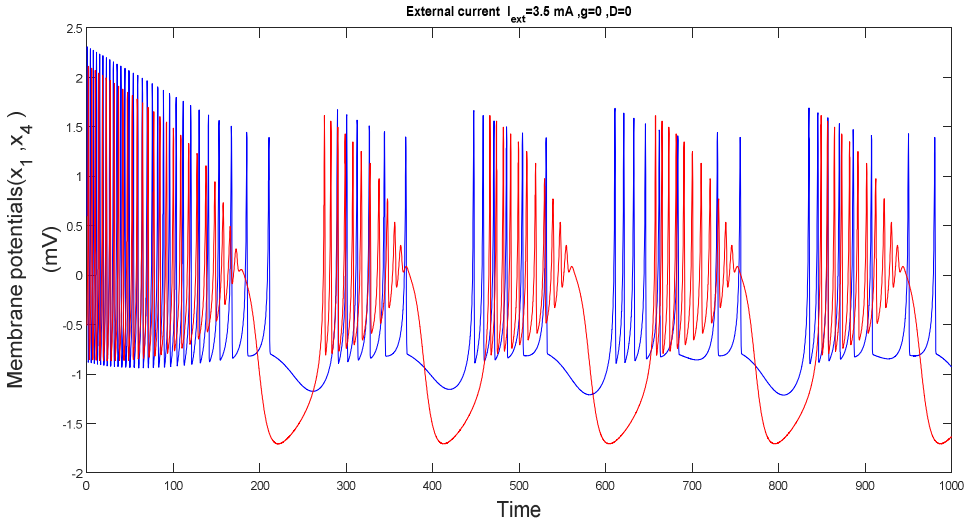
External current I_{ext}=3.5 mA ,g=0 ,D=0
Membrane potentials(x_1 ,x_4) (mV)
Time

(b)

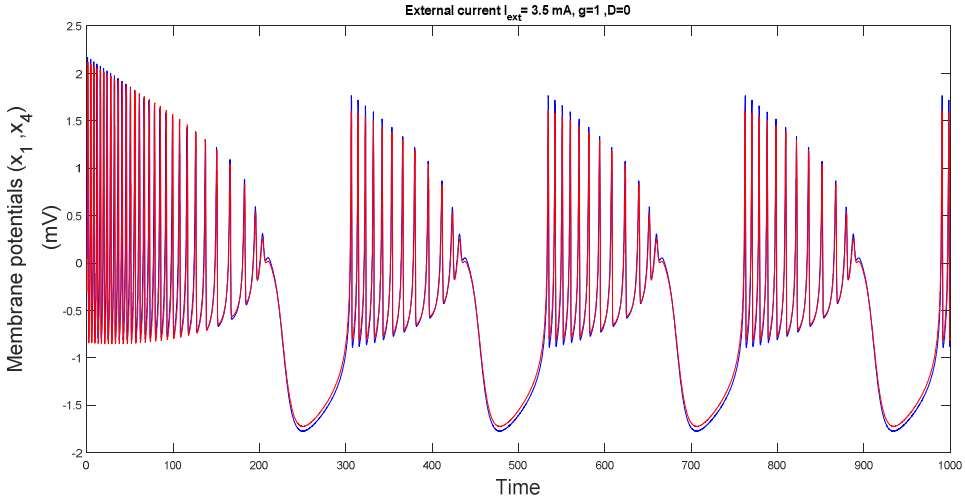
External current I_{ext}= 3.5 mA, g=1 ,D=0
Membrane potentials (x_1 ,x_4) (mV)
Time

(c)

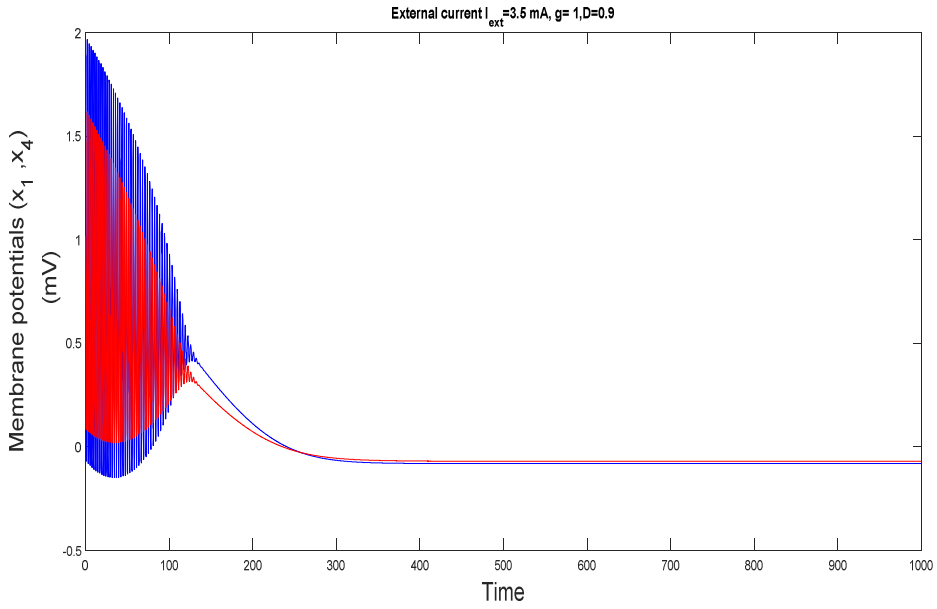

Figure 4.9: Time series for membrane potentials are plotted for fixed external forcing current. For I_{ext}=3.5 mA the synchronization behaviour of the system of neurons (Figure 9b) is achieved with control parameter values g=1, D=0 and the system attains oscillation death state (Figure. 9c) for higher coupling (g=1 and D=0.9) in the presence of high noise.

4.6.1.1 Transverse Lyapunov plot for quadratic flux based memristor

The stability of synchronization can be quantified by master stability approach [172]. The synchronization is stable if the master stability function is negative at each of transverse eigenvalues (Figure 4.10).

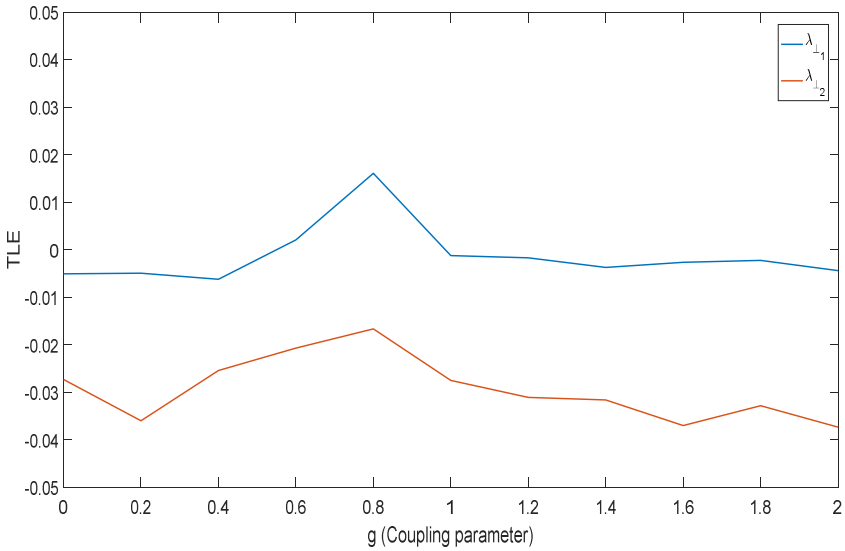

Figure 4.10: The TLE of coupled improved H-R neuron model with quadratic flux induction

The largest TLE crosses zero and becomes negative indicating synchronized state and its stability.

4.7 Influence of exponential flux controlled memristor on coupled neurons

The work is extended to examine neuron dynamics under the influence of exponential flux controlled memristor where the neurons are allowed to interact with each other.

$$\dot{x}_1 = x_2 - ax_1^3 + bx_2^2 - x_3 + I_{ext} - k\rho(\varphi_1)x_1 + g(x_4 - x_1)$$

$$\dot{x}_2 = c - dx_1^2 - x_2$$

$$\dot{x}_3 = r\big(s(x_1 - x_0)\big) - x_3$$

$$\dot{\varphi}=k_1x_1 - k_2\varphi_1 + \xi(t)$$

$$\dot{x}_4 = x_5 - ax_4^3 + bx_5^2 - x_6 + I_{ext} - k\rho(\varphi_2)x_4 + g(x_1 - x_4)$$

$$\dot{x}_5 = c - dx_4^2 - x_5$$

$$\dot{x}_6 = r\big(s(x_5 - x_0)\big) - x_5$$

$$\dot{\varphi} = k_1 x_4 - k_2\varphi_2 + \xi(t) \tag{4.14}$$

The parameter values are selected as a=1, b=3, c=1, d=5, r=0.006, s=4, $k_1 = 0.9$, k_2=0.5.

The exponential flux controlled memristor[173] is represented as

$$q(\varphi) = k_3(a_1{}^{b_1\varphi} - 1) \tag{4.15}$$

Where $a > 1$and $k_3 b_1 > 0$. The Memductance of the function is $\rho(\varphi) = a_1{}^{b_1\varphi} k_3 b_1 ln a_1$. Here a_1= e, $b_1 = 50\log(0.5)\, and\ k_3$=10.

As the values of external current changes, the synchronization pattern shows various patterns as depicted in Figure 4.11 [Figure 4.11(a)-Figure 4.11(c)]. When the magnitude of external forcing current increases, the synchronization pattern shows tonic oscillations, which finally leads to oscillation death state with appropriate value of external forcing current.

(a)

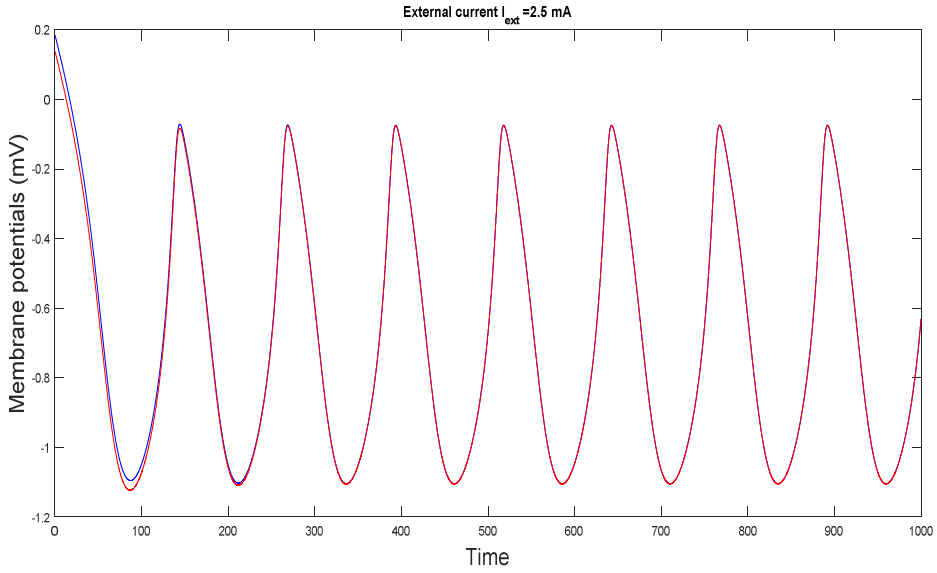
External current I_{ext}=2.5 mA
Membrane potentials (mV)
Time
0.2
0
-0.2
-0.4
-0.6
-0.8
-1
-1.2
0
100
200
300
400
500
600
700
800
900
1000

(b)

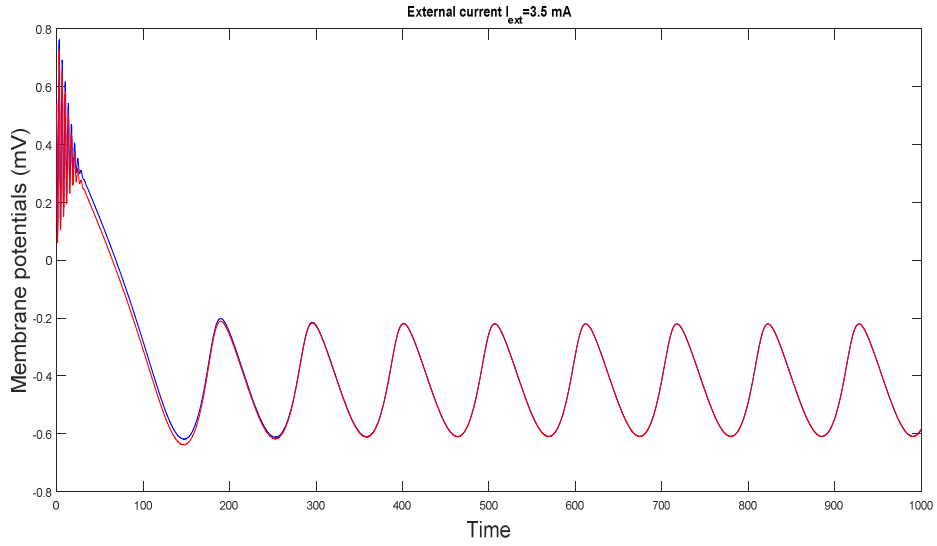
External current I_{ext}=3.5 mA
Membrane potentials (mV)
Time
0.8
0.6
0.4
0.2
0
-0.2
-0.4
-0.6
-0.8
0
100
200
300
400
500
600
700
800
900
1000

(c)

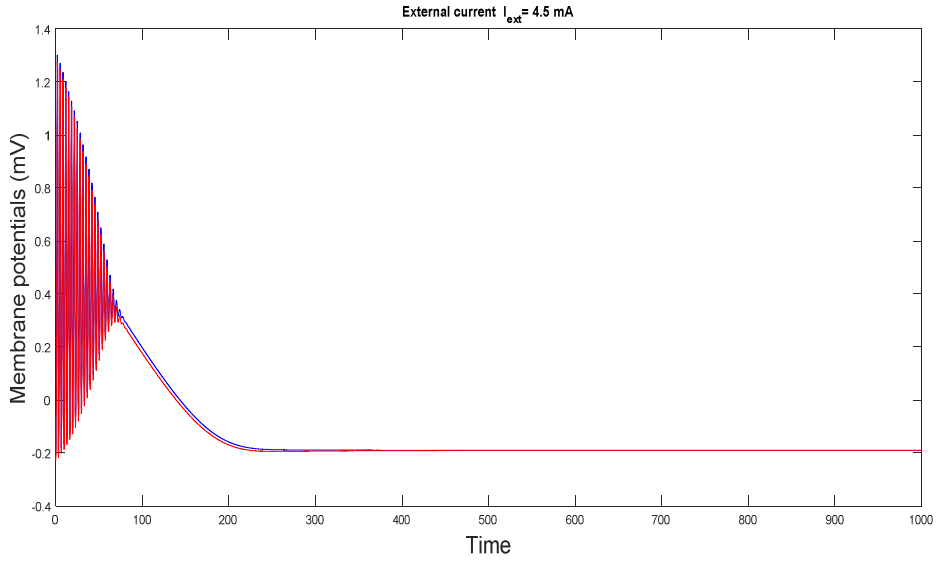

Figure 4.11: Time series for membrane potentials are plotted for different external forcing current I_{ext}=2.5mA, I_{ext}=3.5mA and I_{ext}=4.5mA. As magnitude of external forcing current increases, the synchronization pattern changes to oscillation death state.

On comparing with the dynamics corresponding to quadratic flux controlled memristor, it is interesting to find that for same coupling strength and for same noise intensity ($g = 1$ and D_o=0.6), instead of the tonic behaviour, the system sets into oscillation death state for higher magnitude of external forcing current in the case of exponential flux controlled system.

Further by keeping the external current fixed at I_{ext} =3.5 and changing the coupling parameter and noise intensity terms as (a)g=0.01, D=0.9(b) g=0.5, D=1 and (c) g=1, D=0.3 various patterns are obtained. It is observed that for low values of coupling strength and noise intensity the system exhibits anti phase state [Figure 4.12(a)]. The behaviour is preserved as noise intensity is

stepped up [the pattern is same as that of Figure 4.12(a)]. As g is increased to 0.5 keeping the noise intensity as 1, the behaviour of membrane potential gets changed to chaotic synchronized state [Figure 4.12(b)]. But the decrease in intensity of noise to D=0.3, at high coupling strength causes the time series dynamics to change into that of periodic one [Figure 4.12(c)].

(a)

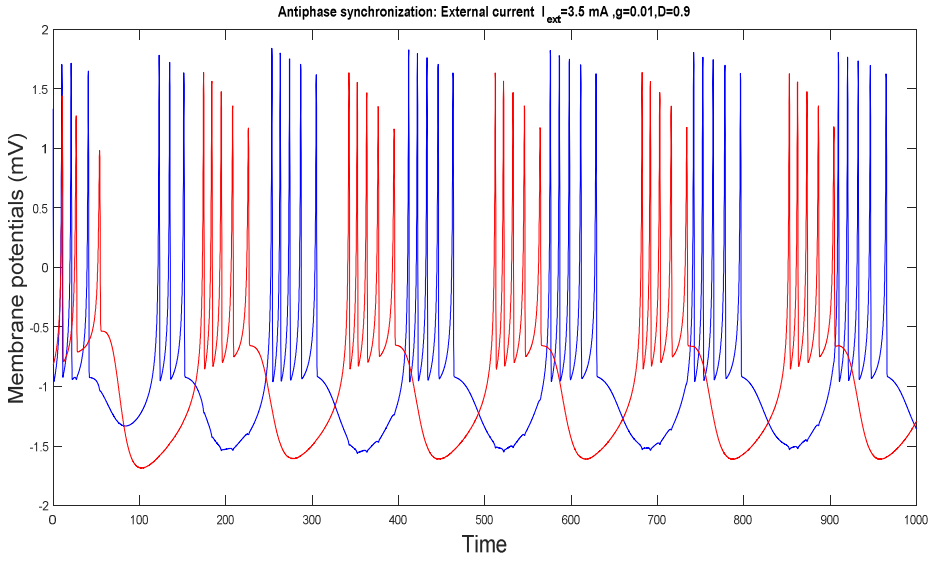

(b)

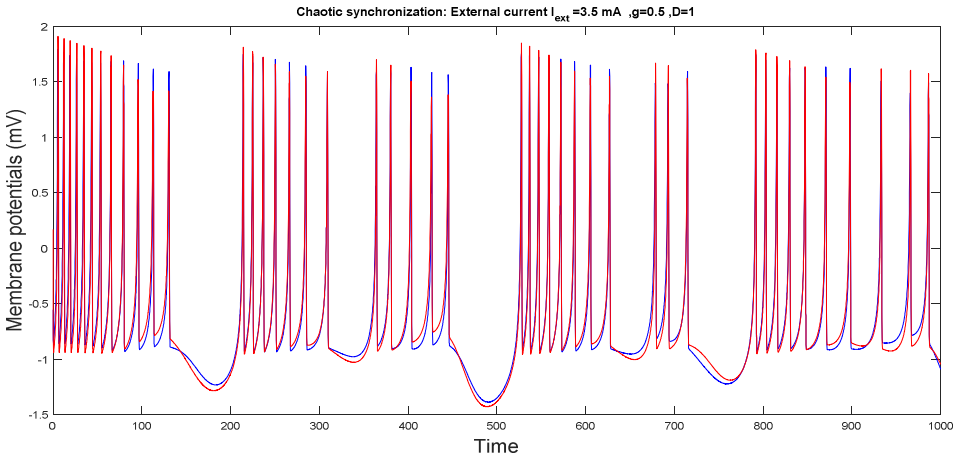

(c)

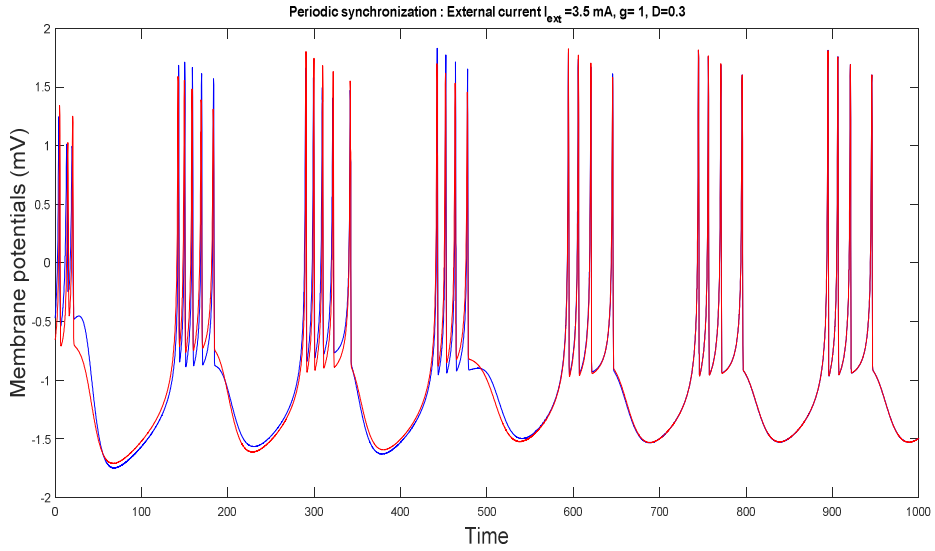

Figure 4.12: Time series for membrane potentials are plotted for different coupling strength and noise intensity. Various patterns such as (a) antiphase (g=0.01, D=0.9), (b) chaotic (g=0.5, D=1) and (c) periodic (g=1, D=0.3) behavior are observed for appropriate values of noise intensity and coupling strength.

Depending upon the low and high values of noise and coupling parameters anti phase state of the system gives way to chaotic and then to periodic type synchronization patterns.

On comparing with the synchronized and oscillation death states found in coupled neurons with quadratic flux based memristor, the system with exponential flux based memristor exhibits chaotic and periodic type synchronization state.

4.8. Discussions and concluding remarks

The essence of brain function consists in how the information is being processed, transferred and stored. The Neuro Electro Dynamic model (NED)[174] is an emerging field which describes the intrinsic computational processes by the dynamics and interaction of charges.

Various studies [130,152,155,165] had been carried out on the effect of electromagnetic induction on H-R neuron under the influence of cubic flux controlled memristor. In the present work influence of quadratic flux and exponential flux based inductions in four-variable H-R neuron model is studied. In the first part we analysed the different modes of electrical activities in single neuron under quadratic memristive term. The system behaviour is studied under the influence of external periodic and non periodic current. It is observed that for nonperiodic current, as the value of external current increases the quiescent states[166]become broadened and also for higher values of external current, the system settles down to oscillation death state. However for the periodic current the action potential shows enhanced quiescent states for the spiking activities and for the higher current the neuron exhibits tonic oscillations in contrast to the suppression of activities observed in non periodic case. So in quadratic flux based mode transition, when compared to cubic flux memristor [130,152,157] the suppression of oscillations is an additional feature.

The influence of control parameter like noise on the neurons is also subjected to study. It is found that when noise is added to the system, the oscillation death is achieved for smaller magnitude of external current. Also the presence of noise leads to the inhibition of quiescent activity under periodic current. The Lyapunov Exponents are plotted which confirm irregularity in the neuron dynamics.

Energy is calculated in terms of Hamilton energy to understand the neuron response to external forcing current and action potential. It is observed that the plot for Hamilton energy versus current shows discontinuity in behaviour. There is a plateau for low values of current which explains the presence of the quiescent states and as current increases tonic behaviour is resulted in. Bifurcation of Inter Spike Interval (ISI) versus current is also plotted and it shows denser pattern as compared with that of cubic flux based electromagnetic induction.

The synchrozation of coupled neurons also is the focus of study. Under the influence of quadratic flux and noise term the system changes through periodic, chaotic and tonic type synchronization as the current is increased. The variation of noise intensity and coupling strength leads to oscillation death of these coupled neurons under constant current. Transverse Lyapunov Exponent plot gives a picture of the stability of the coupled system. The effect of exponential flux controlled memristor based electromagnetic induction on neurons when coupledis also examined. With exponential flux controlled memristor the activity changes to tonic type synchronization with increase in forcing current. Here the synchronization pattern displays oscillation death, antiphase, periodic and chaotic transitions.

The work gives a pathway to understand electromagnetic flux influence on the overall activity of neurons. The activity of neurons is examined with quadratic and exponential flux based memristor. Brain produces an electromagnetic field with specific characteristics. Also Electromagnetic waves are produced due to artificial nano-synapses. The memristor as magnetic flux can also influence neuromorphic quantum computation.

The effect of field coupling under the influence of Lėvy noise on the electromagnetic properties of neuron with quadratic flux is the future focus of

study. In the presence of field coupling and non-Gaussian type noise like Lėvy noise studies may exhibit improved electrical activity of neuronal network with information exchange in the absence of the synapse.

Chapter 5

Electromagnetic induction on neurons through field coupling and Memristor

Chapter 5

Electromagnetic induction on neurons through field coupling and Memristor

5.1 Introduction

Synapse coupling is considered as the most important bridge to exchange signals between neurons. It is possible to analyse the synchronization and pattern selection in neural network under chemical or electric synapse coupling. The possibilities of linear and nonlinear synapse couplings on H-R neuron model[132] are already discussed in chapter 3. It helps to characterize neuronal interactions among the neuron models.

In the present chapter, the effect of field coupling on the electromagnetic induction of neurons is examined. An improved H-R neuron model with cubic flux controlled memristor is selected to analyze the kinetics of neuron. Each neuron is considered as a charged body. It can be controlled by the field triggered by the other neurons. It is observed that under field coupling excitability of neurons can be changed. Field coupling can benefit signal exchange between neurons even if synapse is absent.

Neuron is the basic unit in neuronal network and its electrical activities show distinct nonlinear properties. Various biological neuron models and their modified versions can be used for recognizing and understanding the electrical activities in neurons[67, 68, 193, 194]. External forcing can induce transition in electrical activities namely quiescent state to spiking, bursting and even chaotic states in neurons [194].

The normal function of neural networks always depends on a delicate balance between excitatory and inhibitory synaptic inputs[194-196]. It is

thought that excitatory synaptic inputs are helpful to trigger the electrical activities of neurons, while inhibitory synaptic inputs can calm down the firing in electrical activities. Many evidences confirmed that inhibitory synapse can enhance neural firing pattern or enhance synchronization degree of coupled neurons and of neuronal network[197-199]. It is also observed that some intermediary neurons have autapse connection[200], where the synapse connects to neuron or soma via a closed loop. The modulation of autapse driving can cause a time-delayed feedback on the membrane potential. It can enhance the self-adaption of neuron to external stimuli and can regulate the collective behaviours of neuronal network. Also effect of autapse with time delay can be used to describe the effect of memory in neuron[200,201].

For the neuron and biological cell, the electrical activities also can be changed due to the electromagnetic induction. Here the motion of charged particle can be controlled by electromagnetic field and the spatial distribution of charge particles become complex when these charge particles are exposed to external electromagnetic field. The electromagnetic radiation on neuronal electrical activity can affect energy metabolism, genomic responses, neurotransmitter balance, cognitive function and various brain diseases [194,202]. Lisi et al. [203] investigated the effect of electromagnetic radiations at a frequency of 50 Hz on the development of cerebellar granule neurons (CGN). Masuda et al. [204] presented experimental verification and discussion about effects of 915 MHz electromagnetic field radiation in TEM cell on the blood–brain barrier and neurons in the rat brain.

It is observed that multiple modes of electrical activities[205] can be induced by electromagnetic radiation. These results are consistent with biological experiments. Recent studies based on a new cardiac tissue model[206] explained the potential mechanism for heart disease induced by

electromagnetic radiation. The synchronization behaviour of electrical activities of neurons can be examined when neurons are exposed to noise like electromagnetic radiation [207, 208].

As discussed in **chapter 3**, linear coupling like indirect synaptic coupling and cubic feedback coupling etc. exhibits properties like synchronization, amplitude death and anti synchronization. Different memristor based nonlinear couplings[209] exhibit tonic spiking, bursting, and oscillation death and near death spike etc. and these richdynamical behaviours have much importance in the study of brain cells.

Synaptic coupling and field coupling have distinct features. During chemical synaptic transmission, neurotransmitter may initiate an electrical response. There is no intercellular continuity, thus no direct flow of current from presynaptic to postsynaptic cell. Here action potential triggers the presynaptic neuron to release neurotransmitters. For an electrical synapse gap junctions between pre synaptic and postsynaptic membranes allow current to flow passively through intercellular channels[210]. This current flow changes postsynaptic membrane potential and causes the initiation of postsynaptic action potentials.

Recent researches showed that the field coupling[211] between neurons can also give a new insight to understand the collective behaviours in neuronal networks. Here coupling of adjacent nerve fibers is caused by the exchange of ions between the cells. Here extracellular field feedbacks on to the electrical potential across neuronal coupling. Electrical conduction of nerve impulse occurs without mediation of neurotransmitter and is independent of synapse. Spiking of an active neuron is accompanied by ion flow across the membrane. This may cause an alteration of the electric field at the extracellular space which affect the excitability of nearby inactive neurons. The ephatic or field coupling

depends on the distance between two neurons. A Study of the mouse barrel cortex has reported that during strongly synchronized spiking activity (epileptic discharges or strong evoked responses), spiking could be effectively induced by localized extracellular currents[211].

This chapter examines the effect of field coupling in H-R neurons. Studies on biological Hodgkin–Huxley neuron model were helpful to understand the occurrence mechanism of neuronal systems induced by electromagnetic radiation[209]. Researches based on collective responses in electrical activities of neurons under field coupling were also reported[210]. The contribution of field coupling from each neuron can be analysed by introducing appropriate weight dependent on the position distance between two neurons[209]. Such studies have confirmed that the synchronization degree is much dependent on the coupling intensity. It is possible to modulate the synchronization or pattern selection of network connected with gap junction by field coupling [194,205,206].

In the proceeding sections, the effect of electromagnetic induction on neurons through field coupling and memristor is analysed. Here the four variable modified Hindmarsh -Rose neuron model[68,205] is selected. It is observed that time-varying intercellular and extracellular ion concentration can induce electromagnetic induction and this effect can be described by using magnetic flux according to the law of electromagnetic induction. The induced current from electromagnetic induction can modulate the membrane potential via feedback by using cubic flux controlled memristor. Memductance is dependent on the external stimuli and thus memory can be illustrated[108]. Field coupling is also introduced to understand the collective behaviour and synchronization problems[194]. Different external stimuli are applied to study the effect of field superposition on neuronal discharges. It is possible to analyse

the spatiotemporal evolution of membrane potentials for different external stimulus current and the corresponding dynamics are found to be changed.

For isolated neurons, as the external forcing current increases, the system shows diversity in behaviour under low coupling. Oscillation suppression behaviour for low current is changed into tonic spiking on increase of current. For coupled system the increase of the intensity of external stimuli leads to enhancement of the synchronization of neurons. Similarly for high coupling strength, as intensity of external stimuli is improved, suppression of oscillations is resulted in.

For the neuron networks the neuron oscillators show incoherent as well as synchronization behaviour for various coupling strengths. This is examined for the collective behaviour of 300 H-R neurons.

Stability of synchronization is examined through Transverse Lyapunov Plot. The controller for the system is developed[171] and the activation–inactivation dynamics of fast ion channel for weak and strong coupling is analyzed. This is done by varying the value of coupling parameter.

In the improved H-R neuronal system, each neuron can set electromagnetic field due to the fluctuation of ion concentration and exchange of ion current through the channels embedded into the membrane. Here each neuron is exposed to the integrated electromagnetic field contributed by other neurons according to superposition principle of field. Simulations confirmed that under field coupling the electrical activities in neurons show certain diversity in amplitude and the rhythm and hence can carry more important information because synchronization can be associated with memory[171].

5.2 Model and scheme

The dynamical equations for neuron network can be described by field coupling as follows

$$\frac{dx_i}{dt} = f(x_i, p)$$

$$\frac{d\varphi_i}{dt} = kx_i + g(\sum_{j\neq i}^{N} \varphi_j - \varphi_i) \quad (5.1)$$

Where the subscript i used in equation (5.1) describes i[th] neuron in the network without synapse connection[194]. $\sum_{j\neq i}^{N} \varphi_j - \varphi_i$ represents the field and magnetic contribution of other neurons to the i^{th} neuron. Here $x_i$and $\varphi_i$denotes the membrane potential and magnetic flux for neurons respectively. The coupling intensity is represented by g and p is a parameter which characterizes H-R the neuron. k is the induction coefficient associated with the medium and f (x, p) represents the local kinetics of neuron model.

Schematic diagram of ephatic or field coupling [194]is shown below.

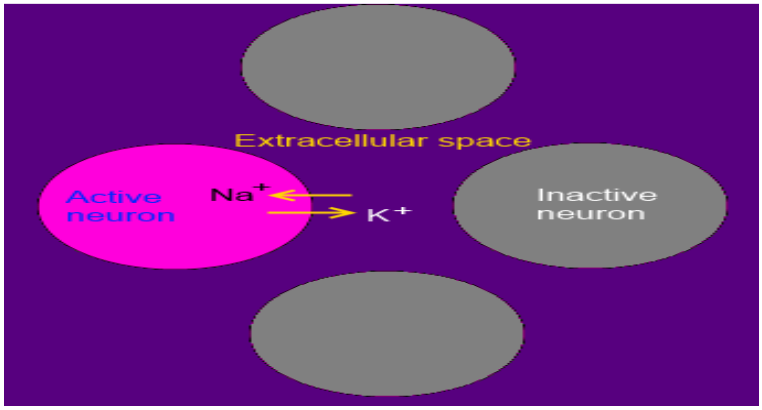

Figure 5.1: Spiking of an active neuron is accompanied by ion flow across the membrane. This results in alteration of the electric field at the extracellular space and in change the excitability of nearby inactive neurons (adapted from [194,206]).

The Hindmarsh-Rose(H-R) neuron model[68] mainly used to describe the nonlinear dynamic characteristics of neurons. The dynamical kinetics can be understand by the ordinary differential equations (ODE). It is composed of three variables. Here memristor is used as coupling term between membrane potential and magnetic flux. Hence the induction field and action potential can be bridged in physical view.

In this work, an improved H-R neuron model is selected which incorporate the magnetic flux as fourth variable. Based on an improved neuron model, the effect of field coupling on electromagnetic induction is analysed and the modulation of magnetic flux on membrane potential can be understand by using cubic flux controlled memristor coupling. Each neuron regarded as a non uniform charged body and the corresponding distribution of the charged ions are not in a uniform way. The contribution to the field distribution from each neuron could be different in biological and nervous systems. So appropriate weight can be considered in the neuronal network [202].

A chain distribution for Hindmarsh–Rose neuron with field coupling is given by

$$\dot{x}_{1i} = x_{2i} - ax_{1i}^3 + bx_{2i}^3 - x_{3i} + I_{ext} - k\rho(\varphi_i)x_{1i}$$

$$\dot{x}_{2i} = c - dx_{1i}^2 - x_{2i}$$

$$\dot{x}_{3i} = r\big(s(x_{1i} - x_0)\big) - x_{3i}$$

$$\dot{\varphi} = k_1 x_{1i} + g(\textstyle\sum_{i\neq j}^{N} \varphi_j - \varphi_i) \qquad (5.2)$$

The membrane potential, slow current associated with recovery variable and adaption current are represented by $x_1, x_2\ and\ x_3$respectively, where the memductance $\rho(\phi_i)$ is cubic flux controlled memristor term. The parameter

values are selected as a=1, b=3, c=1, d=5, r=0.006, s=4, x_0= -1.6. Here kx_{1i} denotes the changes in magnetic flux induced by membrane potential. Hence the interaction between membrane potential and magnetic flux are represented by the variables k and k_1. Relation between memristor magnetic flux, membrane potential and current is shown as follows.

$$i = \frac{dq(\varphi)}{dt} = \frac{dq(\varphi)}{d\varphi}\frac{d\varphi}{dt} = \rho(\varphi)V = k\rho(\varphi)x_1 \tag{5.3}$$

5.3 Simulation Results

The spatiotemporal evolution of membrane potentials is calculated for dynamical analysis for different node positions when external stimulus current is changed. In order to illustrate the effect of field superposition on neuronal discharges, different external stimuli I_{ext} are applied. The excitability of neuron can be changed in response to the external forcing current. This is well understood through numerical studies. Collective responses in electrical activities of H-R neurons under field coupling and stability of synchronization through Transverse Lyapunov Exponent are also analysed.

5.3.1 Modes of electrical activity of isolated H-R neuron under field coupling

Sampled time series analysis are done using Matlab platform for the isolated neuron [194] system by changing control parameters. As the intensity of external current I_{ext} increases the dynamics of single H-R neuron model under field coupling shows distinct behaviours. For the value of external current I_{ext} =0.5 mA the neuron system shows the suppression of activity. But as the current changes to 1.5 mA its activity gets changed to sudden spiking behaviour. For higher values of external current it shows a tonic or continuous spiking activity. Figure 5.2 shows the different dynamics of the system. Larger

external stimuli are much helpful to excite neurons. By increasing the intensity of external stimuli the suppression of oscillatons are modified to spiking states. Hence it is shown that the field coupling[202] along with the magnetic flux of memristor can control the mode transitions.

(a)

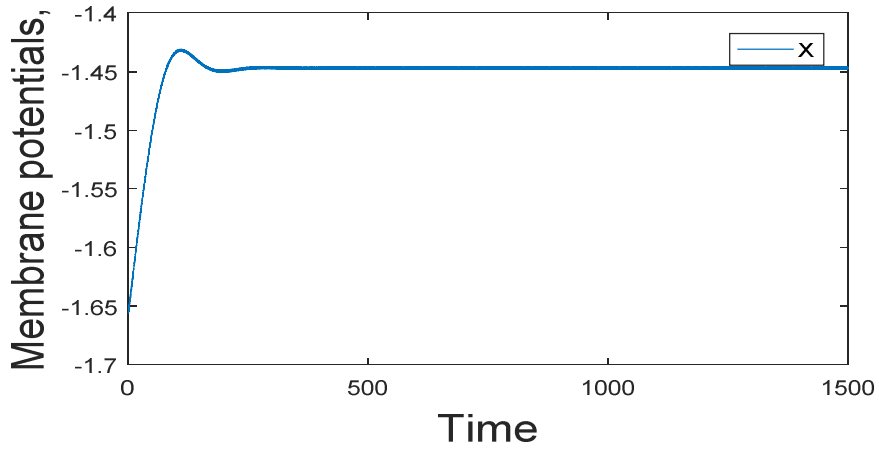

(b)

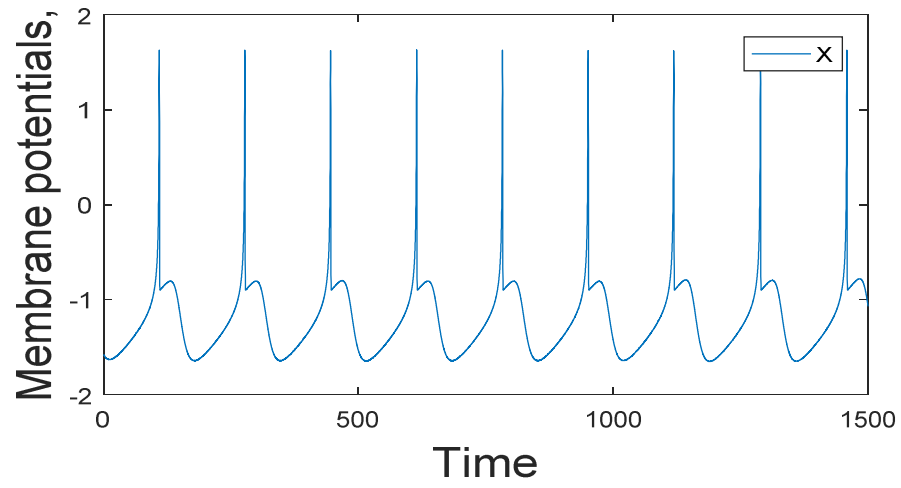

(c)

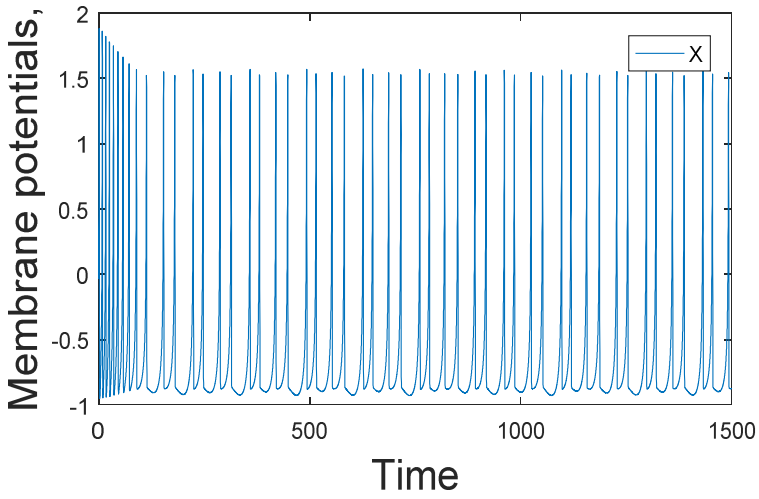

Figure 5.2: Time series plot of membrane potentials for coupling stength g=0.5(a) Oscillation suppression of neuron under I_{ext}=0.5. (b) spiking activity I_{ext}=1.5 (c) tonic spiking for I_{ext}=3.5

5.3.2. Synchronization behaviour of neurons under field coupling

Here the two improved H-R neurons are selected and its dynamics is analysed for coupled neurons under field coupling. The corresponding mode transitions of electrical activities under electromagnetic induction due to field coupling are analysed[194,205,209]. For low coupling strength (g=0.3), the system shows distinct dynamics such as suppression of activity, spiking and death of neuron, antiphase state and chimera state etc. under various external forcing currents (Figure 5.3).

(a)

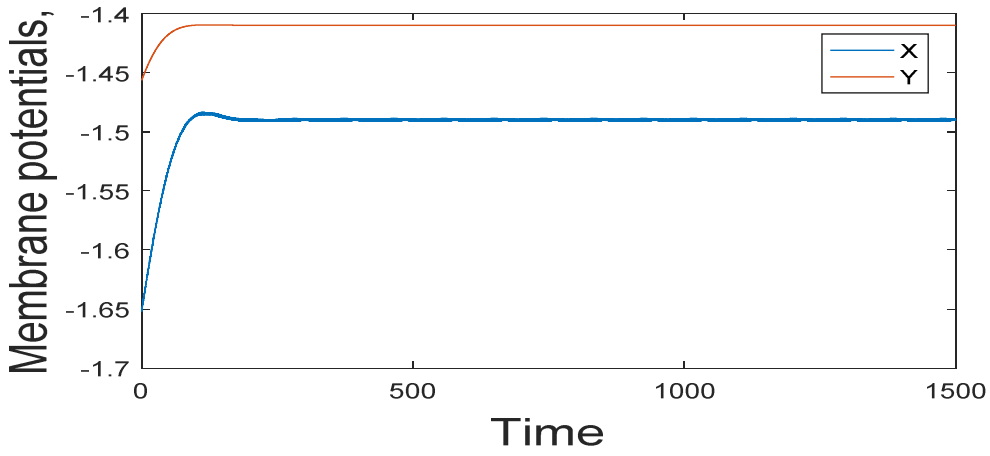
Membrane potentials,
-1.4
-1.45
-1.5
-1.55
-1.6
-1.65
-1.7
0
500
1000
1500
Time
X
Y

(b)

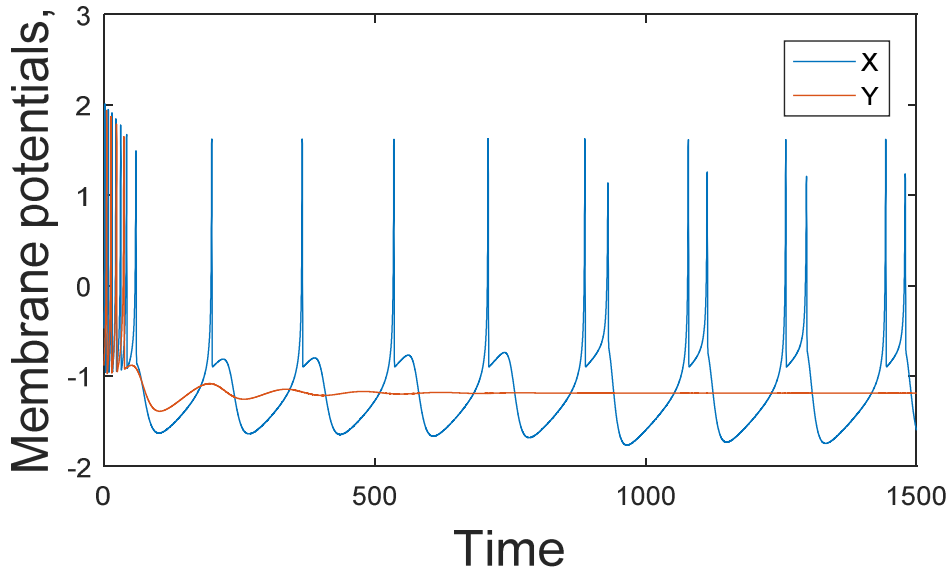
Membrane potentials,
3
2
1
0
-1
-2
0
500
1000
1500
Time
X
Y

(c)

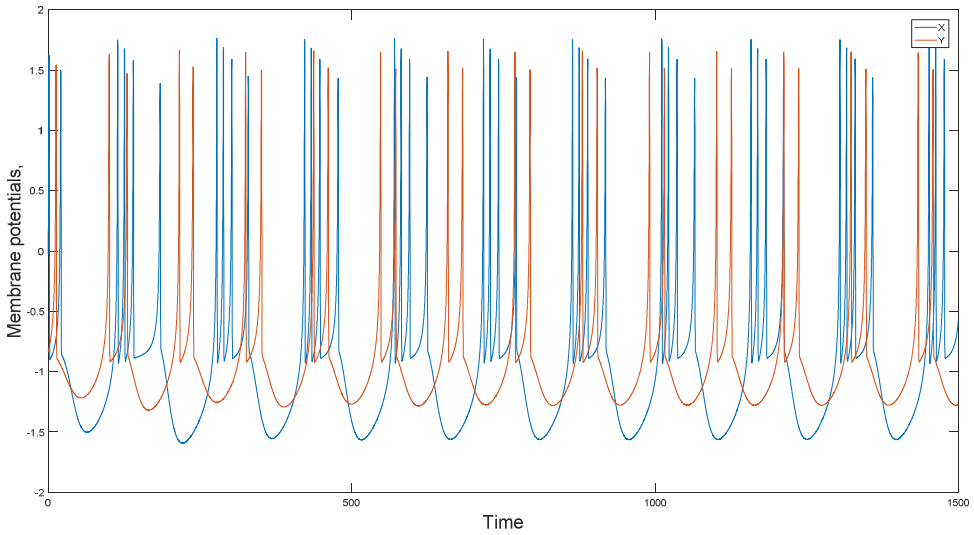

(d)

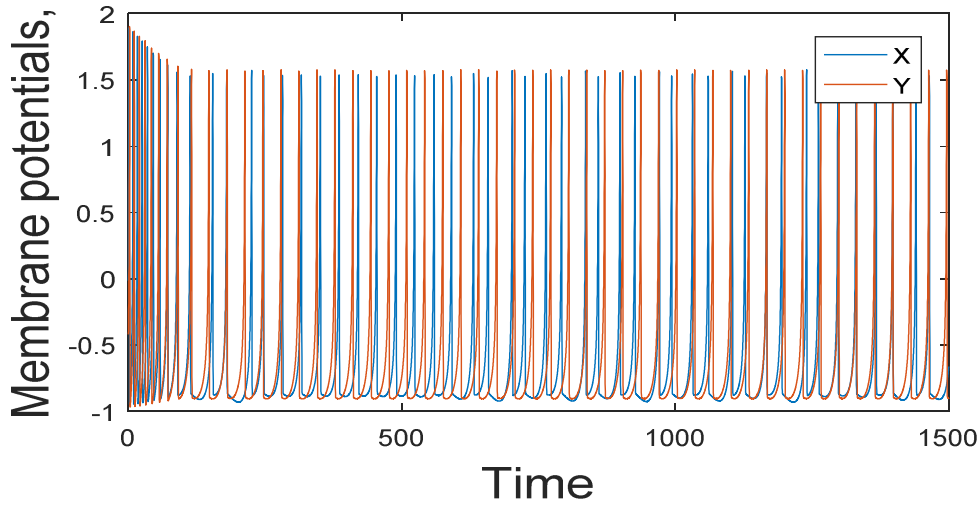

Figure 5.3: The time series analysis of coupled neuron for coupling strength g=0.6.(a) Two neurons are in oscillation death state for I_{ext}=0.5.(b) For the current I_{ext}=1.5, the spiking of one neuron and death of other one takes place. (c) Antiphase synchronization/desynchronization observed for I_{ext}=2.5(d) chimera states occurs at I_{ext}=3.5

Further the study is extended with high value of coupling strength (g=1). The system dynamics exhibits quiescent modes, bursting, oscillation death as the values of external current increases. The result is quite different comparared to that of low coupling intensity. For low coupling strength the oscillation death occurs under low values of external stimulating current. But as coupling strength increases suppression of oscillation may takes place even under high stimulating current. Hence we can reign the dynamic behaviours under field coupling by selecting appropriate control parameters Figure 5.4.

(a)

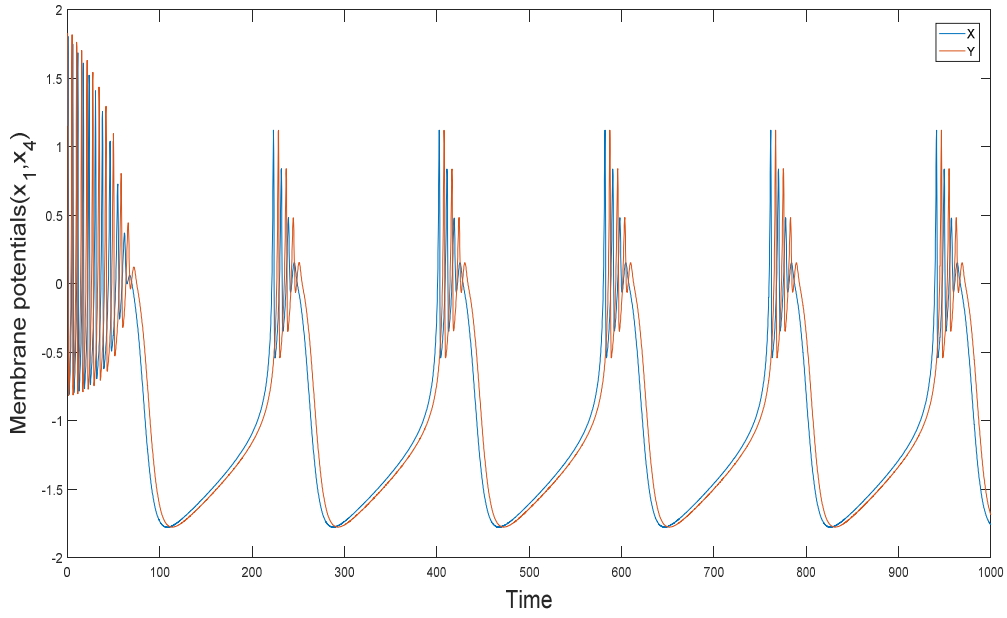

(b)

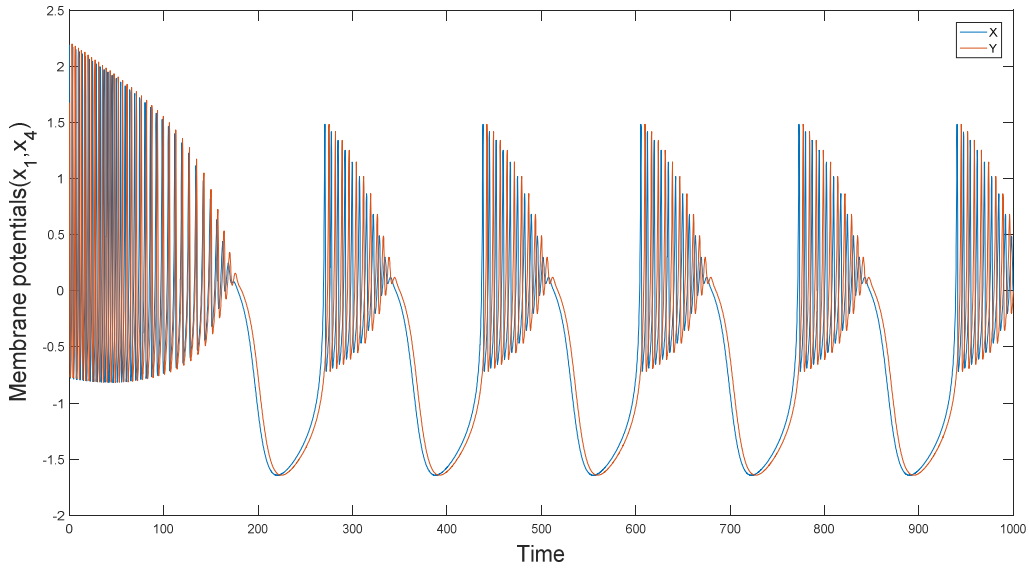

(c)

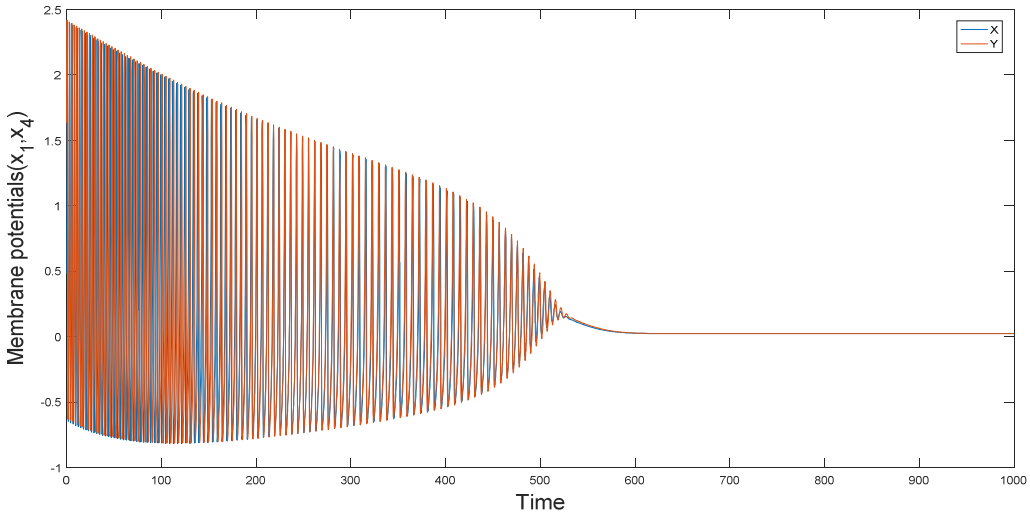

Figure 5.4: The time series analysis of coupled neuron for coupling strength g=1 (a) Two neurons are in quiescent state for I_{ext}=0.5 (b) For the current I_{ext}=2.5, the quiescent states gets broadened (c) oscillation suppression occurs at I_{ext}=3.5.

The field interaction between each neuron can change discharge period of a neuron. The field coupling can drive neurons to give appropriate response in time. Here the synchronization degree varies with external forcing current.

5.4. Collective responses in electrical activities of H-R neurons under field coupling.

The influence of field coupling on the collective behaviours in neuronal network connected by electric synapse[200,210,171] between adjacent neurons is also analysed.

Transition to synchronized state with increase in coupling strength is observed for 300 H-R neurons. In Figure 5.5, i denotes the oscillator (neuron) number and x_i denotes the membrane potential of ith neuron. Figurers (a) and (b) represents the dynamics of 300 H-R neurons for g = 0 . 1 (desynchrony) and 1.0 (complete synchrony) respectively.

(a)

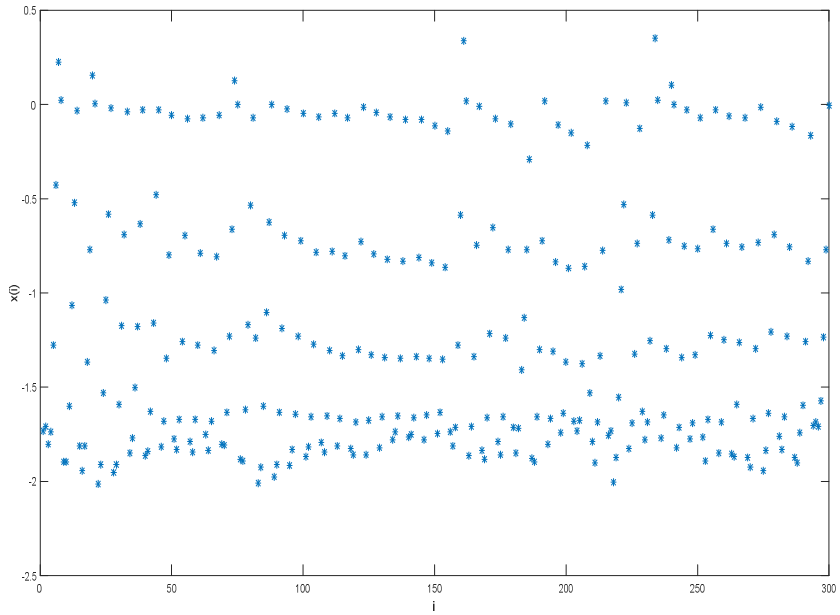

(b)

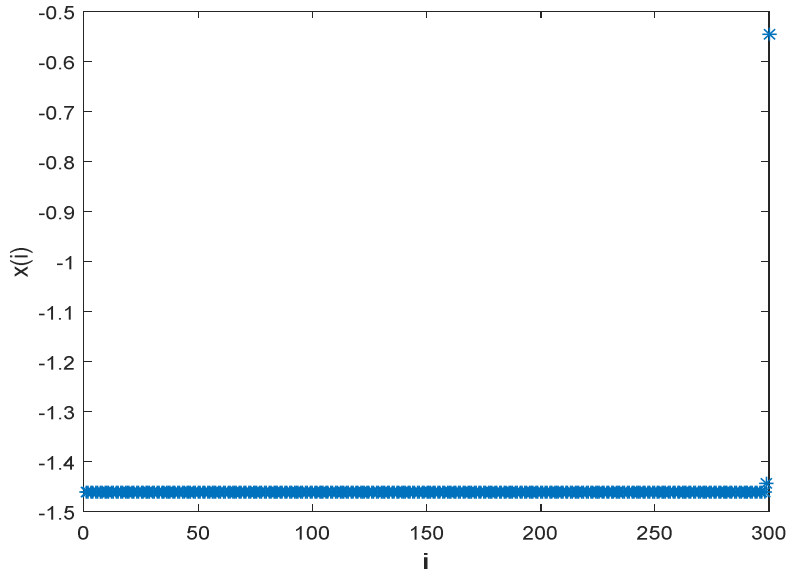

Figure 5.5: Transition from desynchronized state(incoherent) to complete synchrony with increase in coupling strength, where i denotes the oscillator number and x_i denotes the membrane potential of i th neuron. (a) and (b) represents the dynamics of 300 H-R neurons for g = 0. 1 (desynchrony) and 1.0 (complete synchrony) respectively.

5.5. Analysis with control inputs.

The control law serves as a bridge to estimate the unknown parameters of the model[210,211,171]. The analysis based on control law can indicate disease condition in the case of biological neurons. It can be used as a bridge network in between the abnormal and normal network. The method of deriving control laws for synchronization can be used in many complex networks, such as electronic circuits, computer networks and may be used as a potential method for adjusting neuronal rhythm to cure mental disorders in future. In the following section the synchronization condition for the model including the

control inputs are developed. Control inputs can be analysed by Lyapunov function method. The dynamics of system with control input can be written as

$$\dot{x}_{1i} = x_{2i} - ax_{1i}^2 + bx_{2i}^3 - x_{3i} + I_{ext} - k\rho(x_{4i})x_{1i} + u(i, x_{1i})$$

$$\dot{x}_{2i} = c - dx_{1i}^2 - x_{2i} + u(i, x_{2i})$$

$$\dot{x}_{3i} = r\big(s(x_{1i} - x_0)\big) - x_{3i} + u(i, x_{3i})$$

$$\dot{x_{4i}} = k_1 x_{1i} + g(\sum_{i\neq j}^{N} x_{4j} - x_{4i}) + u(i, x_{4i}) \tag{5.4}$$

The synchronization errors are defined as

$$e(i, x_{1i}) = x_{1ni} - x_{1i}, \quad e(i, x_{2i}) = x_{2ni} - x_{2i}, \quad e(i, x_{3i}) = x_{3ni} - x_{3i},$$

$$e(i, x_{4i}) = x_{4ni} - x_{4i} \tag{5.5}$$

The error dynamics are taken the form

$$\dot{e}(i, x_{1i}) = e(i, x_{2i}) - a(x_{1ni} - x_{1i})^2 + b(x_{2ni} - x_{2i})^3 - (x_{3ni} - x_{3i}) - k\rho e(i, x_{1i}) - u(i, x_{1i})$$

$$\dot{e}(i, x_{2i}) = -d(x_{1ni} - x_{1i})^2 - e(i, x_{2i}) - u(i, x_{2i})$$

$$\dot{e}(i, x_{3i}) = rs\,(x_{1ni} - x_{1i}) - e(i, x_{3i}) - u(i, x_{3i})$$

$$\dot{e}(i, x_{4i}) = k_1(x_{1ni} - x_{1i}) - g\,e(i, x_{4i}) - u(i, x_{4i}) \tag{5.6}$$

Considering the Lyapunov function using difference variable we get,

$$V = \frac{1}{2}\sum_{i=1}^{N-1} e(i, x_{1i})^2 + e(i, x_{2i})^2 + e(i, x_{3i})^2 + e(i, x_{4i})^2 \tag{5.7}$$

$\dot{V}= e(i,x_{2i})e(i,x_{1i})\text{-}a(x_{1ni}-x_{1i})^2e(i,x_{1i})+b(x_{2ni}-x_{2i})^3e(i,x_{1i})-(x_{3ni}-x_{3i})e(i,x_{1i})-k\rho e(i,x_{1i})^2-u(i,x_{1i})\,e(i,x_{1i})-d(x_{1ni}-x_{1i})^2e(i,x_{2i})-e(i,x_{2i})^2-u(i,x_{2i})\,e(i,x_{2i})+rs\,(x_{1ni}-x_{1i})e(i,x_{3i})-e(i,x_{3i})^2-u(i,x_{3i})e(i,x_{3i})+k_1(x_{1ni}-x_{1i})e(i,x_{4i})-g\,e(i,x_{4i})^2-u(i,x_{4i})\,e(i,x_{4i})$ Here $i=1\ldots\ldots\ldots\ldots\ldots\ldots\ldots n-1$ (5.8)

The controllers are chosen to ensure that the time derivative of Lyapunov function is negative definite. The errors converge to zero as $t\to\infty$, this leads to asymptotically stable synchronization manifold.

So controllers are chosen as

$$u(i,x_{1i})=e(i,x_{2i})a(x_{1ni}-x_{1i})^2+b(x_{2ni}-x_{2i})^3-(x_{3ni}-x_{3i})-k\rho e(i,x_{1i})$$

$$u(i,x_{2i})=-d(x_{1ni}-x_{1i})^2+e(i,x_{2i})$$

$$u(i,x_{3i})=rs\,(x_{1ni}-x_{1i})-e(i,x_{3i})$$

$$u(i,x_{4i})=k_1(x_{1ni}-x_{1i})-e(i,x_{4i}) \quad (5.9)$$

Then

$$\dot{V}=-g\sum_{i=1}^{n-1}e(i,x_{4i})^2 \quad (5.10)$$

Hence H-R neuron network with field coupling analysed with controller shows that Lyapunov function derivative is negative.

5.6. Stability of Synchronization

The stability of synchronization of the selected model can be quantified using the master stability approach developed by Pecora and Carroll [211] . The master stability function allows to establish whether any linear coupling

arrangement will produce stable synchronous dynamics. It also helps to reveal the desynchronization bifurcation mode which occur when the coupling scheme or strength changes. The synchronization is stable if the master stability function is negative for each of the transverse eigenvalues. The analytical expressions for estimating the synchronization threshold for diffusively coupled continuous and discrete time chaotic systems have been reported earlier [211,212].

For the stability of synchronization, complete stable synchronization occurs,when the difference between neural oscillator coordinates $x_i = x_n - x_i$, $y_i = y_n - y_i$ and $z_i = z_n - z_i$ vanish in the limit of t→ ∞ and there exists a synchronous solution $\eta_1(t)$= $\eta_2(t)$=……= $\eta_n(t)$.Where $\eta_i(t)$=(x_i, ,y_i,z_i). Hence the stability of equations for perturbations transverse to synchronization corresponding to given equation can be calculated.

The activation–inactivation dynamics of fast ion channel for coupling has been analyzed by varying the value of coupling strength from 0 to 5. The minimal condition for the stability of synchronized state[211,171] is the negativeness of the Transverse Lyapunov Exponents (TLEs) associated with equation (5.2).

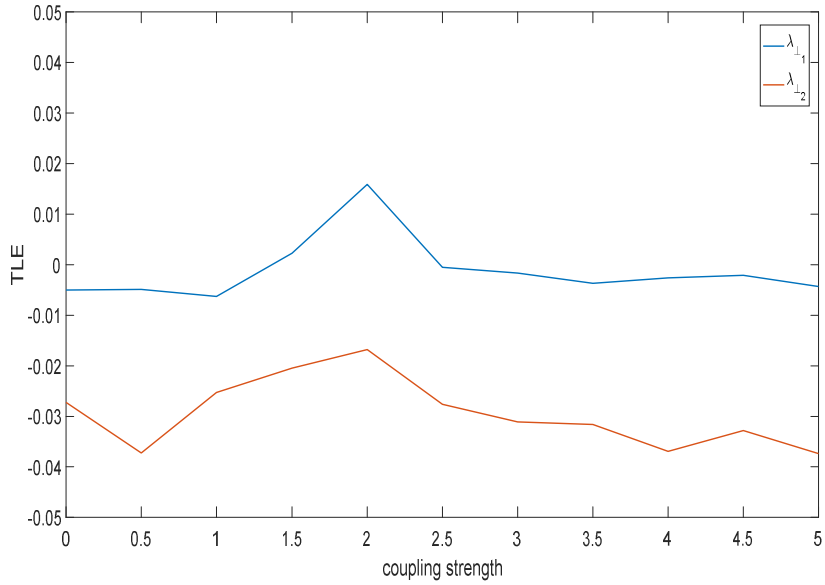

Figure 5.6: The TLEs of coupled HR neural network. (a) Coupling strength is plotted along *x* axis and TLE along *y* axis. The largest (blue color) TLE (λ⊥ 1) become positive under coupling strength 1.1<g<2.7.

Variation of two largest TLEs (λ⊥ 1 and λ⊥ 2) with increase in *g* are shown in Figure 5.6. As the coupling strength is increased, the largest TLE (λ⊥ 1) increases initially, reaches a peak, and then decreases. The largest TLE crosses zero and become negative indicating a transition from desynchronized state to complete synchrony.

5.7 Summary

In the complex physical and biological conditions (for example, noise driving and electromagnetic radiation), it is very difficult to achieve the complete synchronization between neurons [194,196,212,213]. But the phase synchronization or rhythms are available in such cases. In the work presented here it is observed that magnetic coupling is an effective way to realize synchronization. The effect of field coupling on the electromagnetic induction is

examined. The corresponding modes of electrical activities with cubic flux controlled memristor are examined by finding the influence of the magnetic flux on membrane potential. For isolated and coupled neurons, different mode transitions in electrical activities can be analysed by increasing the intensity of field coupling. Under low coupling strengt has the external forcing current increases the system shows diversity in behaviour. Various dynamics such as oscillation death, tonic spiking, desynchronization and chimera state etc. are resulted in. As coupling strength increases, dynamics of spiking, bursting and oscillation suppressions etc. are resulted in. Hence under high coupling strength oscillation suppression can be observed for high stimulating current. It is observed that for network of 300 H-R neurons, the neuron oscillators show incoherent as well as synchronization behaviour. Stability of system is confirmed by negativeness of Transverse Lyapunov Exponent plot.

The mode in electrical activities can be controlled by field coupling. The excitability of neuron can varies with the external forcing current, and larger external stimuli are much helpful to excite neurons. This is well understood through the numerical studies. So present studies gives ideas to understand the signal encoding and exchange when synapse coupling is absent.

Chapter 6

Dynamics of Josephson Junction model with Memristor and H-R neuron

Chapter 6

Dynamics of Josephson Junction model with Memristor and H-R neuron

6.1 Introduction

In Josephson Junction the quantum-mechanical effect is responsible to produce a non-ohmic current between two superconductors separated by an insulator. Complex chaotic behaviours can be simulated in the Josephson Junction (JJ) circuits when it is coupled with other electric elements such as resistance and inductance coil [214].

The superconducting circuits with Josephson Junctions can model biologically realistic neurons. Josephson Junction neurons can mimic many characteristic behaviour of biological neurons with respect to action potentials, refractory periods and firing thresholds [163]. Action potential is of the order of picosecond roughly a billion times shorter than that of other neuron models (H-H neuron, FHN neuron etc.)[164]. The individual junctions behave like ion channels. Josephson Junctions are easy to design and inexpensive to fabricate. It is easy to fabricate up to 20,000 junctions using rapid single flux quantum technology (100 GHz). Here a Single chip can model 10000 neurons. Hence it can be used for larger brain regions. Shorter transit time and less power dissipation is an added advantage of the model. It is possible to model single neurons with two Josephson Junctions [214,215].

Single flux quantum technology is used for neuromorphic computing. When operating in a low current regime near critical current, Josephson Junctions naturally behave like spiking devices[214]. It is possible to compare numerical solutions of the voltage and current equations for the Josephson circuit with simulations of other well-known biological models. The results

exhibit striking quantitative similarities between the models. Josephson Junction can operate in parallel and a single Josephson neuron in isolation can run as quickly as a thousand fully interconnected ones. It is faster than computer simulations of any other neuron model and that of actual biological ones.

The study of dynamics of Josephson Junction also shows potential applications in many fields such as secure communication and the study of high frequency of circuit[215]. The memristor coupled Josephson Junction circuit is effective to apply in the encryption and decryption of an image[216]. The present studies could be useful to construct a network of neuronal circuits in a large scale so that the collective behaviours of neurons could be detected and investigated.

The effect of electromagnetic induction in Josephson Junction circuit model can be analysed by introducing the magnetic flux variable into the model. Here memristor[218] is used to realize feedback between magnetic flux and Junction potential. When memristor is used in circuits the nonlinearity of electric circuit is enhanced. Memristor can describe the effect of memory and can bridge the output voltage and magnetic flux by generating induction current. Using improved model with memristor, the different modes of electrical activities can be detected which is consistent with biological experiments [219-221]. Wu and et al. [220,221] imposed phase noise on the improved neuron. A time-varying electromagnetic field was induced to trigger different modes of electrical activities and coherent resonance behaviour was observed[220]. Studies[221-223] showed that the chaotic system coupled by flux controlled memristor can enhance the communication security and nonlinear properties.

Recent studies[222] proposed a new nonlinear logarithmic model to characterize memristor and an effective memristor emulator has been designed.

This enables the relationship between memductance and flux to be expressed by an inverse proportional function. It is significant to focus on the application and analysis of this model in neuromorphic computing.

It is possible to simulate the neuronal electrical activity using the biological neuron model and Josephson Junction neuron model. They can be coupled together to mimic electrical and chemical synapses[214-217]. It helps to understand the dynamics of collections of neurons. It is observed that the biological neuron models, such as Hodgkin–Huxley (H-H), Hindmarsh–Rose (H-R), Morris–Lecar (M-L) can be used to measure and simulate the electric activities of neurons[219, 222, 223, 68, 69, 67]. The time series of membrane potential variables can be periodical or chaotic in different parameter regions. Recent studies [222-229] showed that resistive-capactive-inductive-shunted Josephson Junction(RCLSJ) model could be controlled to reproduce some electric activities of FitzHugh–Nagumo neuron model. The larger gain coefficients were reported to be active to speed up the process of synchronization. Studies [223,224] showed that the power consumption of controller is independent of the selection of gain coefficients. Xinyi Wu and et al. [221] confirmed electric activities in Josephson Junction coupled resonator and in Morris–Lecar neuron. It is possible to design electric circuits using the Personal Simulation Program with Integrated Circuit Emphasis (PSPICE)[230]. The parameter regions were detected to generate spiking and bursting for neurons and these were consistent with the numerical results. It is possible to detect the excitability of the neuron model with Bifurcation diagrams for Inter Spike Interval (ISI) vs.forcing current [222].

In this chapter the dynamics of Josephson Junction is analysed with different memristors. Study on electromagnetic induction in Josephson Junction with flux controlled memristor shows fast periodical and double periodical

spiking. The studies indicate that the dynamical properties of Junction potential depend on the coupling intensity, the voltage and the magnetic flux. Also numerical studies of Josephson Junction with logarithmic memristor show periodic spiking and suppression of oscillation. In both cases chaotic nature of system is predicted by Lyapunov Exponent versus gain plot. These behaviours are quite different from that of cubic flux controlled memristor[219, 208] where the periodical, multi-periodical and chaotic state were reported for appropriate gains. There it was found that the induction current in the system generates negative feedback at positive values of gain and the excitability and the oscillating behaviours were found to be suppressed[219]. The suppression of oscillating behaviour with logarithmic memristor at positive feedback is a different feature observed in the present work.

The problem is defined in section 6.2, the dynamical behaviour of Josephson Junction with different memristors are discussed in section 6.3. In section 6.4, an improved adaptive scheme is used to control the RCLSJ model to simulate the dynamical properties of H-R neurons. The possibility of generalized synchronization [222] between the two systems is examined in this section. With the controller with suitable gain coefficients, it is effective to reach synchronization. The dynamics is analyzed by the time series, phase portraits and by Lyapunov stability analysis. Time series behaviour shows spiking, bursting and tonic spiking. Also it is shown that the gain coefficient of the membrane potential of Josephson Junction neuron can be reduced such that the H-R neuron membrane potential lies within the same range of variation of the membrane potential of Josephson Junction.

The H-R neuron model can emerge into different states such as quiescent, periodical and chaotic state in appropriate parameter regions [227, 228]. The electric activities of Hindmarsh–Rose neurons can be shown to

be similar to that of Josephson Junction neuron model[176]. Here resistive–capacitive–inductive-shunted Josephson junction (RCLSJ) [216, 214] is exhibitng the same simulated behaviour as that of Hindmarsh–Rose neuronal discharges. Hence this model helps to understand the pattern formation and synchronization on network of neurons.

6.2. Definition of problem

It is possible to enhance the nonlinearity of electric circuits by using memristor in circuits. Here the memductance is dependent on the input current. As a result the more complex dynamical behaviours can be resulted in [214]. Josephson Junction (JJ) coupled resonator also present complex dynamical behaviours in nonlinear circuit because JJ is used as sensitive inductive component.

The Josephson Junction circuit coupled with memristor can be illustrated as below (Figure 6.1)

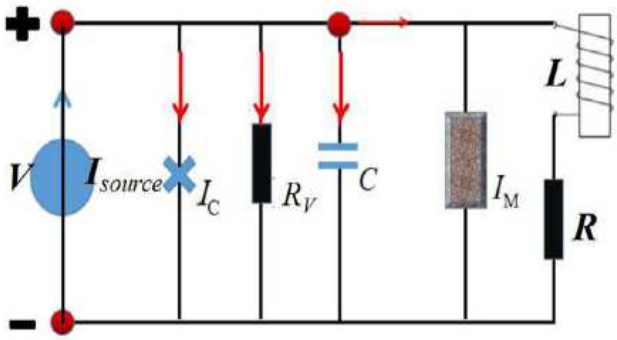

Figure 6.1: Josephson Junction circuit with memristor(adapted from[214])

Josephson junction current with memristor using kirchoff's law can be written as

$$I_{source} = C\frac{dV}{dt}+\frac{V}{R_V} + I_c sin\gamma + I_L + I_M$$

$$V = \frac{h}{2e}\frac{d\gamma}{dt}$$

$$V = L\frac{dI_L}{dt} + I_L R$$

$$\frac{d\varphi}{dt} = V \tag{6.1}$$

Where V is the potential of Josephson junction. I_c represents the junction current. Nonlinear junction resistance is represented by R_V . I_{source} is the external bias current. γ and h represents the phase difference in superconductor and the planks constant respectively. e is elementary charge and R and L denotes resistor and inductor respectively at circuit branch.

According to the Faraday's law of electromagnetic induction, the nonlinear memductance function and the induction current for memristor[8] are described as

$$I = \frac{dq(\varphi)}{dt} = \frac{dq(\varphi)}{d\varphi}\frac{d\varphi}{dt} = \rho(\varphi)V \tag{6.2}$$

Here $\rho(\varphi)$represents the memductance term. The analysis of dynamics of neuronal system with Josephson junction is done in the following sections.

6.3 Dynamical behaviour of Josephson Junction with Different Memristor

6.3.1. Cubic flux controlled memristor

The Josephson Junction circuit employing cubic flux controlled memristor is examined in this section. The dynamical properties of the model are explored also with respect to phase portraits and Lyapunov Exponents.

When the effect of electromagnetic induction is considered, dynamical equations of four variable Josephson Junction model can be represented by [223].

$$\dot{x}_1 = \frac{1}{\beta_c}[i - g(x_1)x_1 - \sin(x_2) - x_3 - k_0 x_1(\delta + 3\varphi^2\mu)]$$

$$\dot{x}_2 = x_1$$

$$\dot{x}_3 = \frac{1}{\beta_L}(x_1 - x_3)$$

$$\dot{\mu} = k_1 x_1 - k_2\mu \tag{6.3}$$

Here μ, the fourth variable (depicted as x_4 in plots) describes magnetic flux and memductance of flux controlled memristor which is represented by $(\delta + 3\varphi^2\mu)$. The parameters k_0, k_1 and k_2 are gains used to calculate the effect of electromagnetic induction on junction. The term $k_2\mu$ describes a feedback of magnetic flux that contributes the induction current.

For a Josephson Junction circuit, the nonlinear memductance function and induction n current for memristor are described by the equation

$$I = \frac{dq(\varphi)}{dt} = \frac{dq(\varphi)}{d\varphi}\frac{d\varphi}{dt} = \rho(\varphi)V = k_0(\delta + 3\varphi^2\mu) \tag{6.4}$$

6.3.1.1 Time series analysis and Lyapunov exponent plot of Josephson junction with Memristor

The fourth order Runge-Kutta algorithm is used for numerical studies. When the parameters $k_1 and\ k_2$ are fixed, the relation between sampled junction potentials and current of the inductance is detected to generate different phase portraits for the selected k_0. It is observed that by selecting appropriate gains k_0, periodic and doubly periodic fast spiking is resulted in. The dynamics is studied for parameter values as $k_0 = 0.1$, $k_1 = 0.4$, $k_2 = 0.6$ and $k_0 = 1.0$, $k_1 = 0.4$, $k_2 = 0.6$ respectively. The parameter values for memristor are selected as α=0.2 and β=0.4. The sampled time series for output voltage are plotted by applying different feedback gain. It is observed that the gain on magnetic flux control the abundant chaotic behaviours.

(a)

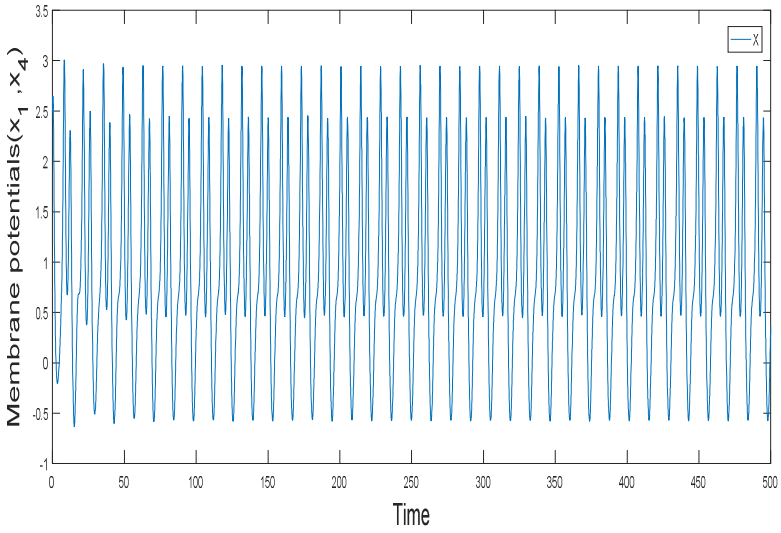

(b)

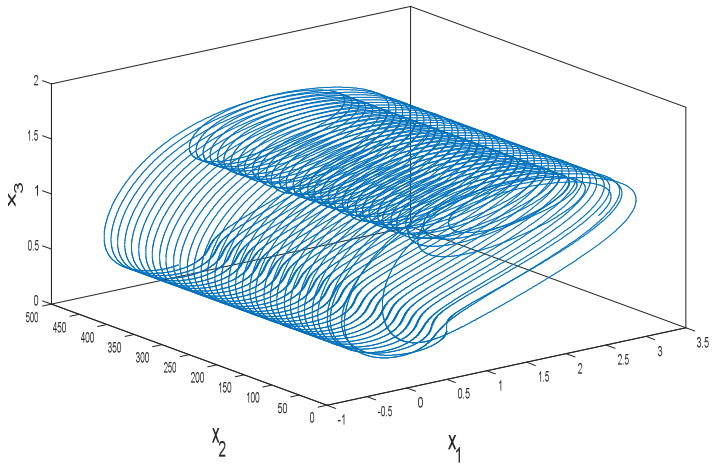

(c)

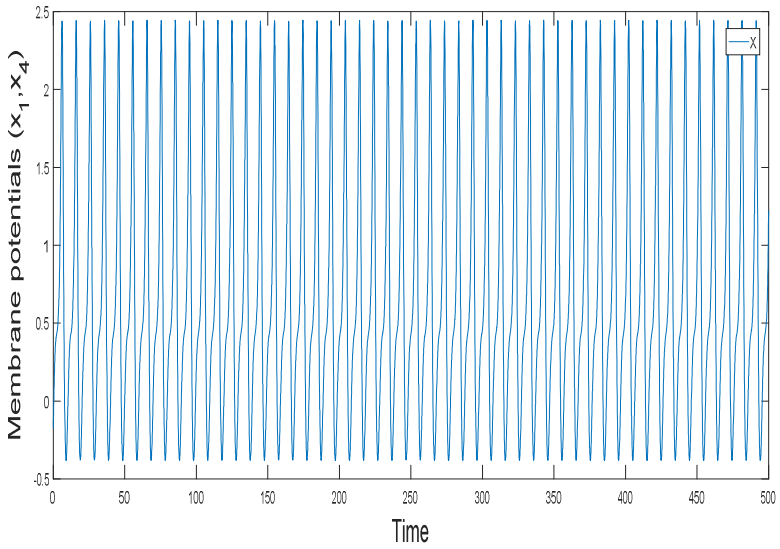

(d)

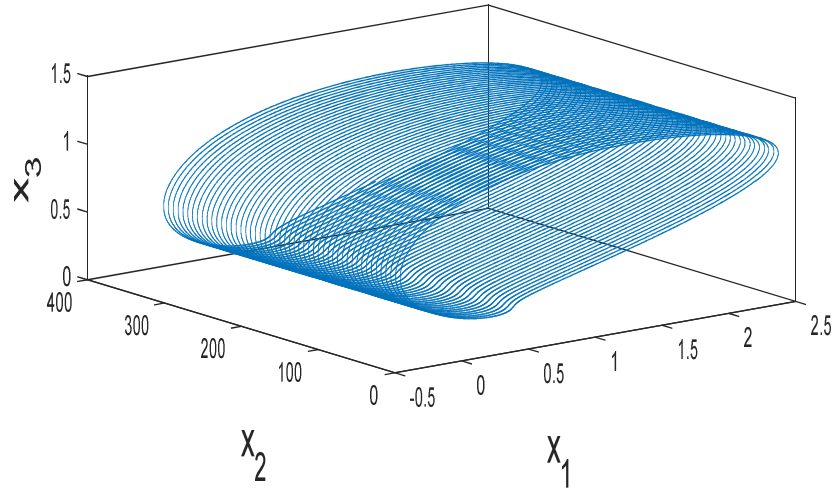

Figure 6.2: (a,b) Fast spiking and corresponding phase portraits for Josephson Junction coupled with memristor for parameters values as k_0=0.1, k_1=0.4, k_2=0.6 and **(c,d)** As gain parameter k_0 changes to 1, the neuron spikes with only one voltage value at all time.

The distribution for magnetic flux in the junction plays important role in changing the dynamical properties of electrical activities. Hence the chaotic dynamics in the system of Josephson Junction with memristor is also analysed with Lyapunov Exponent spectrum. Existence of positive value of Lyapunov Exponent for various values of the gain k_0 of the Josephson Junction circuit shows chaotic nature of the system (Figure 6.3).

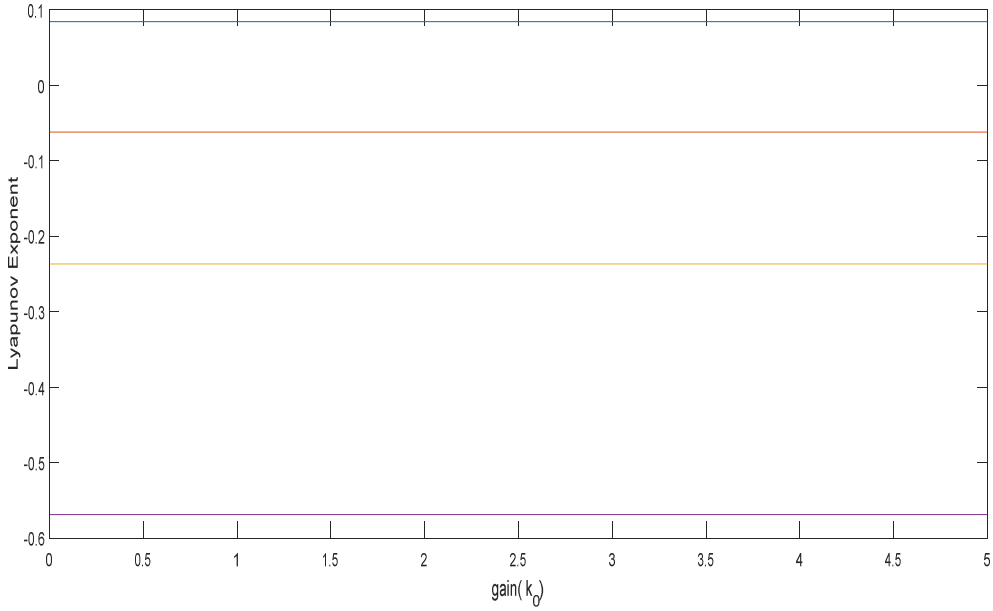

Figure 6.3: Lyapunov Exponent verus gain for JJ circuit coupled with memristor

So the numerical simulations of time series and Lyapunov Exponent plot versus gain confirmed the chaos for all values of feedback gain in induction current. Multiple electrical activities can be found in sampled time series for junction potentials under appropriate feedback gain. The gain k_0 regulates the coupling between junction potential and magnetic flux, which causes diversification of junction current. The other feedback parameters k_1 and k_2 also help to detect the dynamical behaviours [219,222].

By increasing parameter k_0, the transition to doubly periodic spiking is resulted in. It describes electrical activities in response to electromagnetic induction described by the memristor and magnetic flux. Hence gain on magnetic variable is found to be responsible for different dynamical characteristics [219,222].

6.3.2 Logarithmic Memristor

When the effect of electromagnetic induction is considered, the dynamical equations for the four-variable Josephson Junction model are described by

$$\dot{x}_1 = \frac{1}{\beta_c}\left[i - g(x_1)x_1 - \sin(x_2) - x_3 - k_0 x_1\left(\frac{1}{\alpha - \beta x_4}\right)\right]$$

$$\dot{x}_2 = x_1$$

$$\dot{x}_3 = \frac{1}{\beta_L}(x_1 - x_3)$$

$$\dot{x_4} = k_1 x_1 - k_2 x_4 \tag{6.5}$$

Here $g(x_1)$ denotes the correlation between voltage and current of Josephson Junction.

$$g(x) = \begin{cases} 0.366 & x_1 < 2.9 \\ 0.0661 & x_1 \geq 2.9 \end{cases} \tag{6.6}$$

The voltage, phase difference and induction current of Josephson Junction are represented by $\dot{x_1}$, $\dot{x_2}$ and $\dot{x_3}$ respectively. Here i is the external forcing DC current and β_L are parameters of system.

Here x_4, the fourth variable describes magnetic flux and memductance of logarithmic flux controlled memristor which is represented by $\left(\frac{1}{\alpha - \beta x_4}\right)$. The parameters k_0, k_1 and k_2 are gains used to calculate the effect of electromagnetic induction on the junction. The term $k_2 x_4$ describes a feedback on magnetic flux that contributes the induction current. The relation between charge and flux in logarithmic memristor[221] can be obtained by electromagnetic induction

$$I=\frac{dq(\varphi)}{dt} = \frac{dq(\varphi)}{d\varphi}\frac{d\varphi}{dt} = \rho(\varphi)V = k_0\left(\frac{1}{\alpha-\beta x_4}\right) \quad (6.7)$$

The fourth order Runge Kutta algorithm is used for numerical studies with time step 0.01. Initial values for Josephson Junction coupled with logarithmic memristor are selected for $(x_{1,}, x_2, x_3, x_4)$ as (0.2,0.3,0.4,0.2). The MATLAB platform is used for various simulations.

6.3.2.1 Time series analysis and Lyapunov Exponent plot of Josephson Junction coupled with logarithmic memristor

Josephson Junction circuit model modified by a logarithmic memristor is proposed. When the parameters k_1, k_2 are fixed, the relation between sampled junction potentials and current of the inductance is detected to generate different phase portraits by selecting appropriate gains for k_0. It is observed that for different gains k_0, periodic spiking and suppression of oscillations can be resulted in. The dynamics is obtained by selecting parameter values as $k_0 = 0.2,\ k_1 = 0.6,\ k_2 = 0.5$ and as $k_0 = 1.0,\ k_1 = 0.5,\ k_2 = 0.6$. The parameter values for logarithmic memristor are selected as α=0.2 and β=0.4. Here the negative feedback can be made strong enough to suppress oscillations. The sampled time series for output voltage are plotted by applying different feedback gain. Corresponding phase portraits are also shown in Figure 6.4a.

(a)

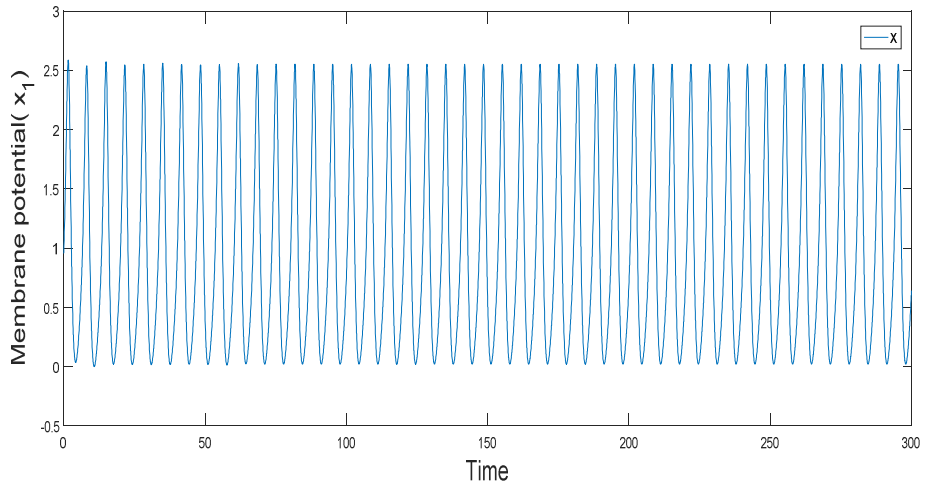
x
Membrane potential(x1)
Time
3
2.5
2
1.5
1
0.5
0
-0.5
0
50
100
150
200
250
300

(b)

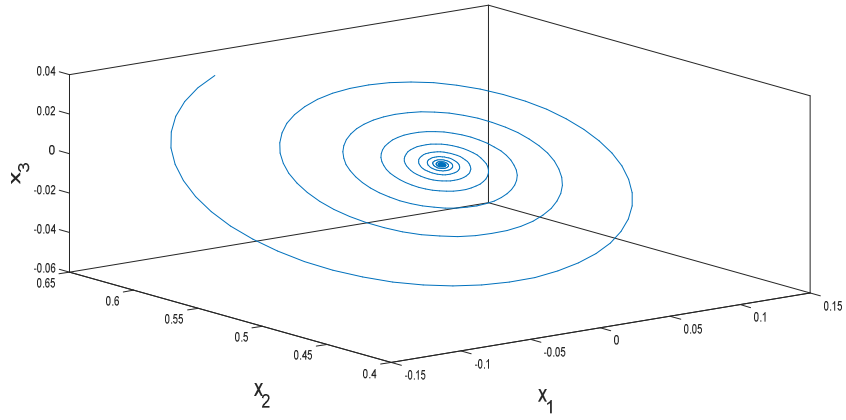
x3
x2
x1
0.04
0.02
0
-0.02
-0.04
-0.06
0.65
0.6
0.55
0.5
0.45
0.4
-0.15
-0.1
-0.05
0
0.05
0.1
0.15

(c)

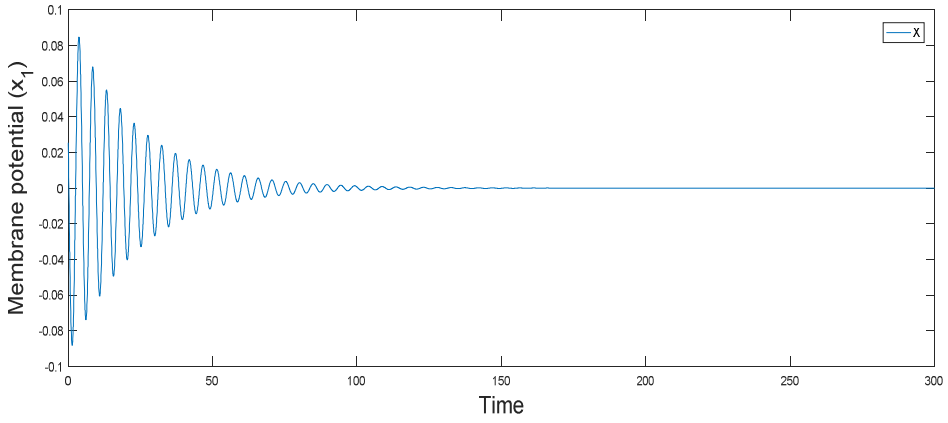

(d)

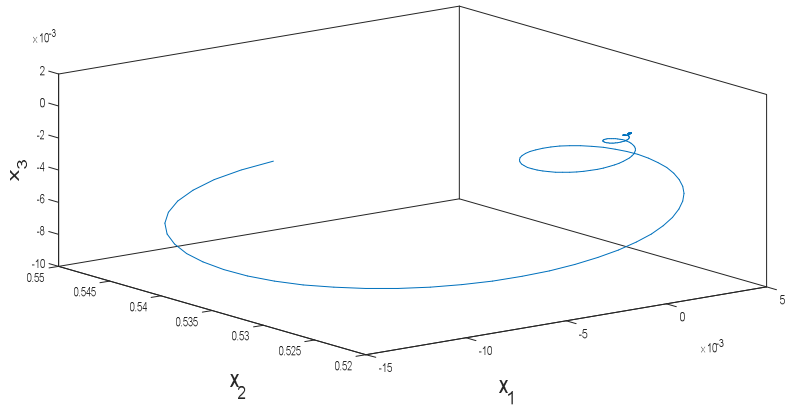

Figure 6.4 (a,b) Periodic spiking and corresponding phase portrait obtained by selecting parameter values as $k_0 = 0.2, k_1 = 0.6, k_2 = 0.5$ (c,d) Suppression of oscillation is observed for $k_0 = 1.0, k_1 = 0.5, k_2 = 0.2$ respectively. The parameter values for logarithmic memristor are selected as α=0.2 and β=0.4 in both cases.

The distribution for magnetic flux in the junction plays important role in changing the dynamical properties in electrical activities. It is interesting to find

the parameter region for chaos by calculating the largest Lyapunov Exponent spectrum [221]. The variation of Lyapunov Exponent versus gain (k_0) confirms chaotic nature of selected system. The other parameters are chosen as $k_1 = 0.6$ and $k_2 = 0.5$ respectively.

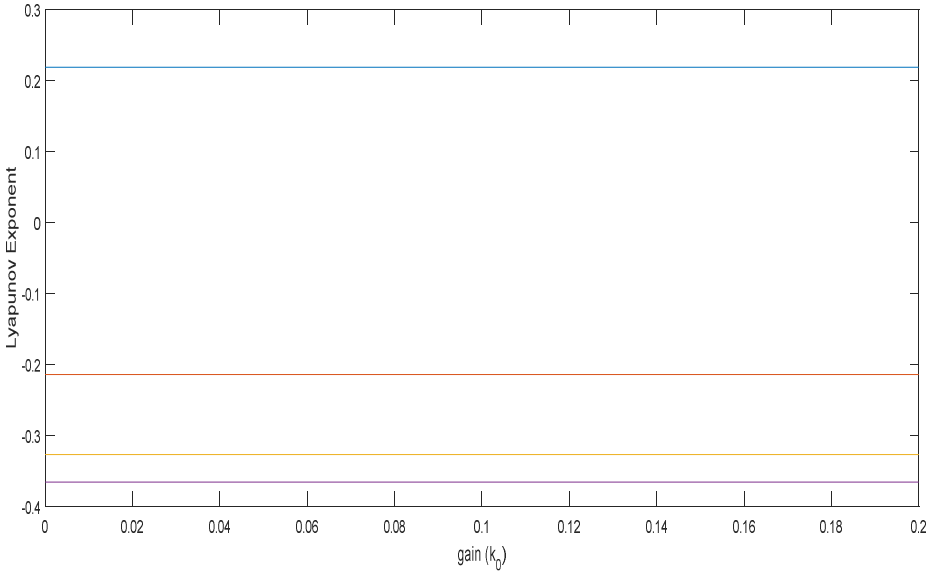

Figure 6.5: Lyapunov Exponent versus gain for Josephson Junction coupled with logarithmic memristor

When the effect of electromagnetic induction is considered, dynamical equations of four variable Josephson Junction model with logarithmic memristor show distinct chaotic behaviour. Numerical studies confirmed that the dynamical properties of Junction potential depend on the coupling intensity (k_0) which bridged the voltage and the magnetic flux.

From numerical studies it is observed that JJ model with logarithmic flux controlled memristor shows distinct behaviours compared with that of cubic flux controlled memristor [219-221]. In cubic flux controlled memristor

sampled time series of membrane potential shows fast periodic and double periodic spiking [215, 221, 227]. The distribution for magnetic flux in the junction changes the dynamical properties in electrical activities. This is confirmed by Lyapunov Exponent spectrum.

6.4 Electric activities and neuronal synchronization of Hindmarsh–Rose neurons simulated by Josephson junction model

The dimensionless model of resistive–capacitive–inductive-shunted Josephson Junction is described by [219, 222, 226]

$$\dot{x_1} = \frac{1}{\beta_c}[i - g(x_1)x_1 - \sin(x_2) - x_3]$$

$$\dot{x_2} = x_1$$

$$\dot{x_3} = \frac{1}{\beta_L}(x_1 - x_3) \tag{6.8}$$

The $g(x_1)$ denotes the correlation between voltage and current of Josephson Junction.

$$g(x) = \begin{cases} 0.366\, x_1 < 2.9 \\ 0.0661\, x_1 \geq 2.9 \end{cases} \tag{6.9}$$

The voltage, phase difference and induction current of Josephson junction are represented by $\dot{x_1}$,$\dot{x_2}$and $\dot{x_3}$respectively. Where i is the external forcing DC current and β_c and β_L are parameters of system.

The original Hindmarsh–Rose (HR) neuron model is given by[68]

$$\dot{x}_4 = x_5 - ax_4^3 + bx_4^2 - x_6 + I_{ext}$$

$$\dot{x}_5 = c - dx_4^2 - x_5$$

$$\dot{x}_6 = r\big(s(x_4 - x_0)\big) - x_6 \tag{6.10}$$

a, b, c, d, r, and s are bifurcation parameters and I is external forcing current. The synchronization between the two corresponding variables is studied by imposing appropriate controller on equation (6.8).

The equation (6.8) for Josephson Junction model can be controlled by a control function u which is governed by the dynamics of both the H-R neuron and Josephson Junction neuron (Equation 6.11)). The control function u is derived from the positive Lyapunov function which is constructed as [219].

$$\dot{x_1} = \frac{1}{\beta_c}[i - g(x_1)x_1 - \sin(x_2) - x_3]$$

$$\dot{x_2} = x_1$$

$$\dot{x_3} = \frac{1}{\beta_L}(x_1 - x_3) + u \tag{6.11}$$

The positive Lyapunov function is constructed as[219]

$$V = \alpha e^2 + (\dot{e} + \alpha\beta e)^2 \tag{6.12}$$

$$\frac{dV}{dt} = 2\alpha e\dot{e} + 2(\dot{e} + \alpha\beta e)(\ddot{e} + \alpha\beta e)$$

$$= -2\alpha\beta V + 2\alpha\beta V + 2\alpha e\dot{e} + 2(\dot{e} + \alpha\beta e)(\ddot{e} + \alpha\beta e)$$

On rearranging

$$\frac{dV}{dt} = -2\alpha\beta V + 2(\dot{e} + \alpha\beta e)[\ddot{e} + 2\alpha\beta\dot{e}(\alpha^2\beta^2 + \alpha)e] \tag{6.13}$$

So condition for negative error dynamic equation

$$[\ddot{e} + 2\alpha\beta\dot{e}(\alpha^2\beta^2 + \alpha)e] = 0$$

$$\frac{dV}{dt} = -2\alpha\beta V < 0$$

$$V = V_0 e^{-2\alpha\beta t} \tag{6.14}$$

$$\begin{aligned} u = -\beta_c[c - dx_4^2 - x_5 - (3ax_4^2 - 2bx_4)(x_5 - ax_4^3 + bx_4^2 - x_5 + I) \\ - r[s(x_4 + 1.6) - x_5) - \frac{g}{\beta_c}(i - g(x_1)x_1 - sinx_2 - x_3) \\ - x_1 cosx_2 - \frac{1}{\beta_L}(x_1 - x_3) \\ - 2\beta_c\alpha\beta\left[x_5 - ax^3 + bx^2 - x_5 + I \right. \\ \left. - \frac{1}{\beta_c}(i - g(x_1)x_1 - sinx_2 - x_3)\right] - \beta_c(\alpha + \alpha^2\beta^2)(x_4 - x_1) \end{aligned} \tag{6.15}$$

The gain coefficients α and β can change the synchronization. By controlling the gain coefficients for the model it is possible to analyse different dynamical properties.

6.4.1 Simulation of electric activity of neuronal synchronization

The initial values for the model are chosen for (x_1, x_2, x_3, x_4) as (0.2,0.3,0.3 and 0.1). Depending upon the gain coefficients different modes in activities are resulted in. Simulation results confirm that at certain values of α and β, the two systems reach phase synchronization. Time series analysis of output variables from H-R and RCLSJ model could not reach complete synchronization for some values of gain parameters within short transient period. It means that system does not settle down to stable values. However, the output time series of the two variables in the H-R and RCLSJ model are locked for appropriate values of gain coefficients.

With suitable values of gain coefficients, both systems show various chaotic activities such as spiking, bursting and synchronized states etc. It is observed that for α=0.1 and β =0.01 both systems are in spiking mode [Figure. 6.6(a)]. The behaviour gets changed to bursting activity for α=0.05 and β =0.01 [Figure 6.6(b)]. On reduction of the gain coefficient to α =0.01 with β =0.01 the tonic synchronization resulted in [Figure 6.6(c)]. The two systems break their complete synchronization for the values of the gain coefficients: both α and β having value 0.001.

(a)

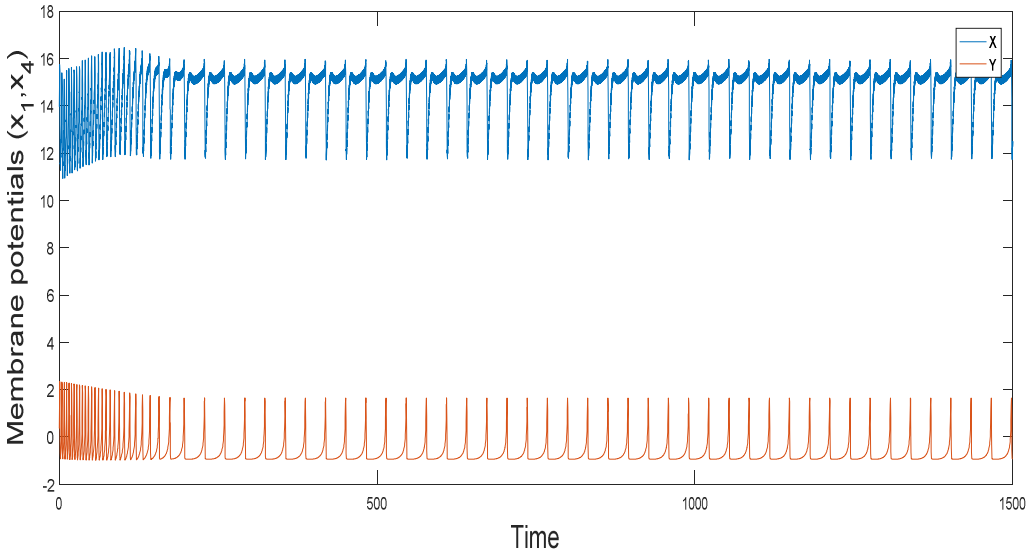

(b)

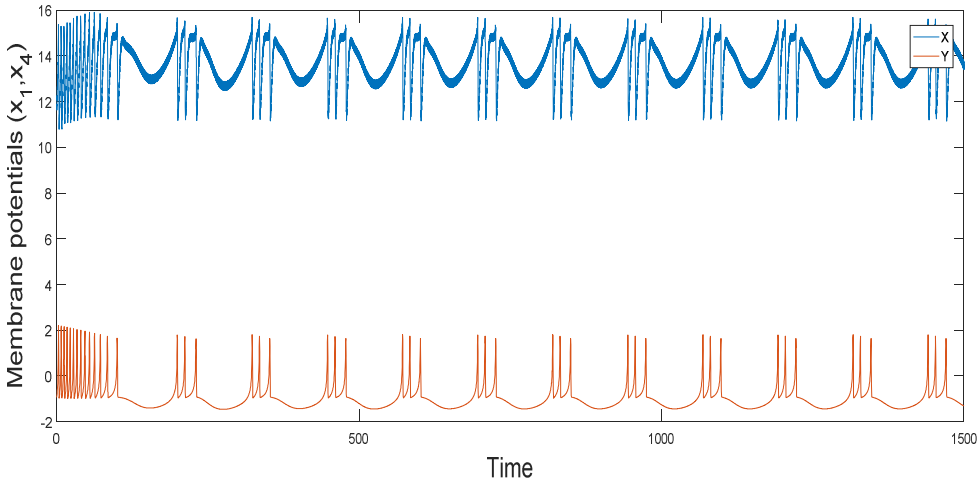
Membrane potentials (x_1,x_4)
Time
X
Y
16
14
12
10
8
6
4
2
0
-2
0
500
1000
1500

(c)

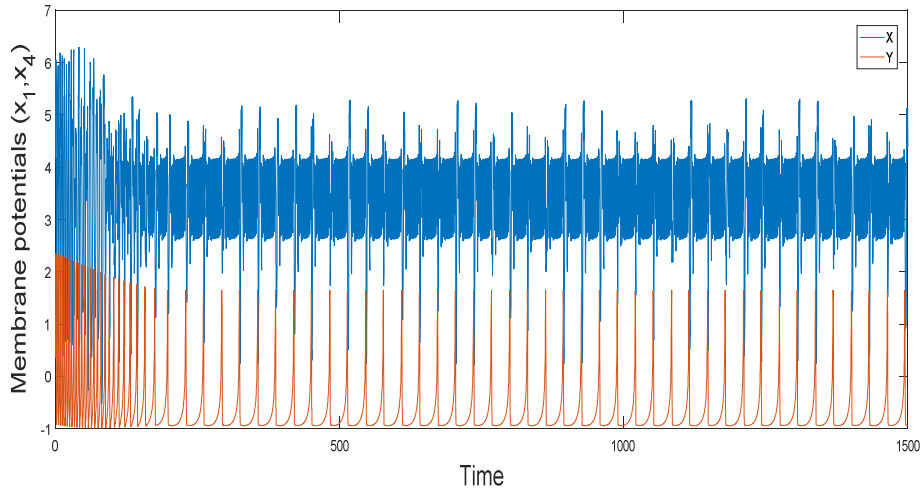
Membrane potentials (x_1,x_4)
Time
X
Y
7
6
5
4
3
2
1
0
-1
0
500
1000
1500

(d)

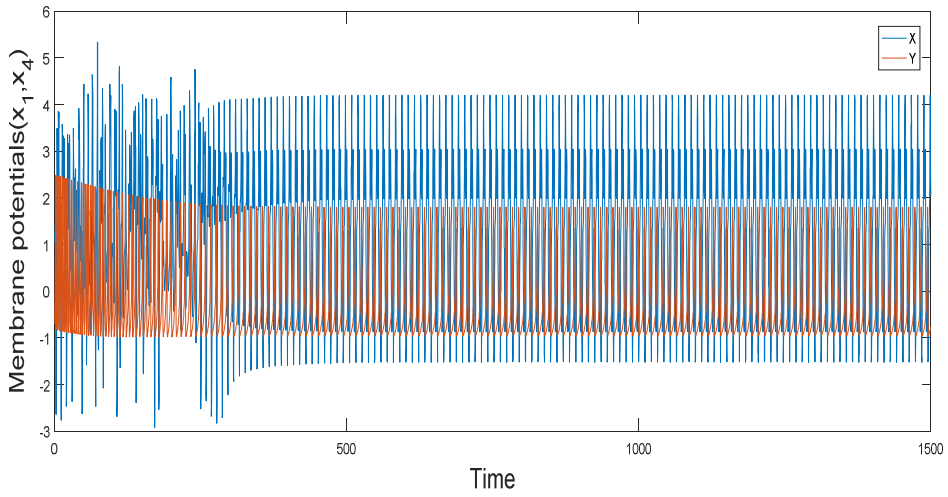

Figure 6.6: Time series behaviour shows spiking, bursting, tonic spiking and finally as α is reduced to value 0.001 the membrane potential of Josephson junction- neuron gets reduced to have values such that the H-R neuron membrane potential lies in the same range of variation.

It is possible to make the time series pattern of two systems identical using controller with appropriate gain coefficients

6.5 Conclusions

The Josephson Junction circuit model (JJ Model) is improved to consider effect of electromagnetic induction by introducing the magnetic flux variable in to the model. Memristor is used to realize feedback coupling between magnetic flux and junction potential(x_1). The sampled time series, phase portraits and Lyapunov plots for junction potentials of circuit in Josephson Junction with the flux of the memristor are investigated by nonlinear analysis. By setting appropriate parameter values, fast spiking of different periodicity is observed. Also with logarithmic memristor, periodic spiking and

suppression of oscillations are resulted in. It is found that dynamical behaviours and electrical modes are much dependent on magnetic flux. This behaviours are different from bifurcation studies of cubic flux controlled memristor, where periodical, multiperiodical and suppression of oscillation were reported in. Hence nonlinear properties can be enhanced by adding memristor term, as a result the present model can be used for potential applications in network.

The chaotic circuit of Josephson Junction is used to simulate behaviour of Hindmarsh–Rose neuronal discharges. The electric activity of H-R neuron is modified by Josephson Junction chaotic circuit which is studied based on the Lyapunov stability theory and using adaptive track control scheme. The controller is approached analytically and two controllable gain coefficients are included. Simulation shows spiking, bursting, tonic type behaviours and finally as gain coefficient (α) is reduced to value 0.001 the membrane potential of Josephson Junction neuron gets reduced to have values such that the H-R neuron membrane potential lies within its range of variation. Hence the junction potential can be modulated in response to external forcing parameters.

The memristor coupled with Josephson Junction circuit is effective to apply in the encryption and decryption of an image. It is observed that when an external ac signal is forced into the junction, the junction voltage has been found modulated in response to the external forcing signal. These behaviours confirm the possible applications of JJs in artificial neural networks [229,230].

Chapter 7
Conclusions

Chapter 7

Conclusions

The thesis mainly focuses on chaotic behaviour of neural systems. The two different biological neuron models, such as Hindmarsh-Rose and Josephson Junction models are selected and the effect of various coupling schemes on them are analysed.

In H-R neuron with memristor based coupling, various behaviours such as synchronization, anti- synchronization, oscillation death, amplitude death etc. are observed which suggests the various possible dynamics of brain cells. Also the observation of near death rare spikes is observed which is consistent with the experimental analysis of rat brain.

The study of influence of electromagnetic inductions on neurons is also done. It gives a pathway to understand electromagnetic flux influence on the overall activity of neurons. The activity of neurons is examined with quadratic and exponential flux based memristor.

Effect of Gaussian white noise on electromagnetic induction is also studied. It is shown that the memristor which produces magnetic flux can also influence neurons. This result is relevant in the context of neuromorphic quantum computation. Electromagnetic waves which can be produced due to artificial nano-synapses is capable of modification of neuron dynamics which is important in the context. Also energy is calculated in terms of Hamilton energy to understand the neuron response to external forcing current and action potential.

The effect of field coupling on the electromagnetic induction and the corresponding modes of electrical activities with cubic flux controlled

memristor are also examined. The influence of the magnetic flux on membrane potential is studied. The field coupling contributes towards magnetic flux and induction current, as a result, the modes in electrical activities are controlled. The excitability of neuron mainly depends on the external forcing current and larger external stimuli are found to be much helpful to excite neurons. The present studies give instructive clues to understand the exchange of ions when synapse coupling is absent and gives further insight into signal encoding.

Further, superconducting circuit with the Josephson Junction is chosen to replace H-R neurons for electromagnetic study of neurons. The model is improved to consider effect of electromagnetic induction by introducing the magnetic flux variable in to the model. Memristor is used to realize feedback coupling between magnetic flux and junction potential. It is observed that when an external ac signal is forced into the junction, the junction voltage has been found to be modulated in response to the external forcing signal.

Electrical activities of H-R neurons can be simulated with Josephson Junction model. Here membrane potential of Josephson Junction- neuron gets reduced to have values such that the H-R neuron membrane potential lies within the same range of variation.

These behaviours confirm the possible applications of JJs as high-frequency oscillator in artificial neural networks.

In an overall perspective, the analysis of the 3-d and 4-d Hindmarsh Rose system, enabled examination of various phenomena like synchronization, oscillation quenching mechanisms and near death rare spikes. The chaotic on set is examined in terms of time series evolutions, Lyapunov Exponents, stability analysis, bifurcation plots and adaptive track control methods etc. Study of influence of electromagnetic induction and noise on neuron,

examination of improvement of superconducting circuits with memristor, investigation of the possibility of controlling the chaotic behaviour in the neuron systems are some other important key points presented in the thesis. Illustration of the role of different types of nanoscale memristors to enhance the nonlinearity of the neuron model is relevant in the context of the memory effects.

BIBLIOGRAPHY

BIBLIOGRAPHY

[1] Robertson, R. and Combs, A.: Chaos theory in psychology and the life sciences. Psychology Press , (2014).

[2] Wolfram, S.: A new kind of science ,Champaign, IL: Wolfram media, 5(130), (2002)., Poincaré, H. and Szumilewicz , I.: *Henri Poincaré*. Wiedza Powszechna, (1978).

[3] Williams, G.:Chaos theory tamed.Taylor & Francis, CRC Press,(1997).

[4] Pikovsky, A., Kurths, J., Rosenblum, M. and Kurths, J.: Synchronization: a universal concept in nonlinear sciences , Cambridge university press,12(2003).

[5] Broer, H.W. and Sevryuk, M.B.: Kam Theory: quasi-periodicity in dynamical systems. Handbook of Dynamical Systems, *3*(C):249-344 (2010).

[6] Lorenz EN. :Deterministic nonperiodic flow. Journal of the atmospheric sciences.20(2):130-41(1963).

[7] Peitgen, H.O., Jürgens, H. and Saupe, D.: Strange Attractors: The Locus of Chaos. In Chaos and Fractals Springer, New York, NY., 655-768 (1992).

[8] Thompson, J.M.T. and Stewart, H.B.: Nonlinear dynamics and chaos. John Wiley & Sons,(2002).

[9] Feigenbaum, M.J.: Quantitative universality for a class of nonlinear transformations. Journal of statistical physics, 19(1):25-52(1978).

[10] Persson, P.B. and Wagner, C.D.: General principles of chaotic dynamics. *Cardiovascular Research*, *31*(3):332-341(1996).

[11] Schuster, H.G. and Just, W.: Deterministic chaos: an introduction. John Wiley & Sons.(2006).

[12] Weisstein.Eric W: "Chaos". From Mathworld-A Wolfram Web Resources.http://mathworld. .wolfram.com/Chaos.html. , Devaney, R., An introduction to chaotic dynamical systems. CRC Press.(2018).

[13] Nolte, D.D.: The tangled tale of phase space. Physics today, 63(4):33-38(2010).

[14] Weisstein. Eric W. "Phase portrait" from Mathworld-A Wolfram Web Resources.http://mathworld. .wolfram.com/Phase portrait.html.

[15] Afraimovich, V.S., Bykov, V.V. and Shilnikov, L.P., May: On the origin and structure of the Lorenz attractor, Akademiia Nauk SSSR Doklady 234: 336-339(1977).

[16] Peitgen, H.O., Jürgens, H. and Saupe, D. :Chaos and fractals: new frontiers of science. Springer Science & Business Media., http://boyangcyqin.wordpress.com.(2006).

[17] Guan, K.: Important Notes on Lyapunov Exponents. arXiv preprint arXiv:1401.3315(2014).

[18] Skokos, C.: The Lyapunov characteristic exponents and their computation, Dynamics of Small Solar System Bodies and Exoplanets , Springer, Berlin, Heidelberg.63-135(2010).

[19] Milnor, J.: On the concept of attractor. In the theory of chaotic attractors Springer, New York, 243-264(1985).

[20] Kapitaniak, T.: Chaotic oscillations in mechanical systems. Manchester University Press.(1991), J. D. Farmer. :Chaotic attractors of an innite-dimensional dynamical system. Physica D, 4:366-393(1982).

[21] Grassberger, P. and Procaccia, I.: Characterization of strange attractors. *Physical review letters, 50*(5): 346(1983).

[22] Boi, L.,: The quantum vacuum: A scientific and philosophical concept, from electrodynamics to string theory and the geometry of the microscopic world. JHU Press(2011).

[23] Al-Shameri, W.F.H., Dynamical properties of the Hénon mapping. *Int. Journal of Math. Analysis, 6*(49):2419-2430(2012).

[24] Tamari, B.:Conservation and symmetry laws and stabilization programs in economics. Ecometry(1997).

[25] Crawford, J.D.: Introduction to bifurcation theory. Reviews of Modern Physics, *63*(4), 991(1991).

[26] J. P. Eckmann. Roads to turbulence in dissipative dynamical systems. Rev. Mod. Phys., 53:643-654(1981.

[27] C. Jeffries and J. Perez.: Observation of a pomeau- manneville intermittent route to chaos in a nonlinear oscillator. Phys. Rev. A, 26:2117-2122(1982).

[28] Vidyasagar, M.:Nonlinear systems analysis,sia,Applied mathematics, 42(2002).

[29] Shevitz, D. and Paden, B.: Lyapunov stability theory of nonsmooth systems. IEEE Transactions on automatic control, 39(9):1910-1914(1994), Murray, R.M.,. A mathematical introduction to robotic manipulation, CRCpress.(2017). (http://web.tuat.ac.jp/~gvlab/ronbun/ ReadingGroupControl/mls-lyap.pdf)

[30] Shintani, M. and Umeno, K.: Conditional Lyapunov exponent criteria in terms of ergodic theory. Progress of Theoretical and Experimental Physics, 1:013A01(2018).

[31] Dabrowski, A.: The largest transversal Lyapunov exponent and master stability function from the perturbation vector and its derivative dot product (TLEVDP). Nonlinear Dynamics, 69(3), 1225-1235(2012).

[32] Galias, Z.: Local transversal Lyapunov exponents for analysis of synchronization of chaotic systems. International journal of circuit theory and applications, *27*(6):589-604(1999).

[33] Fradkov A.L :Control systems,Robotics and automation, Vol.XIII, Control of chaotic systems, Russia, EOLSS publications, Boccaletti, S., Grebogi, C., Lai, Y.C., Mancini, H. and Maza, D.,The control of chaos: theory and applications. Physics reports, 329(3),103-197(2000).

[34] Rega, G., Lenci, S. and Thompson, J.M.T.: Controlling chaos: the OGY method, its use in mechanics, and an alternative unified framework for control of non-regular dynamics. In Nonlinear dynamics and chaos: Advances and perspectives Springer, Berlin, Heidelberg.:211-269(2010).

[35] Pyragas, K.: Continuous control of chaos by self-controlling feedback. *Physics letters A, 170*(6):421-428(1992).

[36] Iroslav· Krsti, Kanellakopoulos, I. and Petar, V.: Nonlinear and adaptive control design. New York: Wiley,Landau, I.D., Lozano, R. and M'Saad, M., *Adaptive control* (Vol. 51). New York: Springer(1998).

[37] Anishchenko, V.S., Vadivasova, T.E., Postnov, D.E. and Safonova, M.A., Synchronization of chaos. International Journal of Bifurcation and Chaos, *2*(03):633-644(1992).

[38] N. F. Rulkov, M. M. Sushchik, L. S. Tsimring, and H. D. I. Abarbanel. Generalized synchronization of chaos in directionally coupled chaotic systems. Phys. Rev. E, 51:980-994, (1995).

[39] S. Boccaletti, S. Boccaletti, and A. Pelaez. Unifying framework for synchronization of coupled dynamical systems. Phys. Rev. E, 63:066219(2001).

[40] Skinner, J.E., Molnar, M., Vybiral, T. and Mitra, M., Application of chaos theory to biology and medicine. Integrative Physiological and Behavioral Science, *27*(1):39-53(1992).

[39] Molnar, C. and Gair :Neurons and Glial Cells. Concepts of Biology-1st Canadian*Edition*(2013).

[40] E. R. Kandel, J. H. Schwartz, and T. M. Jessel.Principles of Neural Science. McGraw-Hill, 4 edition(2000).

[41] Lovinger, D.M., Communication networks in the brain: neurons, receptors, neurotransmitters, and alcohol.,Alcohol Research & Health.(2008).

[42] M. I. Rabinovich , P. Varona, and A. I. Selverston. Abarbanel, H.D.I.: Dynamical principles in neuroscience. Reviews of Modern Physics, 78:1213-1265(2006).

[43] H. C. Tuckwell. :Introduction to theoretical neurobiology. Cambridge University Press, (1988).

[44] R. Connie,W. Robert. :How neurons communicate, Biology, Openstax – CNX,35:991(2013).

[45] Alain Destexhe, Zachary F. Mainen, and Terrence J. Sejnowski. Kinetic models of synaptic transmission. In Methods in Neuronal Modeling, pages 125, (1998).

[46] Izhikevich, E.M.:Neural excitability, spiking and bursting. International journal of bifurcation and chaos, *10*(06), 1171-1266.(2000)

[47] W. Gerstner and W. Kistler.: Spiking Neuron Models. Cambridge University Press, (2002).

[48] A.L. Hodgkin and A. F. Huxley.A quantitative description of membrane current and its application to conduction and excitation in nerve. Journal of Physiology, 117:500544(1952).

[49] Eugene M. Izhikevich. Dynamical Systems in Neuroscience: The Geometry of Excitability and Bursting. MIT Press(2006).

[50] Bose, A.: Bifurcations Dynamics of Single Neurons and Small Networks. Encyclopedia of Computational Neuroscience, :371-380(2015).

[51] Bear, M.F., Connors, B.W. and Paradiso, M.A. eds., Neuroscience Lippincott Williams & Wilkins.2(2007).

[52] Tremblay, R., Lee, S. and Rudy, B., GABAergic interneurons in the neocortex: from cellular properties to circuits. Neuron, 91(2), 260-292.(2016).

[53] Squire, L., Berg, D., Bloom, F.E., Spitzer, N.C. :Fundamental neuroscience. Edition 2. Academic Press.(2012).

[54] Holt, C.E., Martin, K.C. and Schuman, E.M.: Local translation in neurons: visualization and function. Nature structural & molecular biology, *26*(7)557-566(2019).

[55] Deco, G., Jirsa, V. and Friston, K.J.: The dynamical structural basis of brain activity. Principles of brain dynamics: Global state interactions*1*(2012).

[56] Rabinovich, M.I., Friston, K.J. and Varona, P.: Principles of brain dynamics: global state interactions. MIT Press.(2012).

[57] Shelley, B.P.: Footprints of phineas gage: Historical beginnings on the origins of brain and behavior and the birth of cerebral localizationism. *Archives of Medicine and Health Sciences*, *4*(2):280(2016).

[58] Simpson, D.: Phrenology and the neurosciences: contributions of FJ Gall and JG Spurzheim. ANZ journal of surgery, *75*(6), 475-482(2005).

[59] Destexhe, A.: Conductance-based integrate-and-fire models. Neural Computation, 9(3), 503-514(1997).

[60] Miranda-Dominguez, O., Mills, B.D., Grayson, D.: Bridging the gap between the human and macaque connectome: a quantitative comparison of global interspecies structure-function relationships and network topology. Journal of Neuroscience, *34*(16):5552-5563(2014).

[61] Kötter, R.: Online retrieval, processing, and visualization of primate connectivity data from the CoCoMac database. Neuroinformatics, 2(2):127-144(2004).

[62] Jung, R.E., Caprihan, A.:Diffusion tensor imaging in neuropsychiatric systemic lupus erythematosus. BMC neurology, 10(1):65(2010).,Salama, G.R., Heier, L.A., Diffusion weighted/tensor imaging, functional MRi and Perfusion weighted imaging in glioblastoma—foundations and future. *Frontiers in neurology*, *8*, :660(2018).

[63] Buschman, T.J. and Kastner, S.: From behavior to neural dynamics: an integrated theory of attention. Neuron, 88(1):127-144(2015).

[64] McCulloch, W.S. and Pitts, W.: A logical calculus of the ideas immanent in nervous activity. The bulletin of mathematical biophysics, 5(4):115-133(1943)., Marsalli, M., 2006. Mcculloch-pitts

neurons. In The 2008 Annual Meeting of the consortium on cognitive science instruction (ccsi) : 172-179(2008).

[65] Rinzel, J., December.:Excitation dynamics: insights from simplified membrane models. In Fed. Proc,44(15): 2944-2946(1985).

[66] Nagumo, J. and Sato, S.:On a response characteristic of a mathematical neuron model. Kybernetik, 10(3):155-164(1972).

[67] Morris, C., Lecar, H.: Voltage oscillations in the barnacle giant muscle fiber. Biophys. J. 35, 193–213 (1981).

[68] Hindmarsh, J.L., Rose, R.M.: A model of the nerve impulse using twofirst-order differential equations. Nature (Lond.) 296:162C164 (1982).

[69] E. M. Izhikevich.: Simple Model of Spiking Neurons. IEEE Transactions on Neural Networks, 14:15691572, 2003.,E. M. Izhikevich. Which Model to Use for Cortical Spiking Neurons? IEEE Transactions on Neural Networks, 15:10631070(2004).

[70] Dahasert, N., Öztürk, İ. and Kiliç.: Experimental realizations of the HR neuron model with programmable hardware and synchronization applications. Nonlinear Dynamics, 70(4):2343-2358(2012).

[71] Foster, W.R., Ungar, L.H. and Schwaber, J.S.:Significance of conductances in Hodgkin-Huxley models. Journal of neurophysiology, 70(6):2502-2518(1993).

[72] Wang, Q., Lu, Q., Chen, G. and Duan, L.:Bifurcation and synchronization of synaptically coupled FHN models with time delay. Chaos, Solitons & Fractals, 39(2):918-925(2009).

[73] Storace, M., Linaro, D. and de Lange, E.: The Hindmarsh–Rose neuron model: bifurcation analysis and piecewise-linear approximations. Chaos: An Interdisciplinary Journal of Nonlinear Science, 18(3):033128(2008).

[74] Xia, S. and Qi-Shao, L.:Firing patterns and complete synchronization of coupled Hindmarsh–Rose neurons. Chinese Physics, 14(1):77(2005).

[75] Crotty, P., Segall, K. and Schult, D.A.: Modeling biological neurons with Josephson junctions. BMC Neuroscience, *10*(S1):44(2009).

[76] Faisal, A.A., Selen, L.P. and Wolpert, D.M.:Noise in the nervous system. Nature reviews neuroscience 9(4):292(2008).

[77] Milton, J.G.:The delayed and noisy nervous system: implications for neural control. Journal of neural engineering, 8(6):065005(2011).

[78] Xia, S. and Qi-Shao, L.: Coherence resonance and synchronization of Hindmarsh–Rose neurons with noise. Chinese physics, *14*(6): 1088(2005).

[79] Wang, Y., Ma, J., Xu, Y., Wu, F. and Zhou, P.:The electrical activity of neurons subject to electromagnetic induction and Gaussian white noise. International Journal of Bifurcation and Chaos, 27(02): 1750030(2017).

[80] Xu, Y., Li, Y., Zhang, H., Li, X. and Kurths, J.:The switch in a genetic toggle system with Lévy noise. Scientific reports, 6:31505(2016). ,Y. Xu , J. J. Li, and J. Feng. :Lévy noise-induced stochastic resonance in a bistable system. Eur. Phys. J. B, 86:1-7(2013).

[81] Mary Vinaya and R P. Ignatius: Effect of Lévy noise on the networks of Izhikevich neurons. Nonlinear Dynamics94(2),1133-1150(2018).

[82] KK Mineeja,R.P.Ignatius,Spatiotemporal activities of a pulse coupled biological neural network.Nonlinear Dynamics 92(4),1881-1897(2018).

[83] Michael. A.Arbib: Handbook of Brain Theory and Neural Network. MIT Press, Cambridge (2002).

[84] Zou, W., Senthilkumar, D. V, Nagao, R., Kiss, I.Z., Tang, Y., Koseska, A., Duan, J., Kurths, J.: Restoration of rhythmicity in diffusively coupled dynamical networks. Nat. Commun. 6, 7709 (2015).

[85] Hongjie Yu, J.P.: Chaotic synchronization and control in nonlinear-coupled Hindmarsh–Rose neural systems. Chaos, Solitons & Fractals. 29, 342–348 (2006).

[86] Volos, C.K., Kyprianidis, I.M., Stouboulos, I.N., Tlelo-Cuautle, E., Vaidyanathan, S.: Memristor: A new concept in synchronization of coupled neuromorphic circuits. J. Eng. Sci. Technol. Rev. 8, 157–173 (2015).

[87] Resmi, V., Ambika, G., Amritkar, R.E.: General mechanism for amplitude death incoupled systems. Phys. Rev. E - Stat. Nonlinear, Soft Matter Phys. 84, (2011).

[88] K.S.Thornburg, Jr.M.moller, R.Roy, T.W.Carr, R.D.Li, T.E.: Chaos and coherence in coupled lasers. Phys. Rev. E. 55, 3865–38 (1997).

[89] Istvan.Z.Kiss, Vilmos Gaspar, J.L.H.: Experiments on synchronization and control of chaos on coupled electrochemical oscillators. J. Phys. Chem. B. 104(31), 7554–7560 (2000).

[90] M.A.Harrison, Y.C.Lai, R.D.H.: Dynamical mechanism for coexistence of dispersing species without trade-offs in spatially extended ecological systems. Phys. Rev. E. 63:051905, 519051–519055. (2001).

[91] Glass L: Synchronization and rhythmic processes in physiology. Nature. 410(6825), 277–84 (2001).

[92] Prasad, A.: Amplitude death in coupled chaotic oscillators. Physics (College. Park. Md). 1–10 (2005).

[93] Koseska, A., Volkov, E., Kurths, J.: Oscillation quenching mechanisms: Amplitude vs. oscillation death. Phys. Rep. 531, 173–199 (2013).

[94] Ahn, S., Rubchinsky, L.L.: Short desynchronization episodes prevail in synchronous dynamics of human brain rhythms. Chaos. 23, 1–7 (2013).

[95] Essaki Arumugam, E.M., Spano, M.L.: A chimeric path to neuronal synchronization. Chaos. 25, (2015).

[96] Sharma, A., Sharma, P.R., Shrimali, M.D.: Amplitude death in nonlinear oscillators with indirect coupling. Phys. Lett. Sect. A Gen. At. Solid State Phys. 376, 1562–1566 (2012).

[97] P. C. Matthews, R. E. Mirollo, and S.H.S.: Complex Time-Delay Systems: Theory and Applications. Phys. D. 52, (1991).

[98] Prasad, A.: Time-varying interaction leads to amplitude death in coupled nonlinear oscillators. Pramana - J. Phys. 81, 407–415 (2013).

[99] Suresh, K., Sabarathinam, S., Thamilmaran, K., Kurths, J., Dana, S.K.: A common lag scenario in quenching of oscillation in coupled oscillators. Chaos An Interdiscip. J. Nonlinear Sci. 083104, (2016).

[100] Hens, C.R., Olusola, O.I., Pal, P., Dana, S.K.: Oscillation death in diffusively coupled oscillators by local repulsive link. Phys. Rev. E - Stat. Nonlinear, Soft Matter Phys. 88, (2013).

[101] Wang, C., He, Y., Ma, J., Huang, L.: Parameters estimation, mixed synchronization, and antisynchronization in chaotic systems. Complexity. 20, 64–73 (2014).

[102] Ma, J., Song, X., Jin, W., Wang, C.: Autapse-induced synchronization in a coupled neuronal network. Chaos, Solitons & Fractals. 80, 31–38 (2015).

[103] XinLin Song, ChunNi Wang, Jun Ma, J.T.: Transition of electric activity of neurons induced by chemical and electric autapses. Sci. China Technol. Sci. 58, 1007–1014 (2015).

[104] Ma, J., Tang, J.: A review for dynamics of collective behaviors of network of neurons. Sci. China Technol. Sci. 58, 2038–2045 (2015).

[105] Ma, J., Qin, H., Song, X., Chu, R.: Pattern selection in neuronal network driven by electric autapses with diversity in time delays. Int. J. Mod. Phys. B. 29, 1450239 (2015).

[106] Song, Y., Wen, S.: Synchronization control of stochastic memristor-based neural networks with mixed delays. Neurocomputing. 156, 121–128 (2015).

[107] Berdan, R., Vasilaki, E., Khiat, A., Indiveri, G., Serb, A., Prodromakis, T.: Emulating short-term synaptic dynamics with memristive devices. Sci. Rep. 6, 18639 (2016).

[108] Merrikh-Bayat, F., Bagheri-Shouraki, S.: Efficient neuro-fuzzy system and its Memristor Crossbar-based Hardware Implementation. 34 (2011).

[109] D.C.Saha: On the Synchronization of Synaptically Coupled Nonlinear Oscillators: Theory and Experimen. Annu. Rev. Chaos Theory, Bifurcations Dyn. Syst. 6, 1–29. (2016).

[110] Alias, L.A., Pai, M.S., George, M.M. V: Near Death Experiences (NDE) of Cardiac Arrest Survivors- A Phenomenological Study Materials and methods : 3, 216–220 (2015).

[111] Zeren, T., Özbek, M., Kutlu, N., Akilli, M.: Significance of using a nonlinear analysis technique, the Lyapunov exponent, on the understanding of the dynamics of the cardiorespiratory system in rats. Turkish J. Med. Sci. 46, 159–165 (2016).

[112] Terman, D., Kopell, N., Bose, a.: Dynamics of two mutually coupled slow inhibitory neurons. Phys. D Nonlinear Phenom. 117, 241–275 (1998).

[113] Fang, X.: Chaotic synchronization of HindMarsh- Rose neurons coupled by cubicnonlinear feedback. In: Advances in cognitive neurodynamics. 315–320 (2007).

[114] Chua: Memristive devices and systems. In: procceedings of IEEE. pp. 209–223 (1976).

[115] Mazumder, P.: Memristors:Devices,Models and application. In: proceedings of IEEE,100:6 (2012).

[116] Well, R. stock: English words;History and structure. Cambridge Univ. Press. (2001).

[117] Corinto, F.: Memristor synaptic dynamics' influence on synchronous behaviour of two Hindmarsh-Rose neurons. IEEE,Neural Networks (IJCNN), 2011 Int. Jt. Conf. 2403 – 2408 (2011).

[118] R. C Johnson: Missing link' memristor created. EE Times. 04, (2008).

[11 9] Abdurahman, A., Jiang, H., Teng, Z.: Finite-time synchronization for memristor-based neural networks with time-varying delays. Neural Networks. 69, 20–28 (2015).

[120] Hengtong Wang, Y.C.: Firing dynamics of an autaptic neuron. Chinese Phys. B, 24(12) 128709, Neurons Cogn. (q-bio.NC); Biol. Phys. 24, 1–10 (2015).

[121] Guo, Q.: Properties of Quadratic Flux-Controlled and Charge-Controlled Memristor. Adv. Eng. Res. 2352–5401 (2015).

[122] Lee U, B.J.: Surge of neurophysiological coherence and connectivity in the dying brain. In: PNAS. p. 110(35) 144432–7 (2013).

[123] Klotz, I.: Brain waves surge moments before death. Chinese Phys. B. 24(11): 118401 (2009).

[124] Yong, E.: In Dying brains, signs of heightened consciousness. PNAS. (2013).

[125] Wei, L.: Exponential flux-controlled Memristor model and its floating emulator. Chin.Phyb. vol.24 (2015).

[126] Friston, K.J.: Book Review: Brain Function, Nonlinear Coupling, and Neuronal Transients. Neurosci. 7, 406–418 (2001).

[127] Spitzer, N.C.: Electrical activity in early neuronal development,Nature 444(7120):707–712 (2006).

[128]Li, J., Liu, S., Liu, W.et al.: Suppression of firing activities in neuron and neurons of network induced by electromagnetic radiation. Nonlinear Dynamics, 83(1-2):801-810(2016).

[129] Wu, F., Wang, C., Xu, Y.et al.: Model of electrical activity in cardiac tissue under electromagnetic induction ,Scientific reports 6(1):28 (2016).

[130] Lv, M., Ma, J.: Multiple modes of electrical activities in a new neuron model under electromagnetic radiation, Neurocomputing 205:375–381 (2016).

[131] Corinto, F., Ascoli, A., Lanza, V. et al.: Memristor synaptic dynamics' influence on synchronous behavior of two Hindmarsh-Rose neurons. IEEE, Neural Networks (IJCNN), Int. Jt. Conf.: 2403–2408 (2011).

[132] Thottil, S.K., Ignatius, R.P.: Nonlinear feedback coupling in Hindmarsh–Rose neurons, Nonlinear Dyn. 87(3):1879–1899 (2017).

[133] Gale, E.: The Memory-Conservation Theory of Memristance, In Computer Modelling and Simulation (UKSim),IEEE,Proc. 16th UKSim-AMSS Int. Conf. Model. Simul. :599--604 (2014).

[134] Petridou, N., Plenz, D., Silva, A.C. et al.: Direct magnetic resonance detection of neuronal electrical activity, Proc. Natl. Acad. Sci. U. S. A. 103(43): 16015–16020 (2006).

[135] Ignatov, M., Ziegler, M., Hansen, M. et al.: Memristive stochastic plasticity enables mimicking of neural synchrony : Memristive circuit emulates an optical illusion,Science advances 3(10): e1700849(2017), Wang C, Lv, M., Alsaedi, A. et al.: Synchronization stability and pattern selection in a memristive neuronal network,Chaos*:* An Interdisciplinary Journal of Nonlinear Science *27(11)*:113108(2017).

[136] Ren, G., Xu, Y., Wang, C.: Synchronization behavior of coupled neuron circuits composed of memristors, Nonlinear Dyn. 88(2): 893–901 (2017)

[137] Ma, J., Wang, Y., Wang, C. et al.: Mode selection in electrical activities of myocardial cell exposed to electromagnetic radiation, Chaos, Solitons and Fractals. 99: 219–225 (2017).

[138] Lindner, B., García-Ojalvo, J., Neiman, A. et al.: Effects of noise in excitable systems.Physics reports,392(6): 321–424 (2004).

[139] Georgiev, D.D.: Electric and magnetic fields inside neurons and their impact upon the cytoskeletal microtubules. Web source http//cogprints. org/3190: 15–19 (2003).

[140] Wang, S., Wang, W. , Liu, F.: Propagation of firing rate in a feed-forward neuronal network. Physical review letters, *96*(1):018103(2006).

[141] Laughlin, S.B.: Energy as a constraint on the coding and processing of sensory information, Curr. Opin. Neurobiol. 11(4):475–480 (2001).

[142] Hrdina,P.D.: Basic Neurochemistry: Molecular, Cellular and Medical Aspects.Journal of Psychiatry and Neuroscience, *21*(5):352 (1996).

[143] Torrealdea, F.J., D'Anjou, A., Graña, M. et al.: Energy aspects of the synchronization of model neurons, Physical Review E - Stat. Nonlinear, Soft Matter Phys. 74(1):011905(2006).

[144] Drapaca, C.S.: An electromechanical model of neuronal dynamics using Hamilton's principle. Front. Cell. Neurosci., 9:271 (2015).

[145] Friston, K.J., Stephan, K.E.: Free-energy and the brain. Synthese, 159(3): 417–458 (2007).

[146] Nabi, A., Mirzadeh, M., Gibou, F. et al. : Minimum energy desynchronizing control for coupled neurons. J. Comput. Neurosci., 34(2):259–271 (2013).

[147] Wang, Y., Wang, C., Ren, G. et al. : Energy dependence on modes of electric activities of neuron driven by multi-channel signals. Nonlinear Dynamics.,89(3):1967–1987 (2017).

[148] Wang, R., Zhang, Z., Chen, G.: Energy coding and energy functions for local activities of the brain. Neurocomputing ,**73**(1–3):139–150 (2009) .

[149] Gu, H., Chen, S.: Potassium-induced bifurcations and chaos of firing patterns observed from biological experiment on a neural pacemaker. Sci. China Technol. Sci., 57(5):864–871 (2014).

[150] Gu, H., Pan, B., Chen, G. et al.: Biological experimental demonstration of bifurcations from bursting to spiking predicted by theoretical models. Nonlinear Dynamics, 78(1): 391–407 (2014).

[151] Lu, L., Jia, Y., Liu, W. et al.: Mixed Stimulus-induced Mode Selection in Neural Activity Driven by High and Low Frequency Current Under Electromagnetic Radiation.Complexity, 2017: 7628537(2017).

[152] Dhamala, M., Jirsa, V.K., Ding, M.: Transitions to synchrony in coupled bursting neurons. Physical Review Letters, *92*(2):028101(2004).

[153] Xie, Y., Kang, Y., Liu, Y., Wu, Y.: Firing properties and synchronization rate in fractional-order Hindmarsh-Rose model neurons. Science China Technological Sciences, *57*(5):914-922(2014).

[154] Xu, Y., Ying, H., Jia, Y. et al.: Autaptic regulation of electrical activities in neuron under electromagnetic induction, Sci. Rep. 7:43452 (2017).

[155] Xu, Y., Jia, Y., Ma, J., Hayat, T., Alsaedi, A.:.Collective responses in electrical activities of neurons under field coupling. Scientific reports, *8*(1):1349(2018).

[156] Ge, M., Jia, Y., Xu, Y. et al.: Mode transition in electrical activities of neuron driven by high and low frequency stimulus in the presence of electromagnetic induction and radiation, Nonlinear Dyn. 91(1):515–523 (2018).

[157] Dewar, R. L., Hudson, S. R.: Magnetic coordinates for systems with imperfect magnetic surfaces. Proc. 1996 Int. Conf. Plasma Physics: 1262 (1997).

[158] G. Schmid, I. Goychuk, P. Hanggï,: Effect of channel block on the spiking activity of excitable membranes in a stochastic Hodgkin–Huxley model, Phys. Biol. 61–66((2004).

[159] Tarazaga, C.C., Campderrós, M.E., Pérez Padilla, A.: Characterization of exponential permeate flux by technical parameters during fouling and membrane cleaning by electric field, J. Memb. Sci. 283(1-2): 339–345

(2006).

[160] Ge, M., Jia, Y., Xu, Y. et al.: Mode transition in electrical activities of neuron driven by high and low frequency stimulus in the presence of electromagnetic induction and radiation, Nonlinear Dyn. 91(1):515–523 (2018).

[161] Innocenti, G., Morelli, A., Genesio, R. et al.: Dynamical phases of the Hindmarsh-Rose neuronal model: Studies of the transition from bursting to spiking chaos.Chaos: An Interdisciplinary Journal of Nonlinear Science, 17(4):043128 (2007).

[162] Xu, Y., Ying, H., Jia, Y. et al.: Autaptic regulation of electrical activities in neuron under electromagnetic induction, Sci. Rep. 7:43452 (2017).

[163] Guo, Q., Gu, W. , Tao, Z.: Properties of Quadratic Flux-Controlled and Charge-Controlled Memristor. Adv. Eng. Res. :2352–5401 (2015).

[164] Gale, E.: The Memory-Conservation Theory of Memristance, In Computer Modelling and Simulation (UKSim),IEEE,Proc. 16th UKSim-AMSS Int. Conf. Model. Simul. :599--604 (2014).

[165] Xia, S., Qi-Shao, L.: Firing patterns and complete synchronization of coupled Hindmarsh–Rose neurons. Chinese Physics,14(1): 77–85 (2005).

[166] Li, J., Liu, S., Liu, W. et al. : Suppression of firing activities in neuron and neurons of network induced by electromagnetic radiation. Nonlinear Dynamics, 83(1-2):801–810 (2016).

[167] Zhan, F., Liu, S.: Response of Electrical Activity in an Improved Neuron Model under Electromagnetic Radiation and Noise. Frontiers in Computational Neuroscience ,11:107 (2017).

[168] Zhan, F., Liu, S.: Response of Electrical Activity in an Improved

Neuron Model under Electromagnetic Radiation and Noise. Frontiers in Computational Neuroscience, 11:107 (2017).

[169] Ma, J., Wu, F., Jin, W. et al.: Calculation of Hamilton energy and control of dynamical systems with different types of attractors. Chaos:An Interdisciplinary journal of Nonlinear Science,27(5):053108 (2017).

[170] Xin-Lin, S., Wu-Yin, J., Jun, M.: Energy dependence on the electric activities of a neuron. Chinese Physics B, 24(12):128710 (2015).

[171] Torrealdea, F.J., Sarasola, C., d'Anjou, A. et al.: Energy efficiency of information transmission by electrically coupled neurons. BioSystems,97(1): 60–71 (2009).

[171] Zhang, G., Wu, F., Wang, C. et al.: Synchronization behaviors of coupled systems composed of hidden attractors. International Journal of Modern Physics B,31(26):1750180 (2017).

[172] Pecora, L.M. and Carroll, T.L.,: Master stability functions for synchronized coupled systems. Physical review letters, *80*(10), 2109(1998).

[173] Wei, L., Fa-Qiang ,W., Xi-Kui, M.: Exponential flux-controlled Memristor model and its floating emulator. Chinese Physics B,24(11):118401(2015).

[174] Aur, D., Jog, M.S., Neuroelectrodynamics: understanding the brain language . IOS Press, Vol. 74: (2010).

[175] Hodgkin, A.L., Huxley, A.F.: A quantitative description of membrane current and its application to conduction and excitation in nerve. J. Physiol. (Lond.) 117, 500–544 (1952).

[176] Morris, C., Lecar, H.: Voltage oscillations in the barnacle giant muscle fiber. Biophys. J. 35, 193–213 (1981)

[177] Hindmarsh, J.L., Rose, R.M.: A model of the nerve impulse using twofirst-order differential equations. Nature (Lond.) 296, 162C164 (1982)

[175] Ma, J. and Tang, J..A review for dynamics of collective behaviors of network of neurons. *Science China Technological Sciences*, *58*(12), pp.2038-2045 (2015)

[176] Brunel, N., Wang, X.J.: What Determines the frequency of fast network oscillations with irregular neural discharges? I. Synaptic dynamics and excitation–inhibition balance. J. Neurophys. 90(1), 415–430 (2002).

[177] Chih, B., Engelman, H., Scheiffele, P.: Control of excitatory and inhibitory synapse formation by neuroligins. Science 307(5713), 1324–1328 (2005).

[178] Chen, L.F., Cao, H.J.: Synchronization dynamics of two heterogeneous chaotic Rulkov neurons with electrical synapses. Int. J. Bifurc. Chaos 27(2), 1730009 (2017).

[179] Jalil, S., Belykh, I., Shilnikov, A.: Spikes matter for phase locked bursting in inhibitory neurons. Phys. Rev. E 85, 036214 (2012).

[180] Song, X.L., Wang, C.N., Ma, J., et al.: Transition of electric activity of neurons induced by chemical and electric autapses. Sci. China Technol. Sci. 58, 1007–1014 (2015).

[181] Guo, D.Q., Chen,M.M., Perc,M., et al.: Firing regulation of fast-spiking interneurons by autaptic inhibition. EPL 114, 30001 (2016).

[182] Hossmann, K.A., Hermann, D.M.: Effects of electromagnetic radiation of mobile phones on the central nervous system. Bioelectromagnetics 24, 49–62 (2003).

[183] Lisi, A., Ciotti, M.T., Ledda, M., et al.: Exposure to 50 Hz electromagnetic radiation promote early maturation and differentiation in newborn rat cerebellar granule neurons. J. Cell. Phys. 204(2), 532–538 (2005).

184] Masuda, H., Ushiyama, A., Takahashi, M., et al.: Effects of 915 MHz electromagnetic-field radiation in TEM cell on the blood–brain barrier and neurons in the rat brain. Radiat.Res. 172(1), 66–73 (2009).

[185] Lv, M., Ma, J.: Multiple modes of electrical activities in a new neuron model under electromagnetic radiation. Neurocomputing 205, 375–381 (2016) .

[186] Wu, F.Q., Wang, C.N., Xu, Y., et al.: Model of electrical activity in cardiac tissue under electromagnetic induction. Sci. Rep. 6, 28 (2016).

[187] Wu, F.Q., Wang, C.N., Jin, W.Y., et al.: Dynamical responses in a new neuron model subjected to electromagnetic induction and phase noise. Phys.A 469, 81–88 (2017).

[188] Wu, F., Wang, C., Jin, W. and Ma, J.: Dynamical responses in a new neuron model subjected to electromagnetic induction and phase noise. *Physica A: Statistical Mechanics and its Applications*, *469*:81-88(2017).

[189] Xu, Y., Jia, Y., Ma, J., Hayat, T. and Alsaedi, A.: Collective responses in electrical activities of neurons under field coupling. *Scientific reports*, *8*(1), 1349(2018).

[190]. Pecora, L.M. and Carroll, T.L.: Master stability functions for synchronized coupled systems. *Physical review letters*, *80*(10): 2109(1998).

[191] Stefański, A., Wojewoda, J., Kapitaniak, T. and Yanchuk, S.: Simple estimation of synchronization threshold in ensembles of diffusively coupled chaotic systems. *Physical review e*, *70*(2): 026217(2004).

[192] Usha, K., Subha, P.A. and Nayak, C.R.: The route to synchrony via drum head mode and mixed oscillatory state in star coupled Hindmarsh–Rose neural network. *Chaos, Solitons & Fractals*, *108*, 25-31(2018).

[193] Hodgkin, A.L., Huxley, A.F.: A quantitative description of membrane current and its application to conduction and excitation in nerve. The Journal of physiology, 117(4):500-544(1952).

[194] Ma, J. and Tang, J..:A review for dynamics of collective behaviours of network of neurons. *Science China Technological Sciences*, *58*(12):2038-2045 (2015)

[195] Reato, D., Rahman, A., Bikson, M. et al.: Low-intensity electrical stimulation affects network dynamics by modulating population rate and spike timing. Journal of Neuroscience, 30(45):15067-15079 (2010).

[196] Brunel, N., Wang, X.J.: What Determines the frequency of fast network oscillations with irregular neural discharges? I. Synaptic dynamics and excitation–inhibition balance. J. Neurophys. 90(1), 415–430 (2002).

[197] Chih, B., Engelman, H., Scheiffele, P.: Control of excitatory and inhibitory synapse formation by neuroligins. Science 307(5713), 1324–1328 (2005).

[198] Chen, L.F., Cao, H.J.: Synchronization dynamics of two heterogeneous chaotic Rulkov neurons with electrical synapses. Int. J. Bifurc. Chaos 27(2), 1730009 (2017).

[199] Jalil, S., Belykh, I., Shilnikov, A.: Spikes matter for phase locked bursting in inhibitory neurons. Phys. Rev. E 85, 036214 (2012).

[200] Song, X.L., Wang, C.N., Ma, J., et al.: Transition of electric activity of neurons induced by chemical and electric autapses. Sci. China Technol. Sci. 58, 1007–1014 (2015).

[201] Guo, D.Q., Chen,M.M., Perc,M., et al.: Firing regulation of fast-spiking interneurons by autaptic inhibition. EPL 114, 30001 (2016).

[202] Hossmann, K.A., Hermann, D.M.: Effects of electromagnetic radiation of mobile phones on the central nervous system. Bioelectromagnetics 24, 49–62 (2003).

[203] Lisi, A., Ciotti, M.T., Ledda, M., et al.: Exposure to 50 Hz electromagnetic radiation promote early maturation and differentiation in newborn rat cerebellar granule neurons. J. Cell. Phys. 204(2), 532–538 (2005).

[204] Masuda, H., Ushiyama, A., Takahashi, M., et al.: Effects of 915 MHz electromagnetic-field radiation in TEM cell on the blood–brain barrier and neurons in the rat brain. Radiat. Res. 172(1), 66–73 (2009).

[205] Lv, M., Ma, J.: Multiple modes of electrical activities in a new neuron model under electromagnetic radiation. Neurocomputing 205, 375–381 (2016).

[206] Wu, F.Q., Wang, C.N., Xu, Y., et al.: Model of electrical activity in cardiac tissue under electromagnetic induction. Sci. Rep. 6, 28 (2016).

[207] Wu, F.Q., Wang, C.N., Jin, W.Y., et al.: Dynamical responses in a new neuron model subjected to electromagnetic induction and phase noise. Phys. A 469, 81–88 (2017).

[208] Thottil, S.K., Ignatius, R.P.: Influence of memristor and noise on H-R neurons, Nonlinear Dyn. 95(1):239–257 (2019),Ma, J., Mi, L., Zhou, P.et al.: Phase synchronization between two neurons induced by coupling of electromagnetic field,Appl. Math. Comput. 307:321–328 (2017).

[209] Wu, F., Wang, C., Jin, W. and Ma, J.,Dynamical responses in a new neuron model subjected to electromagnetic induction and phase noise. *Physica A: Statistical Mechanics and its Applications*, *469*, 81-88(2017).

[210] Xu, Y., Jia, Y., Ma, J., Hayat, T. and Alsaedi, A.: Collective responses in electrical activities of neurons under field coupling. *Scientific reports*, *8*(1), 1349(2018).

[211] Pecora, L.M. and Carroll, T.L.: Master stability functions for synchronized coupled systems. *Physical review letters*, *80*(10), 2109(1998).

[212] Stefański, A., Wojewoda, J., Kapitaniak, T. and Yanchuk, S.:Simple estimation of synchronization threshold in ensembles of diffusively coupled chaotic systems. *Physical review e*, *70*(2), 026217(2004).

[213] Noebels JL, prince DA. : Development of focal seizures in cerebral cortex:role of axon terminal bursting.J Neurophysiol. 41(5):1267-1281(1978), Usha, K., Subha, P.A. and Nayak, C.R., 2018. The route to synchrony via drum head mode and mixed oscillatory state in star coupled Hindmarsh–Rose neural network. *Chaos, Solitons & Fractals*, *108*, 25(2018).

[214] Crotty, P., Schult, D. and Segall, K.: Josephson junction simulation of neurons. *Physical Review E*, *82*(1), 011914(2010).

[215] Li, F., Liu, Q., Guo, H., Zhao, Y., Tang, J. and Ma, J.:Simulating the electric activity of FitzHugh–Nagumo neuron by using Josephson junction model. *Nonlinear Dynamics*, *69*(4):2169-2179(2012).

[216] Michael L. Schneider, Christine A. Donnelly, and Stephen E. Russek: Tutorial: High-speed low-power neuromorphic systems based on magnetic Josephson junctions, J. Appl. Phys. 124, 161102 (2018); https://doi.org/10.1063/1.5042425 (2018).

[217] Crotty, P., Segall, K. AbdSchult D.A, Modeling biological neurons with Josephson junctions, BMC NeuroSci. 10; 44 2, (2018).

[218] Jun, M., Long, H., Zhen-Bo, X. and Wang, C.: Simulated test of electric activity of neurons by using Josephson junction based on synchronization scheme. *Communications in Nonlinear Science and Numerical Simulation*, *17*(6):2659-2669(2012).

[219] M Lv, C Wang, G Ren, et al., M.Xie, X., Zou, L., Wen, S., Zeng, Z. and Huang, T.:A Flux-Controlled Logarithmic Memristor Model and Emulator. *Circuits, Systems, and Signal Processing*, *38*(4):1452-1465(2019).

[220] Xie, X., Zou, L., Wen, S., Zeng, Z. and Huang, T.:A Flux-Controlled Logarithmic Memristor Model and Emulator. *Circuits, Systems, and Signal Processing*, *38*(4):1452-1465(2019).

[221] J Ma.:Model of electrical activity in a neuron under magnetic flow effect, Nonlinear Dyn. 85 :1479–1490(2016).

[222] Zhang, G., Ma, J., Alsaedi, A., Ahmad, B. and Alzahrani, F.:Dynamical behaviour and application in Josephson Junction coupled by memristor. *Applied Mathematics and Computation*, *321*:290-299(2018).

[223] M Lv, J Ma.:Multiple modes of electrical activities in a new neuron model under electromagnetic radiation, Neurocomput. 205, 375–381(2016)

[224] M.L.Schneider, Christine A:Tutorial: High spped low power neuromorphic systems based on magnetic Josephson Junctions.Journal of applied Physics.124,161102(2018).

[225] Ambika, G. Chaos in Josephson junctions Pramana - Journal of Physics 48: 637(1997) https://doi.org/10.1007/BF02845666

[226] Ucar, A., Lonngren, K.E., Bai, E.W., et al.: Chaos synchronization in RCL-shunted Josephson junction via active controller. Chaos Solitons Fractals **3**, 105–111 (2007).

[227] HindMarsh, J. L., and R.M.R.: A model of neuronal bursting using three coupled first order differential equations. Proc. R. Soc. Lond. Biol. 221, 87–102 (1984).

[228] Dana, S.K., Sengupta, D.C. and Hu, C.K., 2006. Spiking and bursting in Josephson junction. *IEEE Transactions on Circuits and Systems II: Express Briefs*, *53*(10):1031-1034(2006).

[229] S.Sovilj,R.Magjarević and N.H.Lovell .A simplified 3D model of whole heart electrical activity and 12-Lead ECG generation.Computational and mathematical methods in medicine.134208(10),(2013).

[230] Wu, X., Ma, J., Yuan, L. and Liu, Y.: Simulating electric activities of neurons by using PSPICE. *Nonlinear Dynamics*, *75*(1-2):113-126(2014).